

Research

Carbon-14 in the marine environment of Ringhals nuclear power plant

Report for project SSM2022-4035

2025:08

Author: Kristina Eriksson Stenström¹, Sören Mattsson²,
Guillaume Pédehontaa-Hiaa^{1,2}, Filip Käll³

¹Lund University, Department of Physics, Division of Nuclear Physics

²Lund University, Department of Translational Medicine,
Medical Radiation Physics, Malmö

³Swedish University of Agricultural Sciences, Department of Aquatic
Resources, Institute of Coastal Research, Öregrund

Date: August 2025

Report number: 2025:08

ISSN: 2000-0456

Available at www.ssm.se



Strål
säkerhets
myndigheten

Swedish Radiation Safety Authority

Author: Kristina Eriksson Stenström¹, Sören Mattsson²,
Guillaume Pédehontaa-Hiaa^{1,2}, Filip Käll³

¹Lund University, Department of Physics, Division of
Nuclear Physics

²Lund University, Department of Translational Medicine,
Medical Radiation Physics, Malmö

³Swedish University of Agricultural Sciences, Department
of Aquatic Resources, Institute of Coastal Research,
Öregrund

2025:08

Carbon-14 in the marine environment
of Ringhals nuclear power plant

Report for project SSM2022-4035

Date: August 2025

Report number: 2025:08

ISSN: 2000-0456

Available at www.stralsakerhetsmyndigheten.se

This report was commissioned by the Swedish Radiation Safety Authority (SSM). The conclusions and viewpoints presented in the report are those of the author(s) and do not necessarily coincide with those of SSM.

SSM perspektiv

Bakgrund

Kol-14 förekommer i miljön som ett resultat av naturlig produktion samt atmosfäriska kärnwapentester, vilka främst genomfördes under 1950- och 1960-talen. Kol-14 är en viktig radionuklid ur strålskyddssynpunkt, eftersom den ofta dominerar den dos allmänheten får från verksamheter såsom drift av kärnkraftverk, upparbetning av använt kärnbränsle och förvaring av radioaktivt avfall, etc.

Till skillnad från de flesta andra radionuklider (som ofta är metaller) kan omfördelning och ackumulering av kol-14 i marina ekosystem inte lika enkelt beskrivas med en fördelningskoefficient (K_d). Kol (C), och därmed radionukliden kol-14, är mycket biotillgängligt och tas upp under fotosyntesen av primärproducenter (t.ex. fytoplankton och makroalger). Från primärproducenterna överförs kol-14 vidare till andra delar av det marina ekosystemet.

Utöver sin biologiska tillgänglighet är kol-14 också en del av den säsongsbundna karbonatcykeln i havet, och styrs av havsvattnets säsongsvariationer i temperatur, pH m.m., vilket medför ett varierande utbyte av kol (kol-14) mellan havsytan och atmosfären. På grund av en allmän brist på data om kol-14 i miljön kring kärntekniska anläggningar är möjligheterna att validera dosmodeller för kol-14 generellt sett begränsade.

I detta projekt har en ettårig studie genomförts av den marina radioekologin kopplad till vattenburna utsläpp av kol-14 från Ringhals kärnkraftverk (KKV). Provtagningsplatserna valdes utifrån Ringhals KKV:s ordinarie miljöövervakningsprogram och täckte kustområdet från cirka 9 km norr till cirka 8 km söder om kärnkraftverkets utlopp för kylvatten. Prover togs från följande typer av material och organismer: påväxtplattor, *Fucus vesiculosus* (blåstång), *Symphodus melops* (tångsnälla), *Mytilus edulis* (blåmussla), *Magallana gigas* (stillahavsostren), *Cancer pagurus* (krabba), sediment och partikulärt kol.

Rapporten innehåller även en omfattande beskrivning av källor till kol-14 i miljön samt tidigare studier om kol-14:s radioekologi.

Resultat

Resultaten från studien visar att även om utsläppen till vatten från Ringhals KKV antas vara små jämfört med utsläppen till luft, är de resulterande kol-14-nivåerna i marina organismer avsevärt högre än i terrestra organismer. Resultaten indikerar att den kemiska formen av kol-14 som släpps ut spelar en avgörande roll för dess upptag och spridning i marina organismer.

De högsta koncentrationerna i den marina miljön av kol-14 observerades nära kärnkraftverkets utlopp för kylvatten. Organismer som samlats in från en påväxtplatta uppvisade $F^{14}C$ -värden¹ upp till cirka 700 % över uppskattad marin bakgrundsnivå. Mjukvävnad från *Symphodus melops* (tångsnälla) visade ett överskott på upp till cirka 400 %, *Mytilus edulis* (blåmussla) upp till cirka 170 % och *Fucus vesiculosus* (blåstång) upp till cirka 100 %.

¹ $F^{14}C = 1$ motsvarar ungefär den naturliga specifika aktiviteten på ca 226 Bq/kg C ($F^{14}C = 0$ motsvarar 0 Bq/kg C)

Relevans

Dessa resultat ger viktig kunskap till Strålsäkerhetsmyndigheten (SSM) gällande kol-14:s beteende i miljön, särskilt i akvatiska ekosystem. De antyder att nuvarande övervakning – som enbart baseras på luftburna kol-14-utsläpp – kan underskatta den faktiska radiologiska påverkan i den marina miljön.

Studien belyser behovet av att överväga om kol-14 bör ingå som en rutinmässig del i miljöövervakningsprogram för vattenutsläpp och om krav bör ställas på att redovisa den kemiska formen och spridningsvägen för kol-14 i övervakningen. Denna kunskap är särskilt relevant för att säkerställa skyddet av allmänheten och marina ekosystem, med tanke på att kol-14 dominerar dosbidraget.

Fortsatt forskningsbehov

Vidare studier om variationer och kemisk form av kol-14 i utsläpp till vatten från kärnkraftverk, samt upptag i marina organismer, är av intresse för fortsatt forskning. Det finns också behov av att utvärdera resultatens betydelse för den radiologiska riskbedömningen för allmänhet och miljö.

Projektinformation

Kontaktperson SSM: Karin Aquilonius

Referens: SSM2022-4035/ 4530513

SSM perspective

Background

C-14 occurs in the environment at background levels resulting from natural production and atmospheric testing of nuclear weapons, which were mainly carried out during the 1950s and 1960s. C-14 is an important radionuclide from a radiation protection point of view as it often dominates the dose to the public from activities such as operation of nuclear power plants, reprocessing of spent nuclear fuel and storage of radioactive waste, etc.

Unlike most other radionuclides (which are often metals), redistribution and accumulation in the marine ecosystems of C-14 cannot be described as easily with a distribution coefficient (K_d). Carbon (C), and thus the radionuclide C-14, is highly bioavailable and taken up during photosynthesis by primary producers (phytoplankton and macro algae). From the primary producers, the C-14 is transferred to other parts of the marine ecosystem. In addition to being biologically active, C-14 is also part of the seasonal carbonate cycle in the sea and is controlled by the seawater's seasonal variations in temperature, pH, etc., and thus a varying exchange of carbon (C-14) between sea surface and air. Due to a general lack of data regarding C-14 in the environment around nuclear facilities, the possibilities to validate dose models for C-14 in general are limited.

In this project a one-year study has been conducted regarding the marine radioecology of waterborne C-14 discharges from Ringhals nuclear power plant (NPP). The sampling sites were selected from the regular environmental monitoring programme at Ringhals NPP, and covered the coastal area from up to ~9 km north to ~8 km south of the NPP's cooling water outlet. The sample types and organisms were biofouling plates, *Fucus vesiculosus* (bladderwrack), *Symphodus melops* (corkwing wrasse), *Mytilus edulis* (blue mussel), *Magallana gigas* (pacific oyster), *Cancer pagurus* (crab), sediment and particulate carbon.

The report also includes a comprehensive description of sources of C-14, the fate of C-14 in the marine environment and previous studies of the radioecology of C-14.

Results

The C-14 results from the study demonstrate that, although the liquid discharges from the Ringhals Nuclear Power Plant (NPP) are assumed to be small compared to the total operational C-14 releases, the resulting C-14 levels in marine biota can be substantially higher than in terrestrial biota. The findings indicate that the chemical speciation of discharged C-14 plays a critical role in its transfer and uptake by marine organisms.

The highest concentrations of C-14 were observed near the cooling water outlet of the NPP. Organisms collected from a biofouling plate exhibited $F^{14}C^1$ values up to approximately 700% above the estimated marine background. Similarly, soft tissue from *Symphodus melops* (corkwing wrasse) showed up to ~400% excess, *Mytilus edulis* (blue mussel) up to ~170%, and *Fucus vesiculosus* (bladderwrack) up to ~100%.

Relevance

These results provide important insights for the Swedish Radiation Safety Authority (SSM) regarding the environmental behavior of C-14, particularly in aquatic ecosystems. They suggest that current monitoring practices—based solely on airborne C-14 emissions—may underestimate the actual radiological impact in the marine environment.

¹ $F^{14}C = 1$ approximately corresponds to the natural specific activity of carbon of about 226 Bq/kg C ($F^{14}C = 0$ corresponds to 0 Bq/kg C)

The study supports the need to reconsider whether C-14 should be routinely included in environmental monitoring programs for aquatic discharges and whether it should be required to account for the chemical form and pathway of C-14 releases in the monitoring. This knowledge is particularly relevant for ensuring the protection of the public and of marine ecosystems due to C-14 importance as a major contributor to dose.

Need for further research

Further studies in variations and chemical form in the liquid discharges from nuclear power plants of C-14 in addition to uptake to marine organisms is of interest for further research. There is also a need to evaluate the significance of the results for radiological risk assessment of biota and the public.

Project information

Contact person SSM: Karin Aquilonius
Reference: SSM2022-4035/ 4530513

Carbon-14 in the marine environment of Ringhals nuclear power plant

Report for project SSM2022-4035

Kristina Eriksson Stenström¹, Sören Mattsson², Guillaume Pédehontaa-Hiaa^{1,2}, Filip Käll³

¹Lund University, Department of Physics, Division of Nuclear Physics

²Lund University, Department of Translational Medicine, Medical Radiation Physics, Malmö

³Swedish University of Agricultural Sciences, Department of Aquatic Resources, Institute of Coastal Research, Öregrund

Summary

A one-year study has been conducted regarding the marine radioecology of waterborne ^{14}C discharges from Ringhals nuclear power plant (NPP). The sampling sites were selected from the regular environmental monitoring programme at Ringhals NPP, and covered the coastal area from up to ~9 km north to ~8 km south of the NPP's cooling water outlet. The sample types and organisms were biofouling plates, *Fucus vesiculosus* (bladderwrack), *Symphodus melops* (corkwing wrasse), *Mytilus edulis* (blue mussel), *Magallana gigas* (pacific oyster), *Cancer pagurus* (crab), sediment and particulate carbon.

The ^{14}C -results of the study demonstrate that even though the liquid discharges from Ringhals NPP are believed to be small compared to the total ^{14}C operational releases, the resulting ^{14}C signal in marine biota can be substantially higher than in terrestrial biota. The results point to that the chemical speciation of the ^{14}C -discharges is essential in how ^{14}C is transferred to biota. Previously (in 2006), a few measurements of the activity concentrations of ^{14}C in DIC (dissolved inorganic carbon) and DOC (dissolved organic carbon) were performed for water from the wastewater tanks of the two Ringhals Pressurized Water Reactor (PWR) reactors R3 and R4 (the ones still operational). The inorganic form of ^{14}C dominated in 3 of the 4 samples analysed (the organic fraction being 19%, 29% and 34%), and for the fourth sample the organic form dominated (90% organic). However, since seawater contains more DIC than DOC, inorganic ^{14}C -discharges become more diluted than organic ^{14}C discharges. Higher specific activities can thus be expected in DOC in seawater than in DIC.

The results in this report are expressed in the dimensionless quantity Fraction Modern, $F^{14}\text{C}$. $F^{14}\text{C} = 1$ approximately corresponds to the natural specific activity of carbon of about 226 Bq/kg C ($F^{14}\text{C} = 0$ corresponds to 0 Bq/kg C). The general order of $F^{14}\text{C}$ seen in different marine species was (ordered in increasing specific activity):

Fucus vesiculosus \leq *Magallana gigas* $<$ *Mytilus edulis* $<$ *Symphodus melops*

Cancer pagurus appeared to have somewhat higher specific activity than *F. vesiculosus* collected at the same site.

$F^{14}\text{C}$ in *F. vesiculosus* is representative of $F^{14}\text{C}$ in DIC which is absorbed during photosynthesis. The other types of organisms feed on various forms organic carbon, that can be part of the diet or possibly be directly transferred to the organism, e.g. by the respiratory system. We believe that liquid discharges of water-soluble organic compounds (less diluted in seawater than DIC) play a significant role in the observed excess *S. melops* and *M. edulis*. The results of ^{14}C analysis of particulate carbon, which also shows significantly elevated ^{14}C content, support this hypothesis.

The highest concentrations of ^{14}C were found close to the cooling water outlet of the NPP. Organisms from a biofouling plate had a $F^{14}\text{C}$ value that was up to ~700% greater than the estimated marine background level. Soft tissue of *S. melops* caught at the same site had up to ~400% excess of ^{14}C , *M. edulis* had up to ~170% excess, and *F. vesiculosus* had up to ~100% excess. A similar pattern was seen at other sites (with lower excess due to increased distance from the cooling water outlet).

The spatial variability in marine ^{14}C at Ringhals NPP was consistent with the expected dispersion patterns due to the direction of the liquid discharges (to the south) and due to the Baltic current twisting the dispersed cooling water plume towards the north. The northernmost site (~9.3 km N of the discharge point) appeared more affected than the southernmost site (~7.7 km S of the discharge point). However, the southernmost site may be affected by the outflow of river Viskan. Temporal variability in F^{14}C was seen during the one-year study, in particular at the site close to the cooling water outlet. No consistent patterns of temporal variation in F^{14}C were seen between different species.

We have studied the variability of ^{14}C in *Fucus* spp. along the Swedish west coast over time in order to determine a suitable reference value for ^{14}C -DIC for Ringhals nuclear power plant. Carbon-14 discharged to water from the reprocessing plants for spent nuclear fuel at La Hague (France) and Sellafield (UK) reach the Swedish west-coast via water currents from the North Sea. In samples of *F. vesiculosus* collected between 2020 and 2024 we have seen a gradient in F^{14}C that increases in a northerly direction along the west coast. The northernmost Skagerrak has up to ~10% higher F^{14}C values than southern Swedish coastal areas in the Baltic Sea. In a sample collection series in Särö in Halland, started in 1967, we see a connection between ^{14}C discharges from the French and British reprocessing plants and F^{14}C in *Fucus* spp. From the studies of F^{14}C in *Fucus* spp. collected on the Swedish west coast, we conclude that appropriate selection of reference sites is fundamental to correctly interpreting the F^{14}C values measured around the nuclear power plant. We also see that the current geographical area covered by the regular environmental monitoring programme would need to be expanded, both north and south of the nuclear power plant for the case of ^{14}C assessments.

Since no previous data exist on past marine levels of ^{14}C in the Ringhals area we have evaluated the potential use of annual structures of *M. edulis* shells to estimate past liquid discharges of ^{14}C -DIC. A method was developed to extract the fibrous layer that forms visible annual structures in the shells. The approach has proven to be promising.

We see the need to further investigate the mechanisms behind the observed elevated ^{14}C levels in the marine environment of Ringhals NPP. We suggest further investigations of the distribution of ^{14}C in edible fish to understand the uptake of ^{14}C from Ringhals NPP. Additional investigations are also needed to understand the differences in ^{14}C uptake in *M. edulis* and *M. gigas*. We also propose time-resolved studies of the different fractions of ^{14}C in the discharge water, and simultaneous studies of ^{14}C on, for example, the biofouling plates at the discharge. Such a study would show how well the biofouling plates reflect the actual discharge.

Due to the relative importance of ^{14}C in dose assessments to the public, we strongly recommend that analysis of ^{14}C is included in the regular environmental monitoring programmes of Swedish NPPs. At Ringhals NPP, this is of particular importance in view of ongoing decommissioning of R1 and R2 and potential expansion of nuclear power at the Ringhals site. We also recommend that ^{14}C analysis of liquid effluents should be included in the source monitoring of Swedish NPPs.

Sammanfattning

En ettårig studie har genomförts rörande marin radioekologi av vattenburna ^{14}C -utsläpp från Ringhals kärnkraftverk. Ringhals kärnkraftverks ordinarie miljöövervakningsprogram stod som förlaga för val av provtagningsplatser och täckte kustområdet från upp till ~9 km norr till ~8 km söder om kärnkraftverkets utlopp av kylvatten. Undersökta provtyper och organismer var påväxtplattor, *Fucus vesiculosus* (blåstång), *Symphodus melops* (skärsnult), *Mytilus edulis* (blåmussla), *Magallana gigas* (Stillahavsstron), *Cancer pagurus* (krabba), sediment och partikelburet kol.

Resultaten av studien visar att även om de vätskeburna ^{14}C -utsläppen från Ringhals kärnkraftverk tros vara små jämfört med de totala driftutsläppen av ^{14}C , kan den resulterande ^{14}C -signalen i marin biota bli avsevärt högre än i terrester biota. Resultaten pekar på att den kemiska formen av ^{14}C -utsläppen är avgörande för hur ^{14}C överförs till biota. Tidigare (2006) har ett fåtal mätningar av aktivitetskoncentrationerna av ^{14}C i DIC (oorganiskt kol löst i vattnet) och DOC (organiska kolföreningar lösta i vattnet) utförts för vatten från utsläppsvattentankarna i tryckvattenreaktorerna R3 och R4 (de som fortfarande är i drift vid Ringhals kärnkraftverk). Den oorganiska formen dominerade i 3 av de 4 analyserade proverna (den organiska ^{14}C -fraktionen var 19 %, 29 % och 34 %), och för det fjärde provet dominerade den organiska formen (90 % organiskt ^{14}C). Eftersom havsvatten innehåller mer löst oorganiskt kol än löst organiskt kol, blir de oorganiska ^{14}C -utsläppen mer utspädda än de organiska ^{14}C -utsläppen. Högre specifika aktiviteter kan alltså förväntas i DOC i havsvatten än i DIC.

Resultaten i denna rapport uttrycks i den dimensionslösa storheten Fraction Modern, $F^{14}\text{C}$. $F^{14}\text{C} = 1$ motsvarar ungefär den naturliga specifika aktiviteten för kol på cirka 226 Bq/kg C ($F^{14}\text{C} = 0$ motsvarar 0 Bq/kg C). Generellt rangordnade sig uppmätt $F^{14}\text{C}$ i olika marina arter enligt:

$Fucus\ vesiculosus \leq Magallana\ gigas < Mytilus\ edulis < Symphodus\ melops$

Cancer pagurus verkade ha något högre $F^{14}\text{C}$ än *F. vesiculosus* insamlad på samma plats.

$F^{14}\text{C}$ i *F. vesiculosus* är representativ för $F^{14}\text{C}$ i DIC som absorberas genom algens fotosyntes. De andra typerna av organismer livnär sig på olika former av organiskt kol, som kan ingå i kosten eller som eventuellt kan överföras direkt till organismen, t.ex. via andningssystemet. Vi tror att vattenburna utsläpp av vattenlösliga organiska föreningar spelar en betydande roll i det observerade överskottet av ^{14}C i *S. melops* och *M. edulis*. Resultat av ^{14}C -analys av partikelburet kol, som också visar väsentligt förhöjd ^{14}C -halt, stödjer denna hypotes.

De högsta koncentrationerna av ^{14}C hittades nära kärnkraftverkets kylvattenutlopp. Organismer från en påväxtplatta hade ett $F^{14}\text{C}$ -värde som var upp till ~700% större än den uppskattade marina bakgrunds-nivån. Mjuk vävnad hos *S. melops* från samma ställe hade upp till ~400% överskott av ^{14}C , *M. edulis* hade upp till ~170% överskott och *F. vesiculosus* hade upp till ~100% överskott. Ett liknande mönster sågs på andra platser (med lägre överskott på grund av ökat avstånd från kylvattenutloppet).

Den spatiala variabiliteten i marint ^{14}C vid Ringhals kärnkraftverk överensstämde med de förväntade spridningsmönstren på grund av kylvattnets utsläppsriktning (mot söder) och på grund av att Baltiska strömmen vrider av kylvattenplymen mot norr. Den nordligaste platsen (~9,3 km N om utsläppspunkten) verkade mer påverkad än den sydligaste platsen (~7,7 km S om utsläppspunkten). Den sydligaste platsen kan dock påverkats av Viskans utflöde. Variation i $F^{14}\text{C}$ över tid sågs under den ettåriga studien, särskilt nära kylvattenutloppet. Inga samstämmiga mönster för den tidsmässiga variationen i $F^{14}\text{C}$ sågs mellan olika arter.

Vi har studerat variabiliteten av ^{14}C i *Fucus* spp. längs den svenska västkusten över tid för att kunna bestämma lämpligt referensvärde för ^{14}C -DIC för Ringhalsverket. Kol-14 som släpps ut till vatten från upparbetningsanläggningarna för använt kärnbränsle i La Hague (Frankrike) och Sellafield (UK) når den svenska västkusten via vattenströmmar från Nordsjön. I prover av *F. vesiculosus* insamlade mellan 2020 och 2024 har vi sett en gradient i $F^{14}\text{C}$ som ökar i nordlig riktning längs västkusten. Nordligaste Skagerrak har upp till ~10% högre $F^{14}\text{C}$ -värden än sydsvenska kustområden i Östersjön. I en insamlingsserie i Särda i Halland, påbörjad 1967, ser vi samband mellan ^{14}C -utsläpp från de franska och brittiska upparbetningsanläggningarna och $F^{14}\text{C}$ -halten i *Fucus* spp. Från studierna av $F^{14}\text{C}$ i *Fucus* spp. insamlat på svenska västkusten drar vi slutsatsen att lämpligt val av referensplatser är fundamentalt för att på rätt sätt kunna tolka de $F^{14}\text{C}$ -värden som uppmäts kring kärnkraftverket. Vi ser också att det nuvarande geografiska området som omfattas av det ordinarie miljöövervakningsprogrammet skulle behöva utvidgas, såväl norr som söder om kärnkraftverket för fallet ^{14}C .

Eftersom det inte finns några tidigare data på tidigare marina nivåer av ^{14}C i Ringhalsområdet har vi utvärderat den potentiella användningen av årliga strukturer i skal av *M. edulis* för att på så sätt kunna uppskatta tidigare vattenburna utsläpp av ^{14}C -DIC. En metod har utvecklats för att extrahera det fibrösa skiktet som bildar synliga årsringar i skal. Tillvägagångssättet har visat sig vara lovande.

Vi ser behovet av att ytterligare undersöka mekanismerna bakom de observerade förhöjda ^{14}C -nivåerna i den marina miljön i Ringhals kärnkraftverk. Vi föreslår ytterligare undersökningar av fördelningen av ^{14}C i ätbar fisk för att förstå upptaget av ^{14}C . Ytterligare undersökningar behövs också för att förstå skillnaderna i ^{14}C -upptag i *M. edulis* och *M. gigas*. Vi föreslår också tidsupplösta studier av de olika fraktionerna av ^{14}C i utsläppsvattnet, och samtidiga studier av ^{14}C på t ex påväxtplattorna vid utsläppet. En sådan undersökning skulle visa hur väl påväxtplattor reflekterar det verkliga utsläppet.

På grund av betydelsen av ^{14}C i dosbedömningar för allmänheten rekommenderar vi starkt att analys av ^{14}C ingår i de reguljära miljöövervakningsprogrammen för svenska kärnkraftverk. Vid Ringhals kärnkraftverk är detta av särskild vikt med tanke på pågående avveckling av R1 och R2 och potentiell utbyggnad av kärnkraften vid Ringhalsområdet. Vi rekommenderar också att ^{14}C -analys av utsläppsvatten ska ingå i utsläppsövervakningen av svenska kärnkraftverk.

Abbreviations and notations

AAA	Acid alkali acid
AMS	Accelerator mass spectrometry
BWR	Boiling water reactor
DIC	Dissolved inorganic carbon
DOC	Dissolved organic carbon
EA-IRMS	Elemental analyser – isotope ratio mass spectrometry
EMP	Environmental monitoring programme
HWC	Hydrogen water chemistry
LSC	Liquid scintillation counting
LWR	Light water reactor
NPP	Nuclear power plant
NWC	Neutral water chemistry
PC	Particulate carbon
PIC	Particulate inorganic carbon
POC	Particulate organic carbon
PWR	Pressurized water reactor
SLU	Swedish University of Agricultural Sciences
TC	Total carbon
TDC	Total dissolved carbon

Contents

1. Introduction.....	9
2. Carbon-14 in the environment.....	11
2.1. Sources of ^{14}C	11
2.1.1. Natural and bomb- ^{14}C	11
2.1.2. ^{14}C from the nuclear power industry.....	12
2.1.3. Other sources affecting the ^{14}C concentration in the environment.....	17
2.2. ^{14}C in terrestrial organisms	17
2.3. ^{14}C in the marine environment	19
2.3.1. The solubility, biological and carbonate pumps of DIC	19
2.3.2. ^{14}C -DIC in the oceans	19
2.3.3. ^{14}C -DIC in coastal areas	20
2.3.4. DIC, PIC, DOC, POC and transfer of carbon in the marine environment	22
2.3.5. Concentration factors according to literature.....	23
2.4. Previous studies of the radioecology of ^{14}C in aquatic and marine environments.....	24
2.4.1. Lakes and rivers.....	24
2.4.2. Marine environment.....	25
3. Ringhals NPP – reactors and available ^{14}C release data	26
3.1. Reactors	26
3.2. Airborne ^{14}C releases	26
3.3. Water-borne discharge rates of ^{14}C	28
4. Materials and methods	30
4.1. Sampling sites for investigations of spatial and temporal variations in ^{14}C of the Swedish west coast	30
4.2. The Ringhals site.....	34
4.2.1. Sampling sites.....	34
4.2.2. Characteristics of the Ringhals area.....	37
4.2.3. Dispersion of Ringhals NPP cooling water	38
4.3. Sampling	39
4.3.1. Sampling by Lund University.....	39
4.3.2. Sampling by SLU for the one-year study at Ringhals NPP	40
4.4. Sample preparation	40
4.5. ^{14}C -analysis	41
4.6. EA-IRMS measurement.....	41
4.7. Analysis of ^{99}Tc	41
5. Summary of our previous studies	42
6. Results and discussion	46
6.1. Overview of published papers.....	46
6.2. Terrestrial coastal environment.....	47
6.3. Observed temporal variations of ^{14}C at Särö.....	48
6.4. Observed spatial and temporal variations of ^{14}C at the Swedish west coast.....	51
6.5. Carbon-14 reference level for Ringhals NPP 2020-2024.....	53
6.6. Mussel shells for retrospective ^{14}C -DIC analysis.....	54
6.6.1. Shell annual bands versus <i>Fucus vesiculosus</i> for reference sites	54
6.6.2. DIC versus dietary carbon of <i>M. edulis</i> at reference sites	55

6.6.3. Shell annual bands versus <i>Fucus vesiculosus</i> at Ringhals NPP	56
6.7. Carbon-14 in <i>Fucus</i> spp. at Ringhals 2020-2024 [9]	60
6.8. Carbon-14 in <i>Mytilus edulis</i> versus <i>Fucus vesiculosus</i> at Ringhals NPP in 2022	62
6.9. One-year study of ^{14}C at Ringhals 2023-2024	63
6.10. Sediments	72
6.11. Particulate carbon	73
6.12. Trophic levels and carbon content	75
6.13. Technetium-99	76
6.14. Radioecological discussion	77
7. Summary and conclusions	80
8. Outlook	83
9. Acknowledgement	84
10. References	85
Appendix A – Units for ^{14}C	95
Appendix B – Examples of methods for ^{14}C analysis of water	97
Appendix C – Sites	101
Appendix D – Results	103
Appendix E – Trophic levels and carbon content	111

1. Introduction

Carbon-14 (^{14}C , physical half-life 5730 years) is produced during operation of all types of nuclear power reactors. Its radiological significance is demonstrated e.g. by UNSCEAR [1], estimating that ^{14}C discharged from reprocessing of spent nuclear fuel is the largest contributor to the collective dose from global dispersion of the long-lived radionuclides that are generated by the nuclear power industry. In Sweden, ^{14}C often dominates the committed effective dose to the public from operational releases of nuclear power plants (NPPs) [2-5]. The ^{14}C effluents during normal operations of NPPs are mainly airborne [6, 7], and releases of ^{14}C to air are since 2002 continuously monitored at Swedish reactors. Carbon-14 in the plume from the ventilation stack of the NPP is effectively diluted before reaching ground level, where ^{14}C can be incorporated into living organisms mainly through photosynthesis of ^{14}C in the form of CO_2 .

Liquid discharges of ^{14}C are currently not routinely monitored at Swedish nuclear power plants, partly due to analytical challenges and due to the observation that the liquid discharges often are significantly less than the airborne releases [4, 5, 7]. However, for liquid discharges of ^{14}C , the dilution before reaching biota is less, and the uptake mechanisms in biota of the various chemical forms containing ^{14}C are different than in the atmosphere. Therefore, significantly increased levels of ^{14}C compared to background may be seen in the marine and aquatic environment of nuclear reactors, as we have previously reported for the local marine environment of Ringhals NPP [8]. Local marine biota may even display much higher ^{14}C activity concentrations than local terrestrial biota [8]. At Ringhals NPP, we have in previous studies seen an increase in the specific activity of carbon (Bq ^{14}C per g carbon) of seaweed (*Fucus spp.*) of up to ~25% compared to nearby reference sites (considered not significantly affected by the NPP) [8]. This excess is considerably higher than what we have seen in other investigations of the terrestrial environment close to Swedish NPPs (typically <10% excess compared to a relevant reference site, see [8] and references therein).

The observation that the specific activity of carbon can be considerably higher in biota in the local marine environment of Ringhals NPP than in its terrestrial environment has initiated the research project presented in this report. Previous data on ^{14}C in the local marine environment of Swedish NPPs are sparse (see [8] and references therein), and, as mentioned above, ^{14}C measurements of water-borne effluents are not included in the environmental monitoring programmes at any of the Swedish nuclear power plants.

We report on:

1. a study of long-term trends and temporal variations in the marine ^{14}C background of the Swedish west coast, published in [9]
2. an evaluation the influence from foreign nuclear facilities on ^{14}C in Swedish west-coastal waters, based on results published in [10]
3. a one-year study the local radioecology of ^{14}C in the marine environment of Ringhals NPP
4. a first study to investigate the potential of using shells of blue mussels (*Mytilus edulis*) for retrospective analysis of ^{14}C around Ringhals NPP, published in [11]

In the current report we summarize the findings and refer to the publications [9-11] for details.

The results of this report can be used for dose assessments of liquid ^{14}C discharges from Ringhals NPP. The results can also be used as a base for evaluating if source monitoring or environmental monitoring of ^{14}C at Ringhals NPP should be considered.

The report starts with an introduction to ^{14}C in the environment (chapter 2), where natural and anthropogenic sources of ^{14}C are described, focussing on the nuclear power industry. The behaviour of ^{14}C in the terrestrial environment is briefly described, followed by a more detailed discussion on ^{14}C in various chemical and physical forms in the marine environment. Chapter 3 presents facts about Ringhals NPP and summarizes available data on airborne and liquid ^{14}C discharges from the NPP (the latter data is very sparse). Chapter 4 concerns methodological aspects. To put the results reported in in Chapter 6 into perspective, a Chapter 5 has been included which summarizes our previous studies of ^{14}C in the marine environment of the Swedish west coast and of Ringhals NPP. The project is summarized in Chapter 7, followed by and outlook in Chapter 8.

The report also includes appendices with:

1. notes on various units used to report ^{14}C content, and how to convert between different units,
2. some results from measurements of stable carbon and nitrogen isotopes providing information e.g. about trophic levels and carbon content of various organisms used in the one-year study the local radioecology of ^{14}C in the marine environment of Ringhals NPP, and
3. results in tables.

2. Carbon-14 in the environment

To evaluate the environmental effects of ^{14}C released to air or water from a nuclear facility, the other potential sources of ^{14}C in the environment must be known. The possible spatial and temporal variability in the ^{14}C concentration must also be considered. This chapter starts with a brief summary of the three main sources of ^{14}C in the environment – natural ^{14}C , ^{14}C from nuclear weapons tests, and ^{14}C from the nuclear power industry – and also discusses the behaviour of ^{14}C in the environment in general terms. Despite that the focus of this report is the marine environment, also the terrestrial environment is briefly covered in the chapter. A general introduction to the complex behaviour of ^{14}C in the marine environment is provided.

2.1. Sources of ^{14}C

2.1.1. Natural and bomb- ^{14}C

Carbon-14 is a naturally occurring radionuclide that is continuously produced in the upper atmosphere due to nuclear reactions between atmospheric nitrogen and cosmic-ray induced neutrons ($^{14}\text{N}(\text{n},\text{p})^{14}\text{C}$). The annual production rate of ^{14}C varies with the strength of the Sun's and Earth's magnetic fields, which affects the proportion of the flow of the cosmic radiation that reaches the Earth's atmosphere. The average natural ^{14}C production rate has been estimated to about $1.4 \cdot 10^{15}$ Bq/year, resulting in a global atmospheric inventory of about $140 \cdot 10^{15}$ Bq [12]. The testing of nuclear weapons in the 1950s and 1960s added in total about $350 \cdot 10^{15}$ Bq of ^{14}C to the atmosphere [12].

The natural as well as the bomb- ^{14}C is quickly oxidized to CO_2 , which is spread throughout the atmosphere and taking part in the global carbon cycle, starting with photosynthesis in the terrestrial biosphere. Since CO_2 is highly soluble in water and is dissolved at the water surface (referred to as DIC, dissolved inorganic carbon), natural as well as bomb- ^{14}C enter various hydrological compartments. The half-life of bomb- ^{14}C in the atmosphere has been estimated to about 6 years, with the oceans as the main recipient [12]. This transfer illustrated in Figure 1, showing ^{14}C in CO_2 at atmospheric reference sites (clean air sites in central Europe and Sweden) from 1950, forming the so called bomb-pulse, or the bomb-peak. The ^{14}C concentration is given in the dimensionless quantity $F^{14}\text{C}$ (see definition in

Appendix A; $F^{14}\text{C} = 1$ approximately corresponds to the natural specific activity of carbon of about 226 Bq/kg corresponding to an atomic ratio of ^{14}C to total carbon of about 10⁻¹⁰%) [13].

As can be seen in Figure 1, $F^{14}\text{C}$ was slightly lower than 1 prior to the bomb tests, which is due to large-scale releases of ^{14}C -free CO_2 from fossil fuel combustion. The bomb-pulse spiked in 1963 when the natural pre-bomb-levels had been almost doubled (rising to about 450 Bq/kg C). After the limited test ban treaty in 1963, exchange of CO_2 between the atmosphere and oceans has gradually moved bomb- ^{14}C into the oceans through atmosphere-ocean gas exchange. The decrease in $F^{14}\text{C}$ seen in Figure 1 is amplified by the increasing atmospheric CO_2 concentration due to fossil fuel combustion, causing $F^{14}\text{C}$ to be diluted. Transfer of bomb- ^{14}C into organic material in the biosphere is also partly responsible for the decrease in the atmospheric bomb-pulse since the peak in the 1960s.

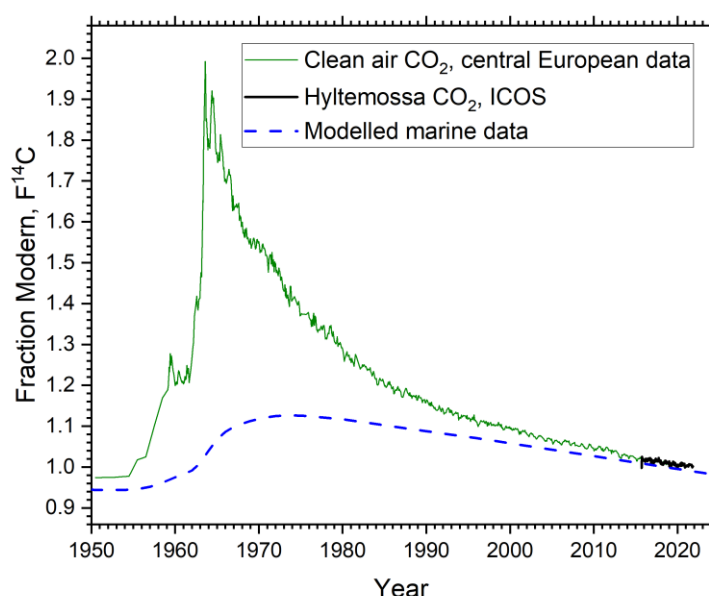


Figure 1 Carbon-14 in atmospheric CO_2 representative of the Northern Hemisphere (atmospheric bomb pulse) and oceans (marine bomb pulse), expressed in units of Fraction Modern ($F^{14}\text{C}$) [13, 14]. $F^{14}\text{C}$ in the atmosphere was approximately 1.0 before the nuclear weapons tests in the 1950s and 60s, corresponding to the natural $^{14}\text{C}/^{12}\text{C}$ ratio of about 10⁻¹⁰%, or 226 Bq (kg C)⁻¹. Carbon-14 data in atmospheric CO_2 has been collected at rural background stations in central Europe [15-18], and at the Swedish ICOS station Hyltemossa [19]. The dashed curve represents the modelled global marine surface mixed-layer bomb pulse for the period 1950 to 1996 [20], and values after this were extrapolated based on linear regression of marine data from 1987 to 1996.

2.1.2. ^{14}C from the nuclear power industry

The nuclear power industry is the third most significant source of ^{14}C in the environment. In contrast to natural and bomb- ^{14}C , which are uniformly distributed in the atmosphere¹, airborne releases and liquid discharges from the nuclear power industry give rise to local excesses in environmental ^{14}C . Apart

¹ There are however differences in bomb- ^{14}C between the northern and southern hemisphere.

from operational releases at nuclear power plants, fuel reprocessing facilities are known to release considerable amounts of ^{14}C to the terrestrial as well as the marine environment.

Various reactor types produce and emit different amounts of ^{14}C to the environment. The production of ^{14}C in nuclear reactors is due to neutron activation of oxygen, nitrogen and for some reactors of carbon in various parts of reactors (coolant, moderator, fuel and structural materials) [6]. The part available for release at the reactor site stems from the coolant and moderator, whereas ^{14}C produced in the fuel may be discharged to the environment if the fuel is reprocessed. Two such reprocessing facilities are of particular interest for the current study, Sellafield in the UK and La Hague in France, since long-range transport of ^{14}C with ocean currents reach the Swedish west coast [8]. The chemical form of the liquid ^{14}C discharges from Sellafield and La Hague is believed to be mainly DIC (see e.g. [21-23]).

A publication by the IAEA from 2004 (TR421) presents data on ^{14}C production and release from various nuclear facilities [6]. In a newer publication (from 2018), Zazzeri et al [24] present a summary of global and regional airborne emissions of ^{14}C from nuclear power plants during the period 1972 to 2016. In a recent report we present updated ^{14}C emission data for light-water reactors (LWRs) [25]. The annual ^{14}C production rate world-wide in nuclear reactors was in end of the 1990ies in the same order of magnitude as the natural annual production [3]. Approximately 10% of the annually produced ^{14}C in nuclear reactors was estimated to be released to the environment [3]. Despite the fact that other reactors types, such as heavy-water reactors, produce and release significantly more ^{14}C than LWRs, LWR reactors dominate the total amount of ^{14}C discharged worldwide to the environment since these are the most common type of reactors [24]. For LWRs of the Boiling Water Reactor (BWR) type the airborne discharges are mainly in oxidised chemical form (as CO_2), while reduced forms (e.g. hydrocarbons) dominate for Pressurized Water Reactors (PWRs) [6].

For operational nuclear reactors in general, the ^{14}C releases to air are considerably higher than the discharges of ^{14}C to water [6]. The available data from operational liquid discharges from nuclear power plants are sparse [26]. Estimated operational liquid ^{14}C discharges from a 1 GW_e LWR is $\sim 1.3 \text{ GBq/a}$ according to the IAEA TR421 from 2004 [6]. The matter of chemical forms of ^{14}C in liquid discharges is not considered in IAEA TR421 [6].

For the fuel reprocessing plants of interest to the current study (La Hague and Sellafield), data exist of the liquid ^{14}C discharges (Figure 2). The magnitude of the annual liquid ^{14}C discharges amounts to TBq/a (Figure 2).

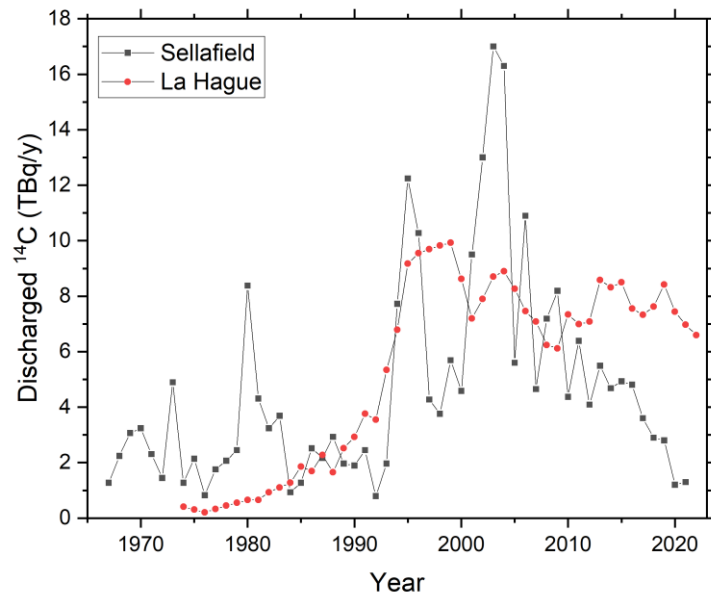


Figure 2 Liquid discharge rates of ^{14}C for the reprocessing plants for spent nuclear fuel at La Hague (France) and Sellafield (UK) for 1967 to 2022 [27].

Light-water reactors (LWRs)

All Swedish nuclear reactors, including those at Ringhals NPP, are LWRs. The production of ^{14}C of relevance for operational releases from LWRs is predominantly neutron activation of ^{17}O ($\sigma=0.24$ barn) and ^{14}N ($\sigma=1.82$ barn) in the water moderator, which also serves as coolant of the core [6]. The main part of the ^{14}C produced in the moderator/coolant is released as airborne effluents through the ventilation stack of the facility. The ^{14}C formed in the fuel, in the cladding (the thin-walled metal tube enclosing the fuel) and in structural materials is usually not available for release to the environment during normal reactor operations (except in cases of leaking fuel rods). However, as mentioned above, significant amount of ^{14}C can be discharged into the environment during fuel reprocessing (see e.g. [8, 23, 27-34]). As mentioned previously, in the present study we demonstrate how liquid discharges from the fuel reprocessing plants in Sellafield (UK) and La Hague (France) are transported to the Swedish west coast.

Table 1, containing data extracted from the IAEA TR421 report from 2004 [6], lists average calculated total ^{14}C production rates and airborne release rates for LWR-PWRs, normalized to electrical energy production, for three periods between 1975 and 1989. Data from 1995 to 2015 in Table 1 are from the publication by Zazzeri et al [24] mentioned above, and consist of median values of release rates from European PWRs and BWRs obtained from the RADD database. As seen in the 1995-2015 data, the airborne ^{14}C release rates are generally notably higher in BWRs than in PWRs, and the variation in release rates between reactors of the same types are large. An updated review of the data in the RADD database can be found in [25]. It should be noted that production rate calculations as well as measurements of ^{14}C effluents may be associated with significant uncertainties. Furthermore, diffuse leakages of ^{14}C from the NPP, not exiting the NPP through the main ventilation stack, where gas is sampled for ^{14}C source monitoring, are not accounted for in Table 1.

Table 1 Average normalized production and release rates of ^{14}C (1975-1989) from PWRs and BWRs [6], and median release rates from European PWRs and BWRs for the period 1995-2015 based on emission data reported the RADD Database and their electricity production (IAEA PRIS) from Zazzeri et al [24]. The interquartile range is within parentheses.

	PWR	BWR	Reference
Production rate ($\text{TBq} \cdot (\text{GW}_e \cdot \text{a})^{-1}$)	1.480	1.290	IAEA [6]
Airborne release rate 1975-1979 ($\text{TBq} \cdot (\text{GW}_e \cdot \text{a})^{-1}$)	0.222	0.518	IAEA [6]
Airborne release rate 1980-1984 ($\text{TBq} \cdot (\text{GW}_e \cdot \text{a})^{-1}$)	0.345	0.330	IAEA [6]
Airborne release rate 1985-1989 ($\text{TBq} \cdot (\text{GW}_e \cdot \text{a})^{-1}$)	0.120	0.450	IAEA [6]
Airborne release rate 1995-2015 ($\text{TBq} \cdot (\text{GW}_e \cdot \text{a})^{-1}$)	0.248 (0.151–0.360)	0.471 (0.371–0.630)	Zazzeri et al [24]

The chemical form of the airborne ^{14}C releases is mainly as hydrocarbons for PWRs (i.e. organic carbon), since PWRs operate under reducing chemical conditions due to excess of hydrogen [6]. BWRs may operate under two different chemical conditions: neutral water chemistry (NWC) or hydrogen water chemistry (HWC). The former (NWC) is most common for Swedish NPPs, and results in that the airborne ^{14}C releases are mainly inorganic (as CO_2) [7].

A smaller fraction of the ^{14}C produced in the coolant/moderator is retained in ion exchange resins of the water purification system [7]. The ion exchange

resins can retain inorganic ^{14}C as carbonates, but the chemical speciation of organic ^{14}C compounds ion exchange resins in NPPs is less well known, but may possibly be acetaldehyde, but various studies suggest acetaldehyde, acetic acid and formate [3]. Examples of studies characterization of ^{14}C in ion exchange resins in Swedish reactors are Magnusson et al [7, 35-38] and Magnusson [7]. A paper from 2008 describes a 4-year study of ^{14}C in different waste streams of Swedish PWRs and BWRs [7]. In BWRs, 0.6–0.8% of the ^{14}C formed in the coolant was found to be accumulated in the ion exchange resins, and for PWRs the corresponding value was 6–10% [7].

Liquid ^{14}C discharges from LWRs

Of particular interest in the present study are liquid discharges of ^{14}C from LWRs. Carbon-14 in liquid discharges stems from ^{14}C produced in the coolant (or from the fuel in case of leaking fuel rods), and which has not been released to air or been accumulated in the ion exchange resins.

As mentioned above, IAEA TR-421 from 2004 estimates that the liquid ^{14}C discharges from BWRs and well as PWRs are about 1.3 GBq/(GW_e·a) [6]. This value is based the average value from studies of one BWR (Oyster Creek) and two PWRs (Haddam Neck and Yankee Rowe) in the USA in the 1970ies (0.7-2 GBq/(GW_e·a)) [39]. Ref [39] states that German measurements support this range of liquid discharge rates. Ref [39] also reports that earlier work by EPA (US Environmental Protection Agency) have found liquid discharge rates of 0.2 GBq/(GW_e·a) for PWRs and 1 GBq/(GW_e·a) for BWRs. In a study by Kunz from 1985 [40] regarding ^{14}C in one BWR (Fitzpatrick) and 2 PWRs (Ginna and Indian Point), the ^{14}C released as liquid and solid wastes was <5% (corresponding to <20 GBq/(GW_e·a)) of the airborne ^{14}C .

In a paper from 2017 Svetlik et al [26] report on measurements of ^{14}C in liquid discharges from two NPPs in the Czech republic, Temelín and Dukovany (Russian VVER reactors of the PWR type). Svetlik et al [26] estimate that in 2015 the liquid ^{14}C discharges from the VVER reactors were low compared to other types of PWRs ($7 \cdot 10^{-5}$ and $4 \cdot 10^{-6}$ of the total ^{14}C released to environment for Temelín and Dukovany, respectively). This study is of less relevance for the present investigation at Ringhals NPP, due different reactor designs.

In the EU RADD database, only few facilities report liquid discharges of ^{14}C . The French NPPs do report liquid ^{14}C data. For the period 2002-2016 all French NPPs report that ~7.5% of the ^{14}C were in liquid form. From 2017 to 2023 the fraction varied considerably between 1% and 21% (average 6.2%, median 5.3%). Is not stated in the RADD database if the reported values are data from measurements or estimations. No information is available if the discharged amounts refer to DIC or the total discharged ^{14}C .

The chemical form of the liquid discharges is of particular interest. Molnár et al [41], who have performed ^{14}C analysis of groundwater at Paks NPP, point out that since DIC dominates over dissolved organic carbon (DOC) in groundwater, ^{14}C discharged as DOC will be significantly less diluted in the water than ^{14}C discharged as DIC. This phenomenon should also be remembered in case of liquid ^{14}C to the ocean. E.g., in a SSM publication by Engdahl [42], DIC (HCO_3) in the waters off Ringhals NPP was typically 100 mg/L (samples from August 2018 to July 2019), whereas DOC typically was single mg/L.

Measurements of ^{14}C in from Swedish reactors are reported in section 3.3.

A note on analytical challenges

There are several reasons for the few available data on waterborne discharges. One reason is that the total amount of ^{14}C emitted to water in previous studies has been shown to be considerably lower than to air. Another reason is the analytical challenges that water analyses of ^{14}C in various chemical forms entail, both on the sample preparation side and on the measurement side. The technology currently available at nuclear power plants is liquid scintillation technology (LSC). Inorganic ^{14}C can be easily extracted by adding acid, degassing the water, and then collecting released carbon dioxide in e.g. NaOH [3]. Precipitation of carbonate may then possibly be required prior to LSC analysis. Analysis of organic ^{14}C is more difficult, requiring e.g. wet oxidation to CO_2 for collection in e.g. NaOH [3, 26]. This analysis can be both time-consuming and labour-intensive. A challenge with the LSC technique is that relatively large sample volumes are required to obtain a sufficiently large signal in relation to the background. It is also necessary to carefully determine the yields in the chemical pretreatment processes to obtain accurate results. Sending effluent water for analysis with AMS (accelerator mass spectrometry) is most likely not feasible, due to too high activity concentrations with too great a contamination risk for the technique (which is also used for age determination with ^{14}C and where a low and stable background is required). However, groundwater and seawater can be analysed with advantage with AMS [41, 43] (see Appendix B).

2.1.3. Other sources affecting the ^{14}C concentration in the environment

Other sources of ^{14}C releases to the environment include research, hospitals and industry, where ^{14}C is commonly used as a tracer. An example from Lund is presented in [44], where up $F^{14}\text{C}$ values were up to ~25% above clean air background in vegetation collected in a research-intensive part of the city. Other such examples can be found in the literature (see e.g. [45, 46] and references therein).

Lowered $F^{14}\text{C}$ values may also be found in environmental samples due to dilution from fossil sources [47].

2.2. ^{14}C in terrestrial organisms

The $F^{14}\text{C}$ in terrestrial organisms depends on $F^{14}\text{C}$ of the diet and on the residence time of carbon in the organism in question. The variations in $F^{14}\text{C}$ in the atmosphere and in the terrestrial biosphere are usually small if the site is not affected by local sources of ^{14}C , such as nuclear power plants (see below), or if being located close to sources with significant releases of fossil CO_2 (such as in heavily industrialized areas [48, 49] and close to volcanoes [50]).

Figure 3 shows an example of the magnitude of temporal variations in atmospheric and terrestrial ^{14}C data (vegetation samples). The ^{14}C data for terrestrial samples in Figure 3 were collected in southernmost Sweden for the pre-operational environmental monitoring programme for the European Spallation Source (ESS), which is under construction in the outskirts of the city

of Lund [51]. Figure 3 also includes atmospheric data from central Europe [15-18] and from the ICOS stations Jungfraujoch (in the Swiss Alps) [52] and Hyltemossa (in a forest area in southern Sweden) [19]. The seasonal trends in atmospheric ^{14}C are due to varying transport of natural ^{14}C from the stratosphere to the troposphere, release of bomb- ^{14}C stored in the biosphere back to the atmosphere, and higher input from fossil fuel sources during winter [16, 53].

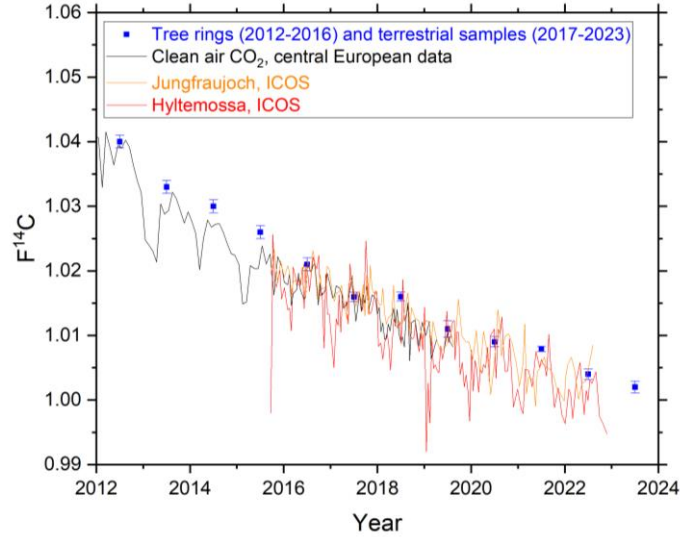


Figure 3 Average $F^{14}\text{C}$ values (uncertainty represented by the SUM) for samples from southern Sweden obtained for the environmental monitoring programme at the European Spallation Source [51]. Carbon-14 data in atmospheric CO_2 are from the rural background stations in central Europe [15-18], Jungfraujoch [52] and at the Swedish ICOS station Hyltemossa [19].

The terrestrial reference values for southern Sweden are also given in Table 2.

Table 2 Reference values of ^{14}C in the terrestrial environment relevant for southern Sweden.

Year	Sample type	Number of samples	Average $F^{14}\text{C}$	Standard deviation of $F^{14}\text{C}$	Standard error of mean of $F^{14}\text{C}$	Ref
2017	Crops, fruits, berries	24	1.018	0.005	0.001	[44]
	Grass	14	1.014	0.006	0.002	[44]
	Milk	2	1.019	0.004	0.002	[44]
2018	Crops, fruits, berries	10	1.016	0.002	0.001	[44]
	Grass	10	1.016	0.004	0.001	[44]
2019	Crops, fruits, berries, grass	8	1.011	0.004	0.001	[44]
2020	Crops, fruits, berries, grass, meat from cow, milk	26	1.009	0.004	0.001	[44]
2021	Fruits, berries, grass, milk	12	1.008	0.002	0.001	[54]
2022	Fruits, berries, grass, milk	18	1.004	0.004	0.001	[55]
2023	Fruits, berries, grass, milk	15	1.002	0.004	0.001	[51]
2024	Fruits, berries, grass, milk	14	0.999	0.002	0.001	[56]

The variations of $F^{14}\text{C}$ in grass collected at various Swedish coastal sites are presented later in this report.

2.3. ^{14}C in the marine environment

2.3.1. The solubility, biological and carbonate pumps of DIC

As stated above, natural or bomb- ^{14}C or other anthropogenic ^{14}C bound in CO_2 enter the oceans as DIC through gas exchange with the atmosphere. The DIC is mainly bicarbonate ions (HCO_3^-), but also carbonate ions (CO_3^{2-}) as well as carbonic acid (H_2CO_3) and the aqueous form of CO_2 ($\text{CO}_{2(\text{aq})}$). There are three fundamental processes that are of importance for transporting DIC within the ocean, known as the solubility pump, the biological pump and the carbonate pump. These are briefly described below.

The solubility pump involves carbon dioxide solubility of water as well as thermohaline ocean circulation. Since the solubility of CO_2 increases with decreasing water temperature, the air-ocean exchange rate depends on the temperature of the water. Surface waters at high latitudes thus have a higher CO_2 absorption capacity than at low latitudes. On a global scale, deep water is formed from dense and cold waters at high latitudes, which drives the thermohaline circulation. Hence DIC concentrations can be higher in deep waters than in surface waters. When deep water rich in DIC upwells in warmer latitudes, CO_2 is outgassed to the atmosphere due to the reduced solubility accompanying the increased temperature.

Another important process which contributes to transfer of ^{14}C (and CO_2) from the atmosphere to the oceans is the so-called biological pump, driven mainly by the primary producer phytoplankton that inhabits surface waters (see e.g. [57]). Phytoplankton residing in the surface ocean photosynthesize CO_2 , leaving room for further uptake of CO_2 into the water. Parts of the phytoplankton is consumed by other organisms, which brings ^{14}C and the carbon up to higher trophic levels of the marine food web. Upon death the phytoplankton and the other organisms sink, transferring carbon from the oceanic surface water downwards into the interior ocean. Respiration of heterotrophic organisms feeding on the dead phytoplankton and other organic materials forms can produce DIC again.

A third important phenomenon associated with the fate of DIC in the ocean water is the carbonate pump (see e.g. [57]). Calcifying organisms, such as bivalves (e.g. mussels and oysters), form their shells of calcium carbonate from DIC in the ocean water. As the calcifying organism dies, the shell sinks to the seafloor, from where it may dissolve and return to DIC.

2.3.2. ^{14}C -DIC in the oceans

As seen in the section above, the ocean-atmosphere fluxes of CO_2 (and hence of ^{14}C) in open sea depends on several factors. Prior to the start of the large-scale testing of nuclear weapons in the late 1950s and early 1960s, the $F^{14}\text{C}$ values in oceanic surface water was lower than in the atmosphere. This is evident in Figure 1 which shows an estimated global average of $F^{14}\text{C}$ in oceanic surface water down to a depth of 75 m [20]: in 1950 $F^{14}\text{C}$ in oceanic surface water was ~ 0.94 compared to ~ 0.97 in the atmosphere. This is a natural consequence of that ^{14}C is formed in the atmosphere prior to entering the oceans and being distributed in the interior ocean by advection-diffusion processes while also

being subject to radioactive decay. Hence, the carbon in the ocean surface water is generally older (with lower specific activity) than in the atmosphere.

A slow carbon cycling between the surface and deep ocean generally implies lowered $F^{14}\text{C}$ values with increasing ocean depths [57]. This phenomenon is contributing to the so-called marine reservoir effect, which must be taken into account e.g. in radiocarbon dating, and which can provide valuable information about ocean circulation. The magnitude of the marine reservoir effect may be huge: carbon in the deep ocean may be thousands of years of age [57]. E.g., the specific activity (and $F^{14}\text{C}$) of carbon of the age of 1000 years is approximately 11% lower than its initial value. The global average marine reservoir effect of ocean surface waters is ~ 400 ^{14}C years [58].

Site-specific vertical ocean circulation rates and mixing are other factors affecting the ^{14}C concentration. Thus, the spatial variation in ^{14}C in DIC in the marine reservoir can be large. This has e.g. been demonstrated by Scourse et al. [59], who found bomb-pulse maxima ranging from $F^{14}\text{C} \sim 1.03$ to ~ 1.24 in annual increments of *Arctica islandica* shells from 4 sites across the coastal North Atlantic (shells are mainly built up of DIC from the surrounding water).

2.3.3. ^{14}C -DIC in coastal areas

Coastal areas, which are of main relevance for the present study, have additional complexity compared to open sea. Here we point out a few mechanisms that are of particular importance to understand how ^{14}C concentrations may vary in coastal areas.

Upwelling is a phenomenon that may bring cold ^{14}C -depleted deep water to the surface (see Figure 4). Upwelling is not only driven by wind (as indicated in Figure 4), but is also the result of the Coriolis force (caused by Earth's rotation) and internal friction of the water (described by so called Ekman transport). River runoff may result in local variations in ^{14}C in coastal areas. River runoff may be in equilibrium with atmospheric ^{14}C , but it may also be depleted in ^{14}C due influence from carbonate-bearing bedrock [60, 61]. Another source of ^{14}C -depleted water entering coastal areas is old groundwater entering the sea water [61]. As an example of the magnitudes, $F^{14}\text{C}$ in fish caught in 2022 and 2023 in two rivers in southern Sweden in the ESS environmental monitoring programme, had $F^{14}\text{C}$ of 0.894 ± 0.004 (year 2022 in Kävlinge river) and 0.929 ± 0.005 (year 2023 in Helge river). Both these values are about 8-11% lower than the average $F^{14}\text{C}$ in the terrestrial samples the corresponding year (see Table 2) and about 7% lower than in DIC in shallow waters in southern Sweden (see Table 5 below).

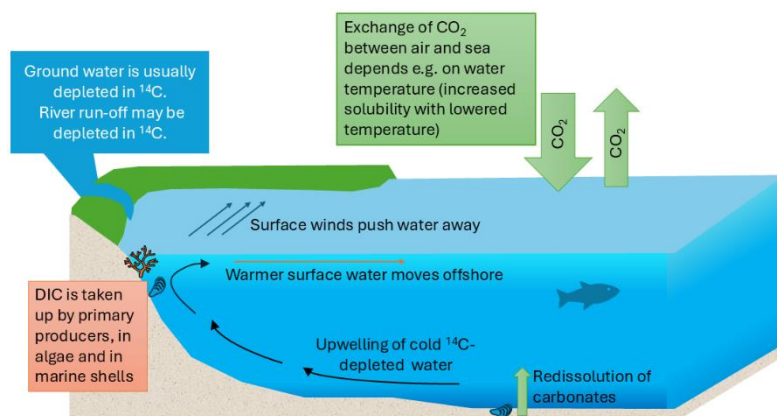


Figure 4 Some factors influencing ^{14}C in DIC in waters of coastal areas.

As an example of recent reference values of ^{14}C in DIC in southern Sweden, Table 3 shows $F^{14}\text{C}$ in *Fucus vesiculosus* from reference sites used in the ESS environmental monitoring programme. Despite the few samples, $F^{14}\text{C}$ in DIC in shallow waters at the sites in

Table 3 for 2021-2024 is very close to atmospheric data at the corresponding years (see Table 2). For 2021 and 2022, the terrestrial $F^{14}\text{C}$ is ~5-6% higher than in marine DIC. For 2023 and 2024, the average $F^{14}\text{C}$ in the terrestrial and in marine DIC data differ by less than ~0.5%. This observation may indicate that $F^{14}\text{C}$ in shallow waters in southern Sweden in the next years may start to exceed $F^{14}\text{C}$ in the atmosphere.

Table 3 Reference values of ^{14}C in in *Fucus vesiculosus*, representative of DIC in seawater, collected at the west coast (Öresund strait) and east coast (Baltic Sea) of Skåne in southernmost Sweden.

Year	Site	Coast	Sampling date (YY-MM-DD)	Coordinates	$F^{14}\text{C}$	Average $F^{14}\text{C}$ ($\pm\text{SUM}$)	Ref
2021	Skillinge	East	21-08-12	55.47N, 14.28E	0.991 ± 0.005	0.950	[54]
	Gamla Bjarred	West	21-09-02	55.71N, 13.03E	0.998 ± 0.005		[54]
2022	Skillinge	East	22-08-13	55.47N, 14.28E	0.984 ± 0.005	0.960	[55]
	Gamla Bjarred	West	22-08-11	55.71N, 13.03E	0.936 ± 0.005		[55]
2023	Vikhög	West	23-08-18	55.72N, 12.95E	0.995 ± 0.005	1.000 \pm 0.004	[51]
	Barsebäckshamn	West	23-08-21	55.75N, 12.90E	1.007 ± 0.005		[51]
	Skillinge	East	23-08-22	55.47N, 14.28E	0.990 ± 0.005		[51]
	Sibbarp	West	23-08-24	55.57N, 12.90E	1.008 ± 0.005		[51]
2024	Vikhög	West	24-08-06	55.72N, 12.95E	0.987 ± 0.004	0.995 \pm 0.002	[56]
	Barsebäckshamn	West	24-08-06	55.75N, 12.90E	0.999 ± 0.005		[56]
	Skillinge	East	24-05-19	55.47N, 14.28E	0.997 ± 0.005		[56]
	Åhus Revhaken	East	24-08-14	55.91N, 14.30E	0.995 ± 0.004		[56]
	Sibbarp	West	24-08-07	55.57N, 12.90E	0.999 ± 0.005		[56]

2.3.4. DIC, PIC, DOC, POC and transfer of carbon in the marine environment

As stated above, ^{14}C of natural origin and bomb- ^{14}C enter the marine environment as CO_2 which is absorbed into surface waters as DIC. Apart from DIC, other biogeochemical forms of carbon in the marine waters include inorganic carbon in particulate form (particulate inorganic carbon, PIC), as well as particulate organic carbon (POC) and DOC. Figure 5 illustrates how these carbon forms interact in the marine environment (some organisms which are studied in this report are inserted as symbols).

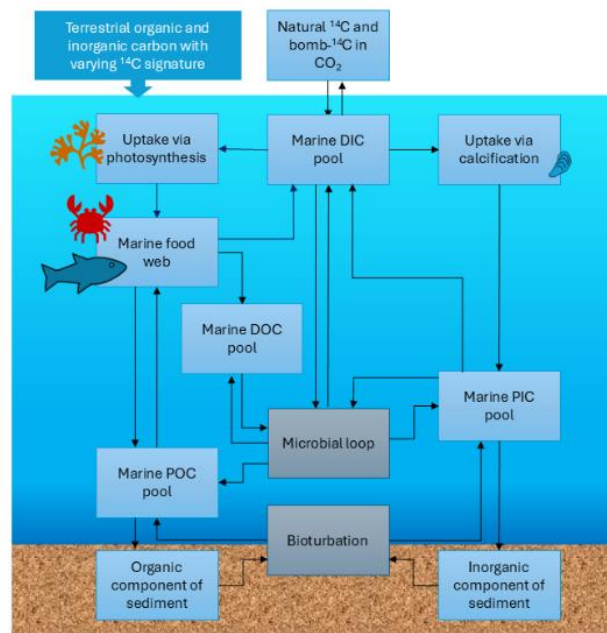


Figure 5 Transfer of ^{14}C from the atmosphere to and in the marine environment. DIC – dissolved inorganic carbon, PIC – particulate inorganic carbon, DOC – dissolved organic carbon, POC – particulate organic carbon. Adapted from [22].

PIC mainly consists of suspended matter from shell material, and hence has its origin in DIC, which is taken up by calcifying organisms during shell formation. The PIC fraction is usually defined as not being able to pass a $0.2\ \mu\text{m}$ filter (whereas DIC does).

POC (typically larger than $0.2\ \mu\text{m}$ in diameter) consists e.g. of phytoplankton, zooplankton, decomposing plankton, detritus from various organisms as well as dead organisms and various aggregates of organic compounds.

DOC comprises organic carbon compounds resulting from decomposition of dead organisms, including animals as well as algae and plants (often defined as $< 0.2\text{--}0.7\ \mu\text{m}$ in diameter). The carbon in marine water bodies may also be of terrestrial origin (allochthonous sources, such as organic materials carried from the terrestrial environment with water runoff, or by rain or dust).

Appendix B contains a brief summary of methods that can be used to extract and measure DIC, DOC, POC and PIC in water samples. In the present study we have analysed particulate carbon ($\text{PC} = \text{PIC} + \text{POC}$) in a few samples.

2.3.5. Concentration factors according to literature

When ^{14}C is homogenously distributed in the environment, the specific-activity approach can be used [1] to assess the ^{14}C -concentration in various organisms. The specific activity approach assumes that the concentration of ^{14}C (expressed in Bq/kg of stable carbon, or as $F^{14}\text{C}$), is the same in organisms as in the surrounding media (air or water). In its most simple form for the marine environment, all carbon pools and organisms have the same specific activity of carbon as in DIC. Isotope fractionation is usually not taken into account (this is a minor and often negligible effect).

A way of expressing the relation between the concentration of a radionuclide in seawater to that in marine biota is by using the concentration factor (CF). In the present report we do not use CFs, but instead compare $F^{14}\text{C}$ values between different compartments and organisms. However, since some reports in the literature refer to CFs for ^{14}C , the concept is introduced here.

The CF is a dimensionless quantity which is defined as [62]:

$$\text{CF} = \frac{\text{Concentration per mass unit of organism } \left(\frac{\text{kg}}{\text{kg}} \text{ or } \frac{\text{Bq}}{\text{kg wet weight}} \right)}{\text{Concentration per mass unit of sea water } \left(\frac{\text{kg}}{\text{kg}} \text{ or } \frac{\text{Bq}}{\text{kg}} \right)}$$

The CF may also be expressed in L/kg [62]:

$$\text{CF} = \frac{\text{Concentration per mass unit of organism } \left(\frac{\text{kg}}{\text{kg}} \text{ or } \frac{\text{Bq}}{\text{kg wet weight}} \right)}{\text{Concentration per mass unit of sea water } \left(\frac{\text{kg}}{\text{L}} \text{ or } \frac{\text{Bq}}{\text{L}} \right)}$$

It is important to note that the term CF itself does not imply that that radionuclide in question is concentrated by direct accumulation from the water. Instead, CF “relates the concentration in the organism, which may have been derived by uptake from sea water, particulate matter and food, to that of the medium in which it lives” [62].

The IAEA technical report IAEA-TR422 [62] provides recommendations on CF values for marine biota and for different elements. In the IAEA-TR422 report, dry or freeze-dried weights are converted to wet weight activity concentrations by multiplying by 0.18. The IAEA-TR422 report also states that for carbon it was decided to use only the organic carbon concentration in sea water in the denominator in the CF equations, and not the total carbon concentration consisting of dissolved organic carbon, carbonate, bicarbonate and CO_2 . A generic value of $7.2 \cdot 10^{-6} \text{ kg/kg}$ was used as the organic carbon in sea water, based on measurements from the Mediterranean Sea [62]. Furthermore, IAEA-TR422 use the following wet weight tissue values for carbon: 95 g/kg for fish, 80 g/kg for crustaceans and molluscs, 65 g/kg for benthic algae, 80 g/kg for zoo plankton and 45 g/kg for phytoplankton [62]. Recommended CFs are presented in Table 4, and are based on the specific activity approach.

Table 4 Generic concentration factors for carbon according to [62].

Species	Recommended value IAEA-TR422
Fish	$2 \cdot 10^4$
Crustaceans	$2 \cdot 10^4$
Molluscs	$2 \cdot 10^4$
Zooplankton	$2 \cdot 10^4$
Phytoplankton	$9 \cdot 10^3$
Macroalgae	$1 \cdot 10^4$

It should be noted that the CFs in Table 4 are generic, and their applicability to Swedish coastal waters may be limited due to different concentrations of organic carbon in the Swedish seawater compared to the Mediterranean Sea.

For various organic carbon substances of anthropogenic origin, the CFs have different values, and direct absorption from water to fish can occur via the gills (see e.g. [63] where common carp, *Cyprinus carpio*, exposed to ^{14}C -labelled arginine in water under laboratory conditions, absorbs the organic compound directly from the water and incorporates a fraction into its tissue).

2.4. Previous studies of the radioecology of ^{14}C in aquatic and marine environments

In this section we give examples of the findings of previous studies on the radioecology of ^{14}C in the aquatic and marine environment. The summary is not covering all available data in the literature, but a selection that can be useful to understand the radioecology of ^{14}C at Ringhals NPP. Our own previous studies are presented in Chapter 5.

2.4.1. Lakes and rivers

A comprehensive report on models for transport of ^{14}C in terrestrial and aquatic environments has been produced within the BIOPROTA project² dedicated to aspects of assessments of long-term impact of radioactive releases from nuclear waste management [64]. The BIOPROTA project has also published a review of carbon uptake in fish [65]. An important experimental study is a Canadian project where a lake was spiked in 1978 with inorganic ^{14}C and the fate of ^{14}C was followed for a 10-year period. Most of the specific activities in various matrices were as expected based on food-chain transfers [66]. Large lake trout was however an exception with unexpectedly high specific activities later than expected. The interpretation was that the fish were in a rapid growth phase at the time of the ^{14}C -spiking and that the muscle tissue of the fish had a very slow turnover rate [66].

Several French studies have regarded NPP-derived ^{14}C in rivers. In a recent paper, Bodereau et al [67] describe a one-year study of the Rhône River, hosting several NPPs, and two of its tributaries. $\Delta^{14}\text{C}$ (see Appendix A for definition)

² <https://www.bioprota.org/>

medians of POC, DOC and DIC were 142, 130 and 42 ‰ (corresponding to $F^{14}\text{C}$ values of 1.15, 1.14 and 1.05). Maximum values observed were ~1400, ~2000 and ~1400 ‰ (corresponding to $F^{14}\text{C}$ values of 2.4, 3.0 and 2.4). Bodereau et al [67] state “there is no information about the proper riverine cycling of artificial ^{14}C and its fate is hard to predict as the riverine carbon cycle exhibits various biogeochemical transfer mechanisms between the three forms of carbon (POC, DOC and DIC), as well as complex mixing with natural carbon sources carrying varying ^{14}C ”. Higher $\Delta^{14}\text{C}$ values were generally found in POC than in DIC, which Bodereau et al [67] attribute to introduction of atmospheric CO_2 or contribution from ^{14}C -depleted carbonates from the bedrock. Other French studies of ^{14}C in rivers with NPPs are e.g. [68-70].

Other examples of studies of the aquatic environment close to a NPP are from Ignalina NPP in Lithuania (e.g. [71, 72]). In the early operational period (1984-1999) ^{14}C in DIC agreed well with the specific activity in fish scales, in accordance with the short transfer from DIC → aquatic primary producers → zooplankton → fish. Later in the operational period, differences were seen between DIC and fish scales, with higher ^{14}C concentrations in fish scales than in DIC. This was interpreted as discharges of water-soluble organic compounds from Ignalina NPP (sediment analyses also support this explanation) [72]. It is also stated in [71] that “Previous research showed that low molecular weight (<3.5 Da) xenobiotics and their metabolites can be easily taken up and accumulated by freshwater plants and organisms...”.

2.4.2. Marine environment

Several studies relate to liquid discharges from reprocessing plants for spent nuclear fuel in the UK and France and it is generally accepted that ^{14}C is mostly in the form of DIC [21, 23, 34]. The resulting ^{14}C activity concentrations in various organisms in the marine environment has been examined e.g. in [21-23, 29-32, 34, 73-75]). Close to the reprocessing plant in Sellafield, Begg et al [21] showed that higher ^{14}C activity concentrations were found in mussels (*Mytilus edulis*, ~7×contemporary ambient level) than in wrinkles (*Littorina littorea*, 5×contemporary ambient level) than in seaweed (*Fucus* spp., ~3.5×contemporary ambient level). The differences between organisms were believed to be attributed to differences in feeding behaviour. Shells of mussels showed lower ^{14}C concentrations than the corresponding organic matter. Begg et al [21] state that “The lower activity in the inorganic matter may reflect the fact that the shell carbon accumulates throughout the entire lifespan of the organism, whereas the organic tissue is subject to turnover at a rate that is organism-specific”. Later studies have confirmed species-specific ^{14}C activity concentrations at sites contaminated by e.g. Sellafield liquid discharges [22]. Species-specific feeding behaviour and turnover rates within the organism are believed to cause the differences [22].

A few newer publications have used LSC to determine ^{14}C in marine organisms collected close to various NPPs [76-78]. However, we find quality of the results difficult to assess, and these papers are therefore not discussed further.

3. Ringhals NPP – reactors and available ^{14}C release data

3.1. Reactors

Ringhals NPP (57.26N, 12.11E, Kattegat) on the Swedish west coast currently has two PWRs in operation (R3, Westinghouse, 1070 MW_e, in operation since 1981; and R4, Westinghouse, 1120 MW_e, in operation since 1983). An additional PWR (R2, Westinghouse, 900 MW_e), was in operation from 1975 to the end of 2019. The first reactor constructed at the Ringhals site (R1, 881 MW_e), a BWR from ASEA-Atom, became operational in 1976 and was closed in end of 2020.

3.2. Airborne ^{14}C releases

Figure 6 shows the airborne release rates reported for each of the Ringhals reactors since the ^{14}C measurements started in 2002 [79], including annual electrical energy production since the start of operation. As expected from BWRs, the inorganic form (CO₂, 97%) dominates the airborne ^{14}C releases from R1. There is a clear correlation between released ^{14}C and electricity production, as also seen in previous studies of Swedish BWRs [80]. The same is not valid for PWRs R2, R3 and R4, since PWRs are equipped gas-decay tanks, which delay the release until venting the tanks. Previous studies have shown that the release rate can be highest during power outage due to increased venting during maintenance [80]. For the PWRs R1, R2 and R3, the inorganic form is on average 15%, 7% and 15% respectively.

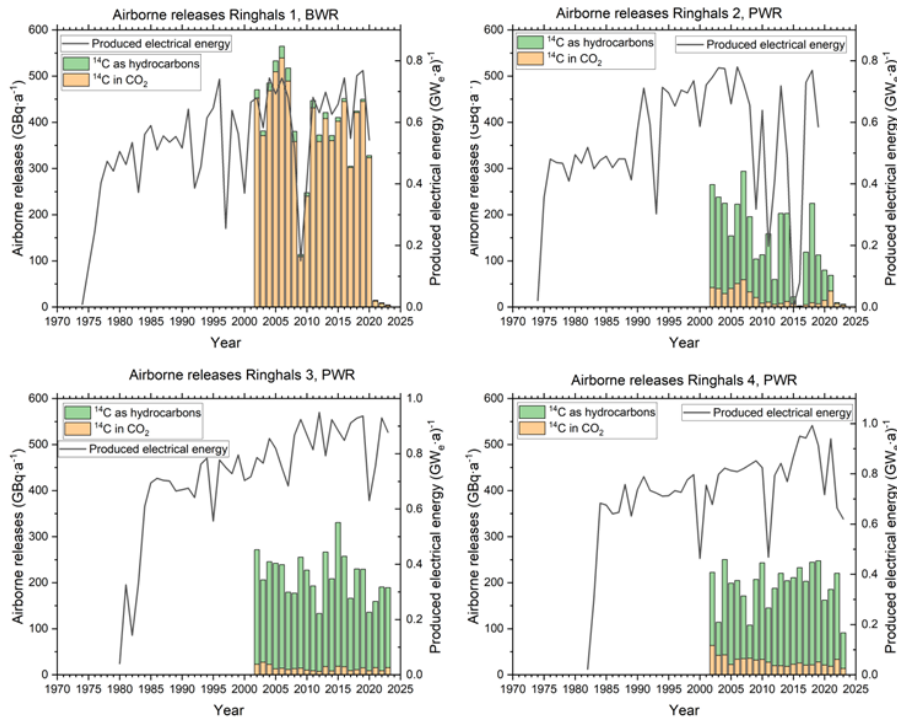


Figure 6 Airborne releases in various chemical forms (organic hydrocarbons and inorganic CO₂) from Ringhals NPP [79] and annual electrical energy production according to the IAEA PRIS database. Measurements of ¹⁴C started in 2002. Note the different scales on the right axes.

The normalized ¹⁴C release rates calculated from the data in Figure 6 is presented in Table 5. Compared to the data from the RADD data base for 1995-2015, presented in Table 1, the oldest Ringhals reactor (the BWR R1) has among the higher values (38% above the median), while the oldest PWR R2 is 25% above the median. R3 and R4 are close to the median for European PWRs (Table 1).

Table 5 Normalised annual airborne ¹⁴C releases from Ringhals NPP during the period 2002-2023.

Reactor	Normalized ¹⁴ C release rate as CO ₂ (inorganic) (GBq/(GW _e ·a))	Normalized ¹⁴ C release rate as hydrocarbons (organic) (GBq/(GW _e ·a))	Normalized total ¹⁴ C release rate (GBq/(GW _e ·a))
R1, BWR	0.63·10 ³	0.02·10 ³	0.65·10 ³
R2, PWR	45	0.26·10 ³	0.31·10 ³
R3, PWR	17	0.24·10 ³	0.26·10 ³
R4, PWR	35	0.20·10 ³	0.24·10 ³

It is of interest, e.g. for dose assessments, to view the airborne ¹⁴C releases for Ringhals NPP as a whole, including all 4 reactors. In Figure 7, showing the summed annual release data and electricity production data, the effect of closing R1 and R2 in the end of 2019 and 2020 is clearly seen, both regarding total ¹⁴C releases and chemical form.

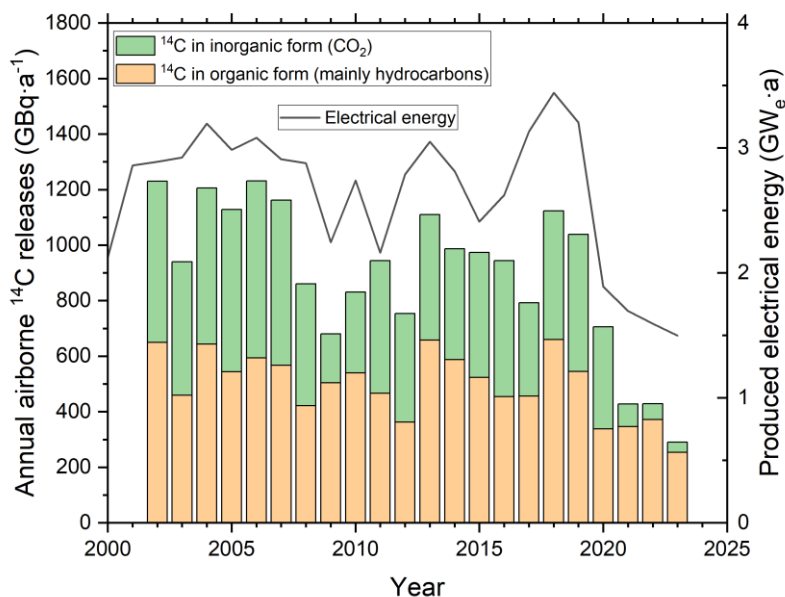


Figure 7 Airborne releases in various chemical forms (organic hydrocarbons and inorganic CO₂) for 2000-2023 from all 4 reactors at Ringhals NPP [79] and total annual electrical energy production according to the IAEA PRIS database.

3.3. Water-borne discharge rates of ¹⁴C

The liquid ¹⁴C waste consists of water that has leaked from the reactor coolant, and from used process water. The leaked and used water is in stored waste storage tanks prior to discharge. Radiometric analysis of key radionuclides is performed to ensure that the activity concentration is below defined maximum values prior to emptying the tanks into the cooling water channels. In a report from 1990, Notter describes that 50-100 tanks are emptied per month during normal operation, and that emptying one tank takes at least 2 hours [81]. The emptying frequency is not rarely doubled during outage [81].

In a former project financed by SSI (the predecessor to SSM), water samples from the wastewater tanks from the PWRs R4 and R3 in 2005 and 2006 (and one water sample from the BWR Barsebäck 2, B2, operating under HWC) were analysed to roughly quantify the waterborne ¹⁴C effluents (Table 6) [82]. The results indicated that the Barsebäck BWR discharges (note: only one sample) were significantly lower than the Ringhals PWRs discharges. The five samples from R3 and R4 show highly variable ¹⁴C concentrations, from <29 Bq/kg to over 1 kBq/kg. The organic fractions of the wastewater at the Ringhals PWRs were also highly variable, from 19% to 90% in the four samples with measurable ¹⁴C activities (one sample was below the detection limit). However, the report [82] states that: “However, the organic fraction of the samples measured should be treated with caution. Organic compounds may be converted into inorganic compounds and vice versa in both wastewater tanks and sampling bottles by e.g. microbial activity.”

In another paper, large variations were observed in concentration as well as distribution of ¹⁴C species in the reactor cooling water of the R4 reactor during

the fuel cycle [7]. Reactor cooling water collected before the reactor water clean-up system (RWCU) had ~60% volatile organic compounds (such as methane), and ~40% non-volatile organic compounds, presumably acetate and formate [7]. These chemical forms may thus also be expected in the wastewater. If discharged into the marine environment, these non-volatile organic compounds containing ^{14}C will behave differently in the ecosystem than inorganic carbon (DIC, which will behave as natural or bomb- ^{14}C).

Table 6 ^{14}C activity in wastewater tanks at the BWR Barsebäck (B2), and the two PWRs at the Ringhals nuclear power plant (R3 and R4). From [82].

Reactor type	Reactor	Sampling period	^{14}C activity concentration (Bq/kg)	Organic fraction (%)
BWR-HWC	B2	March - May 2005	5.9	76
PWR	R4	June 2005	$0.19 \cdot 10^3$	29
	R3	March 2006	$1.2 \cdot 10^3$	19
	R4	March 2006	<29	
	R4	April 2006	$0.43 \cdot 10^3$	90
	R4	June 2006	$0.84 \cdot 10^3$	34

In the previous SSI study from 2005-2006 [82], liquid discharge rates from R3 and R4 were estimated using the data in Table 6, assuming these data to be representative over a year. A value of $1.2\text{--}2.1 \text{ GBq}\cdot\text{a}^{-1}$ was obtained for a single PWR, corresponding to 0.5–1 % of the measured gaseous ^{14}C releases [82]. This is similar to the value reported by the IAEA ($1.3 \text{ GBq/GW}_e\cdot\text{a}$) [6].

A mass balance assessment, performed in a study by Magnusson et al in a publication from 2008 [7], estimated the ^{14}C liquid ^{14}C discharges to be less than 0.5% of the production in the coolant (0.3% for PWRs and 0.04% for BWRs). However, the latter value was deemed as highly uncertain. Estimations made by Ringhals AB of the ^{14}C liquid discharges from Ringhals NPP in 2022 and 2023 are shown in Table 7 [4, 5].

Table 7 Calculated ^{14}C liquid discharges from Ringhals NPP 2022 and 2023 [4, 5].

	^{14}C activity discharged to water, 2022 (Bq)	^{14}C activity discharged to water, 2023 (Bq)
R1 (BWR), not in operation	$3.0 \cdot 10^6$	$1.5 \cdot 10^6$
R2 (PWR), not in operation	$0.21 \cdot 10^9$	$0.13 \cdot 10^9$
R3 (PWR), operational	$5.1 \cdot 10^9$	$4.8 \cdot 10^9$
R4 (PWR), operational	$3.7 \cdot 10^9$	$1.5 \cdot 10^9$
Total	$9 \cdot 10^9$	$8 \cdot 10^9$

4. Materials and methods

4.1. Sampling sites for investigations of spatial and temporal variations in ^{14}C of the Swedish west coast

The sampling sites of relevance for the present studies of ^{14}C mainly in DIC in the waters of the Swedish west coast (Skagerrak and Kattegat) are outlined in Figure 8 (see also Table C1 in Appendix C). The Skagerrak strait is the part of the Atlantic that is located between southeastern Norway, the north of the Danish Jutland peninsula and the Swedish west coast. It connects the North Sea to the Kattegat sea and has an average depth of 218 m, with a maximum depth of >700 m (the Norwegian trench). Kattegat is a relatively shallow strait, with an average depth of only 23 m (maximum depth ~130 m).

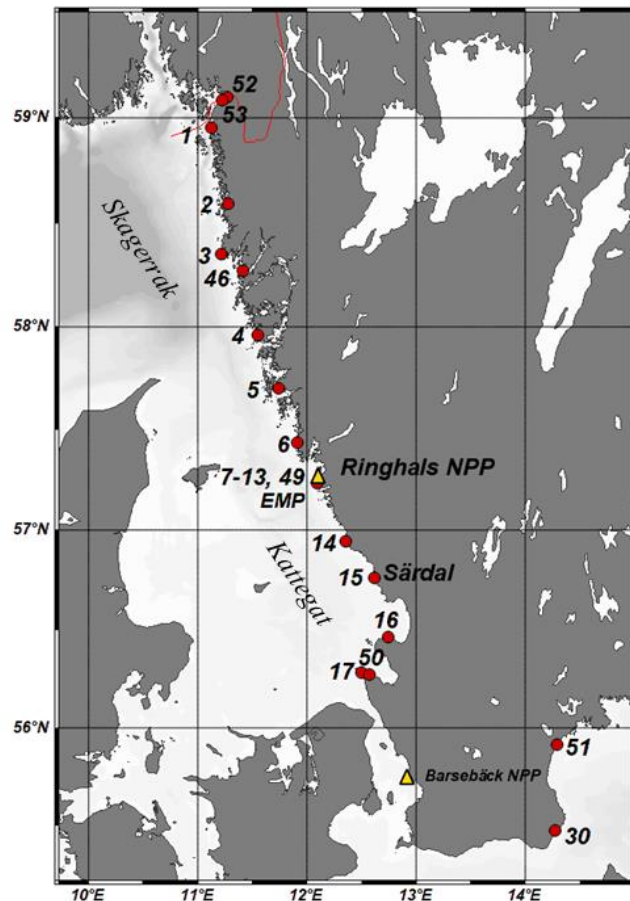


Figure 8 Map indicating the sampling sites. EMP: Sites at Ringhals environmental monitoring programme. Maps: Schlitzer, Reiner, Ocean Data View, <https://odv.awi.de>, 2024.

As seen in Figure 9, bottom water of high salinity from the North Sea enters the Skagerrak and then Kattegat, while surface water of low salinity from the Baltic

Sea most frequently flows towards the north. This results in a significant salinity gradient along the Swedish west coast, increasing towards the north (see e.g. measured salinities in [8]). The high-salinity water from the North Sea may carry radionuclides discharged from the reprocessing plants for spent nuclear fuel in La Hague (France) and Sellafield (UK), as has been demonstrated in previous studies e.g. for ^{14}C (see chapter 5).

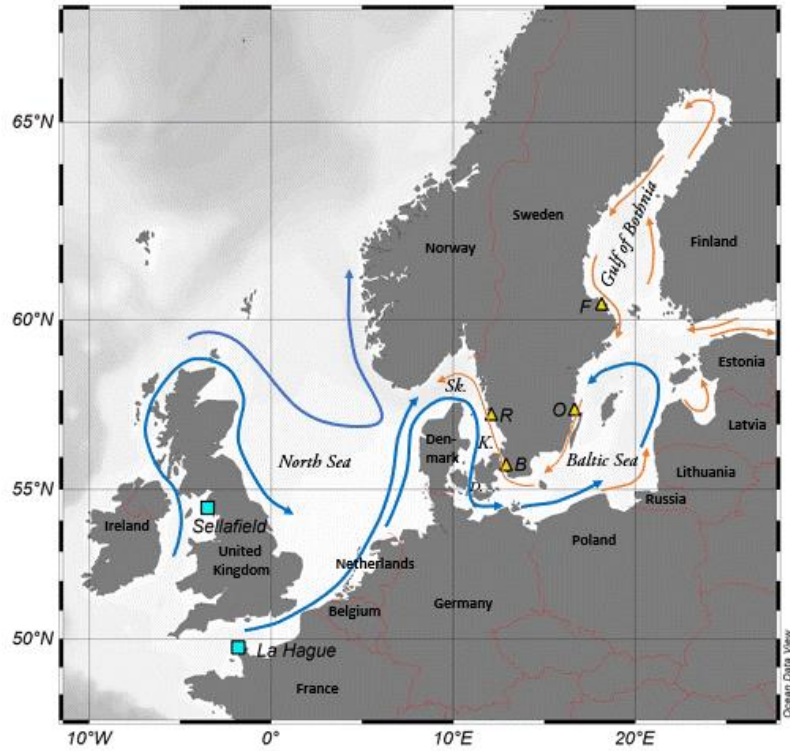


Figure 9 Ocean currents (surface water movement in orange and bottom water movement in blue) (adapted from [83, 84]) of relevance for transport of liquid discharges from Sellafield (UK) and La Hague (France) to Swedish coastal waters. *R*: Ringhals NPP, *B*: Barsebäck NPP, *O*: Oskarshamn NPP, *F*: Forsmark NPP., *Sk.* - Skagerrak, *K.* - Kattegat, *D.* - Danish Straits. Barsebäck NPP is located at the Öresund Strait (not marked in the figure). Maps: Schlitzer, Reiner, Ocean Data View, <https://odv.awi.de>, 2021.

The sampling sites used mainly for studies on spatial and temporal variations in Swedish coastal waters [9] are presented in Table 8 (samples collected by staff at Lund University). Types of samples collected at the various sites are also listed in Table 8. Sites 52 (Svinesund) and 53 (Saltbacken) at Ringdalsfjorden by the Norwegian border were used to investigate potential ^{14}C signals from the Halden reactor in Norway, which is located about 10 km further into the fjord from Saltbacken and about 10 km from Svinesund [11]. The two sites in the Baltic Sea (30 Skillinge and 51 Åhus Revhaken) are used as reference sites.

Table 8 Sampling sites for studies of spatial and temporal variations in ^{14}C on the Swedish west coast (sampling between 2020 and 2024). The two sites in the Baltic Sea are used as reference sites. PC – Particulate carbon. *IRMS analysis of C and N.

Sea	Site	Site name	Latitude	Longitude	Sample types
Skagerrak	52	Svinesund	59.10N	11.27E	<i>Fucus</i> spp.
	53	Saltbacken	59.08N	11.22E	<i>Fucus</i> spp.
	1	Båtevik, Strömstad	58.95N	11.13E	<i>Fucus</i> spp. *, <i>Mytilus edulis</i> * (shells and soft tissue), <i>Poaceae</i> sp., Sediment*
	2	Fjällbacka, Sälvik	58.59N	11.28E	<i>Fucus</i> spp.
	3	Smögen, Kleven	58.35N	11.22E	<i>Fucus</i> spp.
	46	Lysekil	58.27N	11.42E	<i>Fucus</i> spp., <i>Poaceae</i> sp., Sediment*, PC
	4	Stockevik, Tjörn	57.96N	11.55E	<i>Fucus</i> spp., Sediment*
	5	Hällsvik	57.70N	11.74E	<i>Fucus</i> spp.
	6	Smarholmens badplats	57.43N	11.92E	<i>Fucus</i> spp.
	49	Åsa	57.35N	12.12E	<i>Fucus</i> spp., <i>Poaceae</i> sp.,
Kattegat	7	Frillesås	57.31N	12.15E	<i>Fucus</i> spp. <i>Mytilus edulis</i>
	8	Sallebacka	57.28N	12.14E	<i>Fucus</i> spp. <i>Mytilus edulis</i>
	9	Ringhals Gloppe	57.27N	12.11E	<i>Fucus</i> spp., <i>Poaceae</i> sp., Sediment*
	10	Videbergshamn	57.25N	12.11E	<i>Fucus</i> spp., <i>Poaceae</i> sp., Sediment*, PC
	11	Bua lighthouse	57.24N	12.10E	<i>Fucus</i> spp. *, <i>Mytilus edulis</i> *, <i>Poaceae</i> sp., Sediment*
	11B	Bua pier	57.24N	12.10E	<i>Fucus</i> spp., <i>Mytilus edulis</i> ,
	11C	Bua strand	57.23N	12.11E	<i>Fucus</i> spp., <i>Poaceae</i> sp.,
	12	Skeatången, Årnäshalvön	57.20N	12.17E	<i>Fucus</i> spp.
	13	Getterön	57.12N	12.21E	<i>Fucus</i> spp.
	14	Glommen	56.94N	12.36E	<i>Fucus</i> spp.
	15	Särdal	56.76N	12.63E	<i>Fucus</i> spp. <i>Mytilus edulis</i> (shells and soft tissue)
	16	Kattvik	56.46N	12.75E	<i>Fucus</i> spp.
	17	Mölle	56.28N	12.50E	<i>Fucus</i> spp.
	50	Arild	56.27N	12.58E	<i>Fucus</i> spp., <i>Poaceae</i> sp., Sediment*
	30	Skillinge	55.47N	14.28E	<i>Fucus</i> spp., <i>Poaceae</i> sp., PC
	51	Åhus Revhaken	55.91E	14.30E	<i>Fucus</i> spp., Sediment*
Baltic Sea					

We use *Fucus* spp. as an indicator of DIC in seawater, as *Fucus* spp. photosynthesise from DIC. *Fucus* spp. may also absorb CO_2 directly from the atmosphere if exposed to air [28]. In [10] we use *Fucus* spp. collected at Särdal (site 15 in Figure 8) to reveal temporal variations in ^{14}C (and ^3H , ^{60}Co , ^{99}Tc , ^{129}I , ^{131}I , ^{137}Cs , ^{134}Cs , ^{236}U , ^{238}U , ^{239}Pu , and ^{240}Pu) since 1967. The characteristics of the Särdal site, used in [9-11], is described in detail in [10].

In [9], we use *Fucus* spp. to study temporal (2020-2024) variations in ^{14}C -DIC at different sites at the west coast (mainly sites 1. Båtevik, 3. Smögen, 46. Lysekil, 4. Stockeviken and 17. Mölle/50. Arild; see Figure 8) and at two reference sites in the Baltic Sea (sites 30. Skillinge and 51. Åhus; see Figure 8). Several sites were included close to Ringhals NPP (sites 49. Åsa, 7. Frillesås, 8. Sallesbacka, 9. Ringhals Gloppe, 10. Videbergshamn, 11. Bua, 11B. Bua pier, 11C. Bua strand; see map in Figure 10). For reference, we also present data on F^{14}C in grass collected at some of these sites at the Swedish west coast and at the Baltic Sea.

In [11], we analyse ^{14}C in soft tissue and in annual band structures in shells of *Mytilus edulis* collected at sites 1. Båtevik, 15. Särda and at Bua (close to site 11 in Figure 8). The purpose of the study presented in [11] was to investigate if shells of *Mytilus edulis* could be used to retrospectively determine ^{14}C in DIC at Ringhals NPP. The study also generated results on the temporal and spatial variability of ^{14}C at the two sites far from Ringhals NPP (1. Båtevik and 15. Särda). The potential use of blue mussel shells for retrospective assessment of ^{14}C in DIC in seawater is based on that mussels incorporate DIC from seawater into their shells as they grow [22]. Metabolic carbon may also be incorporated into the shell only as a minor fraction [85]. The shell is composed of several layers with different mechanisms for incorporating carbon. The layer that forms visible structures (annual bands) in the shells is called the fibrous layer, and this is suitable for extracting material representative of DIC over the growth period of the shell. Being a filter feeder, F^{14}C in the mussel soft tissue should represent F^{14}C in the dietary carbon of the mussel. Blue mussels are semi-sessile, meaning that they usually are stationary at a specific location, but may occasionally move voluntarily or involuntarily. This fact may limit their use as bioindicators for long-term studies. However, due to lack of other suitable carbon archives in the marine environment of Ringhals NPP (sediment accumulation bottoms are not available in the close vicinity of the discharge point), mussel shells may constitute a valuable resource of information of past ^{14}C discharges.

Seven sites were used for collection of sediments, and water samples for extraction and ^{14}C analysis of particulate carbon (PC) was collected at three sites (Table 8).

4.2. The Ringhals site

4.2.1. Sampling sites

Figure 10 shows the Ringhals area and the sites used in the radioecological marine one-year study (see also Table C2 in Appendix C). The sites labelled “SLU” are identical to the sites in the regular environmental monitoring programme at Ringhals NPP (except site SLU5b.1) [86], and these samples have been collected by staff from the Swedish Agricultural University (SLU). The other sampling sites (49, 7-12) refer to the sites listed in Table 8 (sampling performed by staff from Lund University). Details for the SLU samples, including e.g. sample types and sampling occasions, are listed in Table 9.

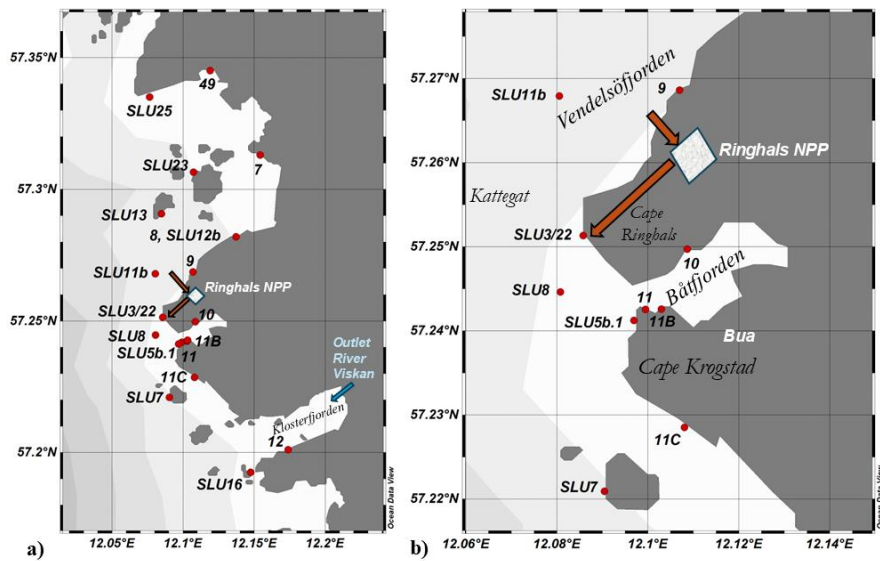


Figure 10 a) Sampling sites in the Ringhals area. Sampling sites denoted SLU are sites included in the environmental monitoring programme of Ringhals NPP. The arrows at Ringhals NPP indicate the location of the cooling water inlet and outlet. The discharge is directed to the south. b) Enlargement of the area close to the NPP. SLU5b is close to site 11B. Maps: Schlitzer, Reiner, Ocean Data View, <https://odv.awi.de>, 2025.

Table 9 Sampling sites, sample types and sampling months for the one-year radioecological study of ^{14}C in the marine environment at Ringhals NPP. The sampling sites are the same as in the environmental monitoring programme at Ringhals NPP. *FV* – *Fucus vesiculosus* (bladderwrack); *SM* – *Symphodus melops* (corkwing wrasse); *CP* – *Cancer pagurus* (crab); *ME* – *Mytilus edulis* (blue mussel); *MG* – *Magallana gigas* (Pacific oyster); *Sed* – Sediment; *Bio* – Biofouling plates. * Sample subjected to IRMS-analysis.

Site	Name	Latitude	Longitude	Sample type, month sampled						
				YY-MM						
				<i>FV</i>	<i>SM</i>	<i>CP</i>	<i>ME</i>	<i>MG</i>	<i>Sed</i>	<i>Bio</i>
SLU3/ SLU22	Outlet	57.253N	12.088E	23-05	23-04*		23-09*	23-05*	23-07*	23-12
				23-09	23-08*			23-10	23-12	
				23-12	23-12		23-12	23-12		
				24-02			24-02	24-02		24-01 24-03
SLU5b	Bua beacon	57.242N	12.108E	23-04			23-05			
				23-10			23-10			
				23-12						
				24-02						
SLU5b.1		57.241N	12.097E				23-12			
							24-02			
SLU7	Norra Horta	57.223N	12.097E		23-04		23-05*			
				23-09	23-07		23-10*			
				23-12			23-12			
				24-02			24-02			
SLU7.66		57.225N	12.095E	23-05						
SLU8	Gyltan	57.246N	12.062E	23-05		23-04*				
				23-09		23-09				
				23-12		23-12				
				24-02		24-02				
SLU11b	Södra Ledsjär	57.268N	12.081						23-07*	24-01
SLU12b	Stavder	57.282N	12.137E	23-04						
				23-10						
				23-12						
SLU13	Ustö	57.291N	12.083E	23-05			23-09			
				23-09						
SLU13.2		57.290N	12.082E	23-12			23-12			
SLU16	Knarrskär	57.192N	12.088E	23-05						
				23-10						
				23-12						
				24-02						
SLU23	Vendelsö	57.31N	12.11E		23-05					
					23-08					
					23-12	23-12				
SLU25	Näsbykrok	57.335N	12.077E	23-04						
				23-10						
				24-01						
				24-02						

The selected organisms are also used in the regular environmental monitoring programme of Ringhals NPP [86], which is based on SSMFS 2021:6 [87]. In the present study we use the following sample types and organisms:

Algae

In the one-year study of ^{14}C in the marine environment of Ringhals NPP we exclusively used *Fucus vesiculosus* (bladderwrack). The lifespan of *F. vesiculosus* is at least 3 years [88], and sheltered individuals may survive up to 5 years [89] or more [90]. *Fucus vesiculosus* is permanently attached to rocks or stones. *F. vesiculosus* absorbs DIC through photosynthesis [91], from water if submerged, but can also take up CO_2 directly from the atmosphere if exposed to air [28]. Ref [31] estimates that it takes ~2.5 years to return *F. vesiculosus* to ambient ^{14}C levels after withdrawal of anthropogenic ^{14}C discharges to seawater.

Molluscs

Mytilus edulis (blue mussel) is mainly used as a representative for molluscs, but some samples of *Magallana gigas* (Pacific oyster) have also been analysed. As described above (section 4.1), *M. edulis* is a semi-sessile filter-feeder, incorporates mainly DIC into its shell (a small fraction of dietary carbon may also be transferred to the shell), and its soft tissue is built up of dietary carbon. *Mytilus edulis* may live 10-20 years [92], but old individuals are rare. *Mytilus edulis* effectively filters particles (mainly phytoplankton) between 2-200 µm [91], but can also feed on dead particulate organic material and zooplankton larger than 200 µm [93]. As other bivalve filter-feeders, *M. edulis* has mechanisms for selection of particles for ingestion [94]. The filtering capacity is a few L/h [95]. The turnover of carbon in soft tissue has been estimated e.g. by [96] to be ~0.4 day⁻¹ (corresponding to a biological half-life of about 2 days). *Magallana gigas* (Pacific oyster) is a sessile invasive filter-feeder, that first appeared in the waters of the Swedish west coast in 2006 [97]. It can become more than two decades old [98] and filtration rates may be up to 12 L/h [94]. Since different species of bivalve filter feeders may differ in selection of particles to ingest and in absorption efficiencies [94], *M. gigas* may not have identical diet to *M. edulis* [99].

Arthropods

Cancer pagurus (crab) is used as a representative species of arthropods. *Cancer pagurus* may obtain ages of several decades [91]. The males are non-migratory, whereas females are. Hence only males are used in the study. *Cancer pagurus* is a predator feeding on various animals in the benthic environment, such as molluscs (including *M. edulis*) and crustaceans.

Fish

Symphodus melops (corkwing wrasse) is a non-migratory fish residing near the seafloor [91]. It is an omnivorous opportunist, feeding e.g. on molluscs (including *M. edulis*), crustaceans, echinoderms (e.g. starfish), polychaetes (marine annelid worms), oligochaetes (types of soft-bodied marine worms) and insects [100]. The life-span of *S. melops* is up to 8-9 years [91].

Sediments

The sites for sediment samples are the same as in Ringhals environmental monitoring programme [86]. The upper 2 cm of the sediment is sampled.

Biofouling plates

In Ringhals environmental monitoring programme [86] two biofouling plates made of Plexiglass with a surface of 1 m² are located close to the outlet of the cooling water. The plates are located in the eutrophic zone to allow photosynthetic growth of e.g. diatoms and filamentous green algae [86].

Particulate carbon

Particulate matter in seawater is not part of the regular Ringhals NPP environmental monitoring programme, but was collected to obtain additional radioecological information.

4.2.2. Characteristics of the Ringhals area

The Ringhals area (Figure 10) is characterized by open sea with only a few islands. The water outside the NPP is mainly deep (>10 m). The fjord Båtfjorden located just south of the NPP is however shallow and protected from open sea. A channel of ~4 m depth runs in Båtfjorden from open sea to the fishing harbours of Videbergshamn (at site 10) and Bua (see Figure 10). Shallower areas can be found around the island Norra Horta (site SLU7 in Figure 10), around the islands north of the NPP (the Vendel islands, site SLU23) and at the coasts north of the NPP. A few 100 m west of Ringhals NPP the depth is ~10 m, which increases to ~50 m before reaching the shallow waters of Fladen (a popular fishing area located ~17 km west of Ringhals NPP).

The seawater in Kattegat off Ringhals NPP is characterized by stable salinity stratification [101], and two types of water with different salinity between the surface and the bottom are usually present (higher salinity at the bottom) [101]. The salinity typically ranges between 20 and 35‰ [102]. The upper water layer is brackish water originating from the Baltic Sea, carried by the Baltic current, and this layer is characterized by a large mixing, while the lower water layer enters from Skagerrak (see Figure 9). The halocline (salinity leap layer) in Kattegat is often located at depths of 8-25 m with an average of about 15 m [101]. The salinity leap layers of Kattegat are outlined in Figure 11. The surface water of Kattegat is up to ~22 °C in summertime and can reach below 0 °C toward the end of winter and early spring [102].

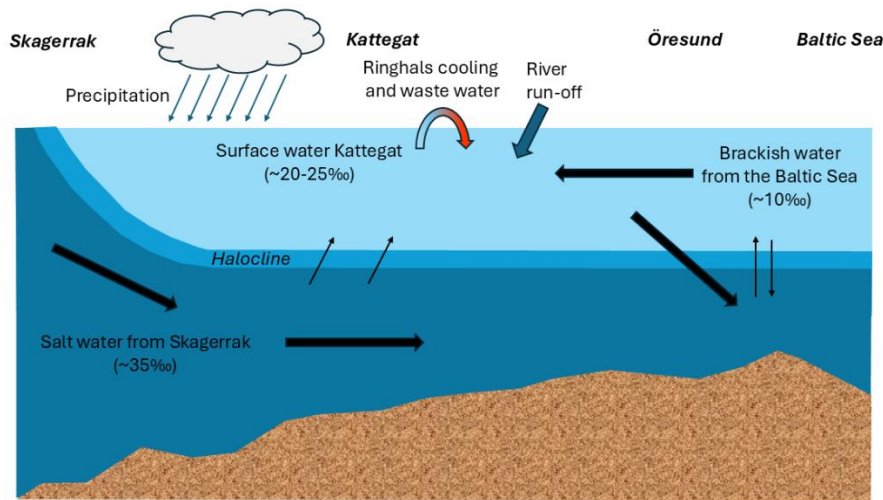


Figure 11 Salinity leap layers on the Swedish west coast. The arrows represent water movement. Inspired by [101].

The river Viskan, which enters Kattegat south of Ringhals in Klosterfjorden (see Figure 10), also affects the salinity of the upper water, and the dispersion from Viskan into Kattegat varies depending on winds and surface ocean currents. The runoff area of Viskan is ~2200 km², with an average water flow of ~35 m³/s [101]. The surface bedrock in the Viskan catchment area is not carbonate-rich (as it is e.g. in southernmost Sweden, see e.g. Loughheed et al [61]). Viskan, and other watercourses in the Ringhals area, are therefore not expected to bring significant amounts of ¹⁴C-depleted DIC into Kattegat (see section 2.3.3).

The water currents outside Ringhals NPP are mainly parallel to the coast, and the surface water mainly travels towards the north. However, the surface water

off Ringhals NPP may change direction on a frequent basis (often more than one change per day between northern and southern currents), giving rise to whirlpools north of the Cape Ringhals [103]. Maximum flow rates are typically ~0.75 m/s in the upper layers and ~0.5 m/s in the lower layers, but the average flow rates are ~0.2-0.3 m/s [102].

As Ringhals NPP is located at open sea, accumulation of bottom sediments is rare in the close vicinity of the NPP, and the seafloor is mainly stony [81]. At greater depths, bottom sediments can be found (see e.g. [81]).

In a previous SSM project, Engdahl [42] performed sampling in the marine environment at Ringhals NPP between August 2018 and July 2019. Seawater and various marine organisms (e.g. *Fucus* spp.) were collected in a reference area (in fjord Klosterfjorden) and in a target area (in Båtfjorden) (see location of the fjords in Figure 10). Parameters such as water transparency, turbidity, salinity, fluorescence, temperature, oxygen content, and carbon content were analysed. The latter, in terms of total organic carbon (TOC), POC, DOC and bicarbonate (DIC), are of particular interest for the current study. DIC (HCO_3) in monthly collected samples of seawater off Ringhals NPP was on average 90 mg/L (23-110 mg/L) in Klosterfjorden and 99 mg/L (70-110 mg/L) in Båtfjorden. DOC was significantly less: Klosterfjorden had on average 4.1 mg/L (2.8-8.3 mg/L) and Båtfjorden 3.5 mg/L (2.4-5.7 mg/L). POC was on average 0.21 and 0.18 mg/mL for Klosterfjorden and Båtfjorden, respectively [42].

The Ringhals area is characterised by a great diversity of species, including plankton. Jellyfish, as well as eggs and larvae of benthic animals and fish (e.g. cod, herring and flatfish), occur frequently in summer. Belts of brown, green and red algae provide habitats for e.g. crustaceans and marine gastropods. Blue mussels, barnacles and crabs are abundant. Greater depths also host snake stars, as well as bristleworms and sea urchins [102].

4.2.3. Dispersion of Ringhals NPP cooling water

The locations of the inlets and outlets of cooling water to Ringhals NPP are indicated in Figure 10. The inlet constitutes two channels in the fjord Vendelsöfjorden. The outlet water carries small amounts of radioactive waste, including ^{14}C , from the reactor coolant water purification and treatment systems. The outlet water is led through two km-long tunnels entering the ocean at 5-6 m beneath the water surface [103]. The heated cooling water is discharged in the southerly direction towards the fjord Båtfjorden [102] (see Figure 10). The discharge volume rate about 40 m³/s per reactor, with a discharge speed a few m/s [103]. In 2022, the total cooling water flow rate was on average 71 m³/s (89 m³/s in January-May and in July-August, and 50.5 m³/s during outage) [104]. The water temperature in the outlet area was in 2022 about 6 °C higher than at Vendelsö (the island at site SLU23 in Figure 10), which used a reference area in Ringhals environmental monitoring programme [104]. Similar values were observed in 2023 [105].

Discharged heated cooling water is usually dispersed as a cohesive cooling water plume, which is mixed horizontally as well as vertically (down to a number of m) with the surrounding water [102]. However, at certain occasions and during winter the cooling water can sink to relatively large depths [102]. Close to the discharge point the cooling water plume is mainly affected by the discharge speed. Due to the higher temperature of the discharged cooling water than of the surrounding seawater, the discharged water (with lower density than

the surrounding seawater) tends to float on the surrounding water, and dispersion will be due to the action of gravity, and factors such as wind, currents, vertical stratification and heat losses to the atmosphere [102].

The momentary direction of the dispersed plume is a result of prevailing water currents and wind conditions. According to a one-year study by Notter [103], the dispersion of the cooling water plume from Ringhals NPP was directed towards the north at 40% of the time, towards the south at 25%, and to the west at 15%. The direction was undefined for the remaining 20% of the time. Ref [102] estimates that recirculation, i.e. that heated cooling water is again taken through the cooling water inlet, occurs at 11% of the time at Ringhals NPP [102]. This is of course of relevance also for recirculation of discharged radionuclides.

The significance of specific oceanographic and meteorological conditions on the direction and magnitude of dispersion of the discharged heated coolant water can clearly be seen in studies of water temperature (see e.g. [101, 102]). As discharged radionuclides are advected with the discharged cooling water, these studies are of relevance for estimates of the dispersion of radionuclides in the discharged cooling water prior to entering the biological systems of the marine environment or being settled by gravitation in case of radionuclides in suspension or associated with particles. The most affected area, starts at the discharge point (SLU3/22 in Figure 10), and has a distribution of ~800 m to the south (to the southern part of Cape Ringhals) and a width of ~400 m [106]. In ref [102] it is stated that in previous measurements by SMHI for Ringhals, an area of ~16 km² between the south of Ustö (site SLU13 in Figure 10), Norra Horta (site SLU7), and out to ~2 km west of the NPP was affected by an excess temperature of at least 1 °C (excess temperature of outlet water 11 °C) [102]. The same publication presents satellite measurements from 1980, when the NPP was run with 50% of the power capacity: an excess temperature of at least 0.1 °C was seen at the water surface up to 8 km west of the cooling water outlet. Furthermore, [102] states that the heated cooling water normally affects the temperature of the water down to a depth of 5-7 m.

Notter [81] states that radiometric analysis of bladderwrack has shown a traceable impact from the NPP up to 60 km north of the NPP.

4.3. Sampling

4.3.1. Sampling by Lund University

Sampling of *Fucus* spp. at Särödal was performed (since 1967) as described in [8, 10, 107]. *Mytilus edulis* sampled in Särödal in 1978 was also used in the study. Sampling of *Fucus* spp. at other sites, mussels, grass, sediment and seawater for PC analysis (Table 8) was performed by Lund University. All samples from the marine environment were collected by entering the water on foot. The *Fucus* spp. samples collected were chosen to be likely to be constantly submerged in water to avoid uptake of atmospheric CO₂. For most of the seaweed samples, a few kg of material (w.w.) was sampled (only 3 *Fucus* individuals were taken further to ¹⁴C analysis). In case of sampling of mussels, <10 mussels were sampled per site and sampling occasion. Sediments were collected by entering the water by foot and scooping sediment down to a depth of ~5 cm into a sterile 100 ml jar (Brandt™).

Seawater for particulate carbon analysis was sampled in a 10 L container (HDPE bottle with airtight lid, Mellerud plast emballator) by entering the water by foot. Salinity and water temperature was measured at sampling (Salinity meter 850, Heraco AB, Holmsund, Sweden; absolute uncertainty in the salinity measurement ~0.1%). For grass, a few strands were collected using a pair of scissors.

4.3.2. Sampling by SLU for the one-year study at Ringhals NPP

The Swedish Agricultural University collected the samples denoted “SLU” (results in this report) and the mussel samples from Bua in paper [11] according to normal procedures in the environmental monitoring programme of Ringhals NPP. Water temperature and salinity was measured at the time of sampling.

4.4. Sample preparation

Sample preparation of biota was performed at Lund University as described in papers [9-11], resulting in dried samples. Sediments were pre-treated as described in [108] (sieving down to 2 mm prior to freeze-drying). The sample preparation of mussel shells, and the division into annual bands, are described in [11]. In brief, a method based on heating the shell to separate the fibrous layer from the other layers was developed, and ^{14}C was analysed by AMS as described above [11]. The soft tissue of the mussel was also analysed, and the results were compared to F^{14}C in *Fucus* spp. collected at the same occasion, or in earlier years (F^{14}C in *Fucus* is representative of F^{14}C in DIC).

All excess material that was not used for ^{14}C analyses was saved for possible future analyses, with *Fucus* spp. as the only exception (dried and grounded material of only 250 ml or 60 ml were saved, except for the Särö samples were all sampled material was saved).

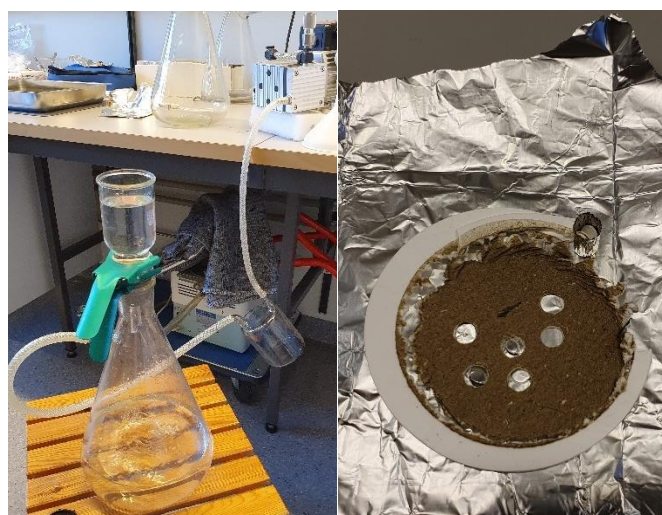


Figure 12 Left: Apparatus for vacuum filtering of seawater samples. Right: Filter with after filtration. The punched smaller pieces are taken further to ^{14}C analysis.

A 5-liter filter flask with associated filter holder and funnel was used for filtering the seawater. Filtration equipment was connected to a membrane pump with a water trap in between. The filter, Whatman QMA (quartz microfiber filter

50 mm diameter, 2.2 µm particle retention), was cleaned by baking in a muffle oven for 30 minutes at 700 °C. The filter was weighed before filtration. The 10 L container with the sampled seawater was shaken and the water was then poured into the funnel and filtered using vacuum. Filtration took place until the filter was saturated and only single drops of water passed through the filter. The filter was detached from the holder and dried in an oven (65°C). The dried filter was weighed, and the filtered amount of water was measured. From the dried filter, filter pieces were punched out with a chisel (4 mm diameter) and the filter pieces were placed in cylindrical tin capsules (fitting into the elemental analyser of the AGE graphitization system (see below). For each filter, 60 pieces were punched out which were distributed in 10 tin capsules. Total sample area was 7.5 cm².

4.5. ¹⁴C-analysis

A few mg of each dried sample was submitted to the Lund Radiocarbon Dating Laboratory at Lund University. The *Fucus* spp. and sediment samples were subjected to acid-alkali-acid (AAA) pretreatment to eliminate carbonates and organic acids prior extraction of a few mg of carbon (graphitization) using an AGE graphitization system, including an elemental analyser for sample combustion [109]. Other biota (soft tissues from fish, mussels, crabs and oysters, and particulate carbon filtered from seawater) were not subjected to acid-alkali-acid pretreatment. Carbon-14 analysis of the samples, standards and blanks was performed using the Single Stage Accelerator Mass Spectrometry facility at Lund University [44, 110, 111]. The results of the ¹⁴C measurements are expressed as F¹⁴C [13, 14]. The conversion of F¹⁴C into specific activity of carbon (in terms of Bq per kg carbon) and activity concentration (Bq per kg dry or wet weight) is described in Appendix A.

4.6. EA-IRMS measurement

A few samples of biota and the sediment samples (see Table 8 and Table 9) were measured with Elemental Analyser – Isotope Ratio Mass Spectrometry (EA-IRMS) at the Department of Forest Ecology and Management, Swedish University of Agricultural Sciences (SLU). Quantities measured were mass fractions of C and N, δ¹³C (¹³C/¹²C ratio expressed using the VPDB scale) and δ¹⁵N (¹⁵N/¹⁴N ratio expressed using the atmospheric nitrogen scale). See Appendix A for a description of the principles behind isotope fractionation. The samples were only subjected to drying prior to analysis (the sediments and *F. vesiculosus* samples were not subjected to acid-alkali-acid pretreatment).

4.7. Analysis of ⁹⁹Tc

Two samples from Särö (site 15) and two samples from the Ringhals area (sites SLU3 and SLU7) from 2023 were subjected to ⁹⁹Tc analysis. A sample of the certified material IAEA-446 (Baltic Sea *Fucus*) was also subjected to ⁹⁹Tc analysis for quality control purpose. The measurement done by liquid scintillation counting after extraction of the ⁹⁹Tc from the seaweed matrix by the Service de Mesure et d'Analyse de la Radioactivité et des éléments Traces (SMART, part of the UMR 6457 SUBATECH) in Nantes, France.

5. Summary of our previous studies

In a previous study of ^{14}C in Swedish coastal waters, *Fucus* spp. was sampled in spring 2020 from shallow waters at 45 sites in Kattegat, Skagerrak, Öresund, the Baltic Sea and the Gulf of Bothnia (Figure 13a) [8]. The Ringhals area was subjected to extended sampling (see Figure 13b).

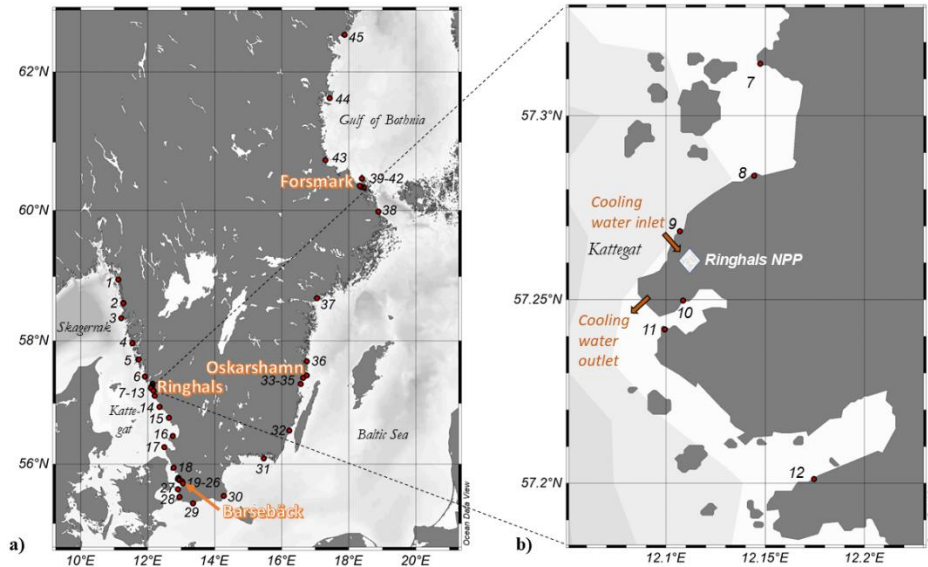


Figure 13 a) Sampling sites for *Fucus* spp. in spring 2020 [8]. b) Enlargement of the Ringhals NPP sampling area [8].

Sampling was performed by entering the water on foot, and the maximum sampling depth was limited to an arm's length (~50 cm). The $F^{14}\text{C}$ data for the various straits and the Baltic Sea are presented in Figure 14 and summarized in Figure 15 (excluding samples collected around Ringhals NPP). Figure 15 also includes data from samples of terrestrial vegetation and foodstuffs in southern Sweden in 2020 [44]. The data in Figure 15 can serve as an example of what variations in $F^{14}\text{C}$ can be expected in *Fucus* spp. grown close to the shore in various parts of Swedish coastal waters.

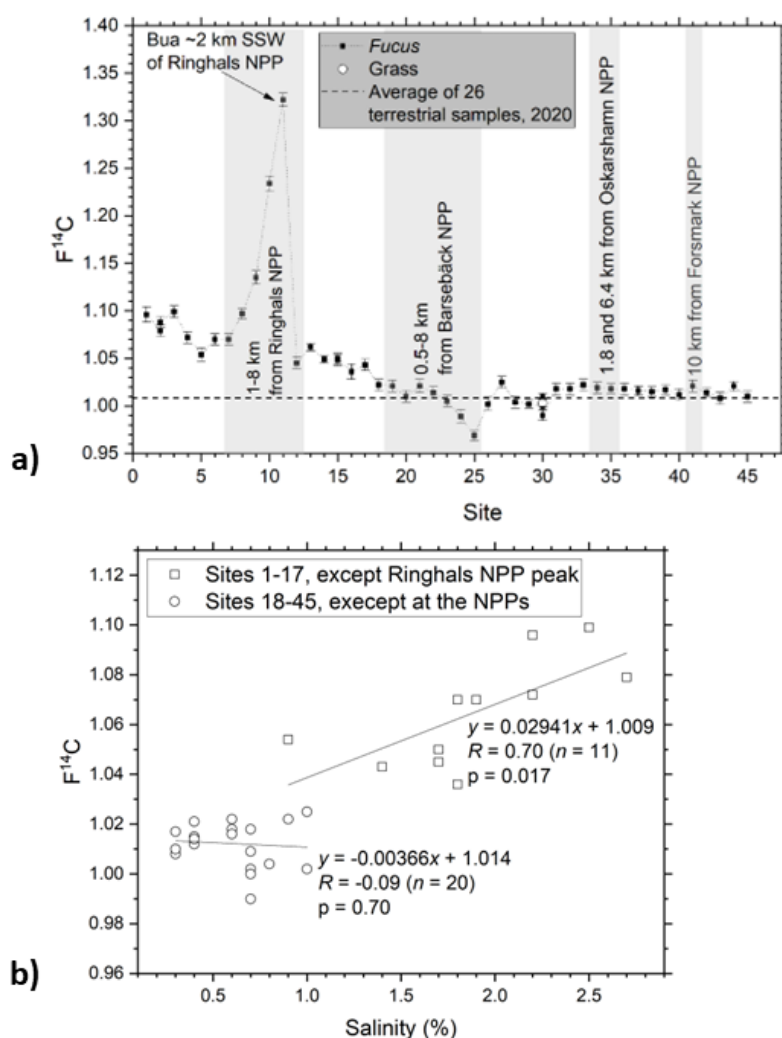


Figure 14 a) $F^{14}C$ in *Fucus* spp. and grass (the latter at Skillinge, site 30) collected along the Swedish coast in spring 2020 [8]. Samples collected within 10 km of the Swedish NPPs are highlighted in the grey areas. The dashed line represents the average $F^{14}C$ value of 26 terrestrial samples collected in southern Sweden for 2020, representing the atmospheric CO_2 reference value for 2020 [112]. Uncertainties represent 1 SD, resulting from repeated measurements of the same sample. b) Linear correlation between $F^{14}C$ and salinity, divided into two sets separated by the border between Kattegat and the Öresund Strait. Sites 8-11 at Ringhals NPP and sites located close to all other NPPs have been excluded (grey shading in upper figure). From [8].

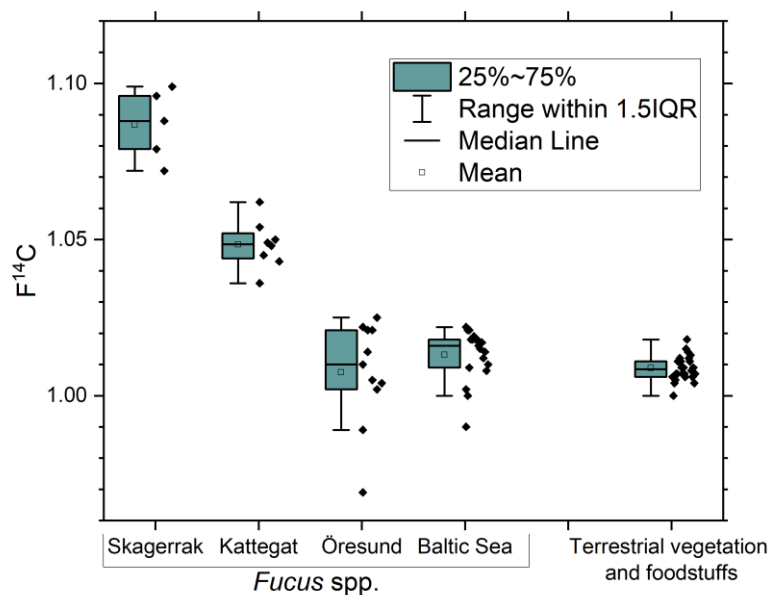


Figure 15 $F^{14}C$ in *Fucus* spp. collected in Swedish shallow coastal waters in 2020 [8], and in $F^{14}C$ terrestrial vegetation and foodstuffs collected in 2020 in southern Sweden [44]. The lowest values in Öresund and in the Baltic Sea are outliers. IQR: Interquartile range. The typical analytical uncertainty in each $F^{14}C$ measurement is typically 0.005.

The main findings (Figure 14) were:

1. A clear increase in $F^{14}C$ was seen in *Fucus* spp. around Ringhals NPP, with a maximum $F^{14}C$ of 1.322 ± 0.007 (31% above the atmospheric ^{14}C reference data for 2020) at site 11 (Bua), located ~1.4 km SSE of the discharge point.
2. No distinct peaks in $F^{14}C$ were detected around the other Swedish NPPs. However, the sampling sites were further away from the discharge points at these NPPs than at Ringhals NPP (the minimum distance was 10 km at Forsmark, and the two sampling sites at Oskarshamn NPP were 1.8 and 6.4 km from the discharge point).
3. $F^{14}C$ in *Fucus* spp. was significantly higher in Skagerrak and Kattegat (west coast) than in the Öresund Strait, the Baltic Sea and the Gulf of Bothnia.
4. On the west coast (excluding the sites close to Ringhals NPP), $F^{14}C$ correlated strongly with salinity ($R = 0.70$, $p < 0.05$; see Figure 15b). This was interpreted as evidence that water of high salinity from the North Atlantic, containing ^{14}C , e.g. from La Hague and Sellafield, reaches the Swedish west coast. Ocean currents of relevance for the transport of radionuclides discharged from La Hague and Sellafield are indicated in Figure 9.

For the Särðal historical samples collected since 1967, the ^{14}C content in *Fucus* spp. in a limited number of samples have been presented in [8, 113] (projects SSM2019-5225 and SSM2020-797). The results showed F^{14}C in the Särðal samples collected after the 1990s were clearly higher than F^{14}C in clean air CO_2 , indicating contributions of ^{14}C of anthropogenic origin (see Fig. 7 in [8]).

6. Results and discussion

This chapter starts with an overview of the published papers and an outline of the results presented in this report only. Section 6.2 describes the observations in the terrestrial environment. Section 6.3 summarizes the ^{14}C measurements in *Fucus* spp. at the Särödal site. Temporal and spatial variation in ^{14}C in *Fucus* spp. along the west coast is described in section 6.4, whereas section 6.5 describes reference levels for the Ringhals site. Analysis of mussel shells for retrospective determination of ^{14}C discharges is summarized in section 6.6. Results for *F. vesiculosus* in at the Ringhals site for 2020-2024 are presented in section 6.7. Section 6.8 compares $F^{14}\text{C}$ in *M. edulis* with *F. vesiculosus*. Section 6.9 is devoted to the one-year study of ^{14}C in marine biota in the close vicinity of Ringhals NPP. A few measurements of sediments are presented in section 6.10, and of particulate carbon in 6.11. The chapter ends with a note on trophic levels and carbon content of the samples (section 6.12), the ^{99}Tc results (section 6.13) and a radioecological discussion (section 6.15).

6.1. Overview of published papers

A summary of studies published from the data obtained in project SSM2022-4035 are presented in Table 10. Some data, e.g. of mussels collected at various sites along the Swedish coast in 2022 and the one-year study at Ringhals NPP, have not been published elsewhere.

Table 10 Summary of the aims, sites, samples and sampling occasions of the papers summarized in the present publication. EMP – Environmental Monitoring Programme.

Paper	Aim	Sites	Main material	Years
[10] Mattsson et al	Temporal variations in ^{14}C in <i>Fucus</i> spp. at Särödal. Long-range transport of ^{14}C from foreign nuclear facilities to Särödal.	Särödal (site 15)	<i>Fucus</i> spp.	Most years 1967-2023
[9] Eriksson Stenström et al	Spatial and temporal variations in ^{14}C in <i>Fucus</i> at the Swedish west coast.	14 Swedish west coast sites (1, 3, 46, 4, 49, 7-11, 11B, 11C, 17, 50) 2 Baltic Sea sites (30, 51)	<i>Fucus</i> spp. <i>Poaceae</i> sp.	Spring 2020 [8] Autumn 2020 Autumn 2022 Spring 2023 Autumn 2023 Spring 2024
[11] Bjarheim et al	Retrospective analysis of ^{14}C at Ringhals NPP using mussel shells.	3 sites on Swedish west coast (1, 11, 15)	<i>Mytilus edulis</i> <i>Fucus</i> spp. <i>Poaceae</i> sp.	Collected in: 2022 (site 1), 2023 (site 11), 1978 (site 15) Years: 2017-2022 (site 1), 2014-2022 (site 11), 1972-1978 (site 15)
This report	Radioecology at Ringhals NPP.	10 sites from Ringhals EMP (SLU3/22, SLU5, SLU7, SLU 8, SLU11, SLU12, SLU13, SLU16, SLU23, SLU25) 6 other sites (49, 7-12)	<i>Fucus</i> spp. <i>Mytilus edulis</i> <i>Cancer pagurus</i> <i>Magallana gigas</i> <i>Symphodus melops</i> <i>Poaceae</i> sp. (grass) Sediment Particulate carbon in seawater	Spring 2023 Autumn 2023 Winter 2023/2024

6.2. Terrestrial coastal environment

$F^{14}\text{C}$ in the grass samples collected and analysed during the project are shown in Figure 16. All the sites are marine sites used for collection of various marine sample types. The trendline is constructed from the data in Table 2, comprising of annual average $F^{14}\text{C}$ in terrestrial samples in southern Sweden. $F^{14}\text{C}$ for all grass samples overlap within 3σ (most overlap within 1σ) with the trend line for southern Sweden (note that the scale on the y axis makes the uncertainties look large: they are however not, the relative uncertainty in $F^{14}\text{C}$ is $< 0.6\%$). Hence, none of the samples can be considered to have deviating $F^{14}\text{C}$ compared to the trendline.

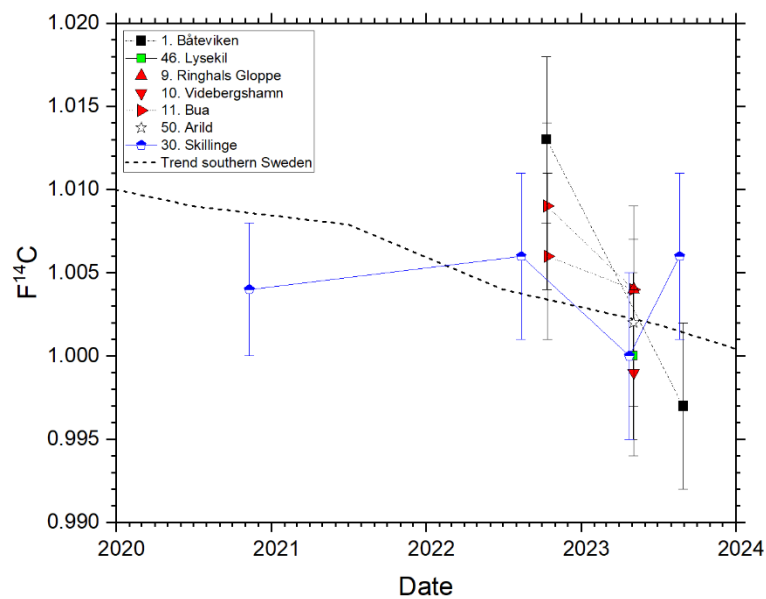


Figure 16 $F^{14}\text{C}$ in grass samples collected in the terrestrial environment at some of the marine sites. A trendline constructed from average $F^{14}\text{C}$ in vegetation in southern Sweden is also shown (data from Table 2). The uncertainty bars of $F^{14}\text{C}$ in the grass samples represent 1σ (relative uncertainty $< 0.6\%$), resulting from repeated measurement of the same sample. Modified from [9].

The sites in red in Figure 16 are from sites located in the close vicinity of Ringhals NPP (9. Ringhals Gloppe, 10. Videbergshamn and 11. Bua, see Figure 8 and Table 8). The absence of excess ^{14}C in these terrestrial samples, despite each reactor emitting several hundred GBq ^{14}C per year as airborne effluents (see Figure 7), can be understood from the chemical form of the airborne ^{14}C releases and the location of the sampling sites. As seen in Figure 7, the operational PWRs mainly release ^{14}C as hydrocarbons, which are not accessible to vegetation by photosynthetic absorption. The amount of ^{14}C released as CO_2 is only 13% for 2022 and 12% for 2023 for the two operational Ringhals reactors. It should be noted that these samples are not located in the main downwind direction of the NPP. These circumstances, in combination with an effective dilution of ^{14}C (released as CO_2) from its upward release through the 45 m high stacks to the ground level and its vegetation, account for the absence of observed ^{14}C in the grass samples collected close to Ringhals NPP.

6.3. Observed temporal variations of ^{14}C at Särödal

The Särödal $F^{14}\text{C}$ *Fucus* spp. results for 1967-2023 are presented in Figure 17 [10] and in Appendix D. Also included are ^{14}C in *Fucus* spp. from some sites nearby Särödal (Glommen, Kärra and Träslövsläge). Atmospheric ^{14}C bomb pulse data, representative for Europe [15-18], and modelled global marine surface mixed-layer bomb pulse, are also included in.

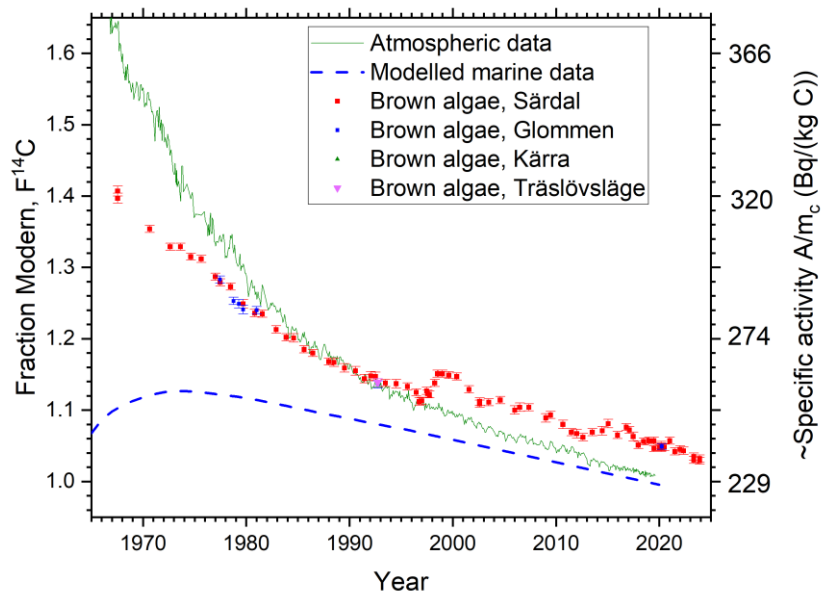


Figure 17 ^{14}C in *Fucus* spp. from Särödal in the period 1967-2023. Additional data from 3 other nearby places (Glommen (56.93N, 12.35E), Träslövsläge (57.06N, 12.27E), and Kärradal (57.19N, 12.21)), on the west coast are also included. The atmospheric data is representative of CO_2 of the Northern hemisphere [15-18]. The dashed curve represents the modelled global marine surface mixed-layer bomb pulse for the period 1950 to 1996 [20], and values after this were extrapolated based on linear regression of marine data from 1987 to 1996. From [10].

In the beginning of the sampling period (from 1967 until the late 1980ies) ^{14}C in *Fucus* spp. is lower than atmospheric ^{14}C data but higher than the modelled marine curve (Figure 17). This is expected since the habitat of *Fucus* spp. is close to the water surface where CO_2 from the atmosphere enters the ocean water as DIC (see section 2.3.2). However, after about 1990 the Särödal ^{14}C values start exceeding the atmospheric CO_2 curve. Furthermore, a pronounced increase can be seen in 1998 and another one in the mid-2010s. As reported previously [8], this mainly believed to be ^{14}C transported by ocean currents from the spent nuclear fuel reprocessing plants La Hague and Sellafield to the Swedish west coast.

Data of liquid discharges of ^{14}C and other radionuclides from La Hague as well as Sellafield are publicly available, e.g. from the OSPAR database [27]. Annual discharge rates of ^{14}C from these two facilities are presented in Figure 18a. As reported in [8], previous studies of other radionuclides have estimated the dilution factors from Sellafield to Särödal to 200, and from La Hague to Särödal to

40 (see Figure 18b). Adding estimated transport times of about 2 years from La Hague to Särödal and 4 years from Sellafield to Särödal (see [8] and references therein) results in Figure 18c. Comparing Figure 17 and Figure 18c, it is evident that the two peaks in $F^{14}\text{C}$ starting in 1998 and in the mid-2010s coincide. This observation further supports that parts of the ^{14}C found in *Fucus* spp. in Särödal originate from La Hague and Sellafield.

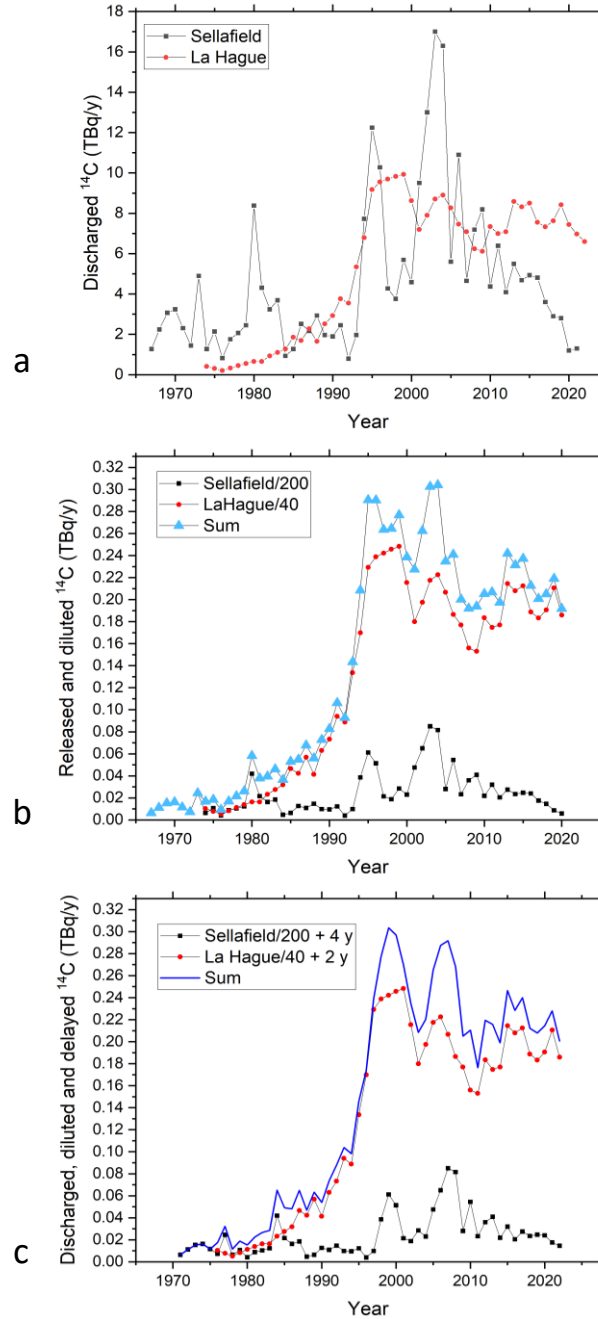


Figure 18 **a)** Liquid discharge rates of ^{14}C for the reprocessing plants for spent nuclear fuel at La Hague (France) and Sellafield (UK) for 1967 to 2022 [27]. **b)** Liquid discharge rates of ^{14}C from La Hague and Sellafield including dilution factors representative for Särödal [8, 10]. **c)** Liquid discharge rates of ^{14}C from La Hague and Sellafield including dilution factors and delay times representative for Särödal [8, 10].

In [8], the limited data set from Särðal ($F^{14}C_{\text{Särðal}}$) suggested that the excess $F^{14}C$ after 1990 at Särðal ($\Delta F^{14}C_{\text{Särðal}}$) compared to marine modelled $F^{14}C$ curve ($F^{14}C_{\text{marine-modelled}}$) was 0.059 ± 0.007 ($\Delta F^{14}C_{\text{Särðal}} = F^{14}C_{\text{Särðal}} - F^{14}C_{\text{marine-modelled}}$), corresponding to a specific activity of $\sim 13 \pm 2$ Bq ^{14}C per kg C. These estimates can be refined based on the new data in Figure 17. Firstly, since *Fucus* spp. is collected in shallow waters, it is reasonable to assume that a representative reference curve for DIC in such shallow waters (referred to as $F^{14}C_{\text{shallow waters}}$) is in between the curves for atmospheric data and for the marine modelled data in Figure 17. Secondly, it is likely that the $F^{14}C_{\text{shallow waters}}$ is closer to the atmospheric curve than to the marine modelled curve, as supported by the early Särðal data in Figure 17 (when discharges from Sellafield and La Hague were presumably low). A very rough estimation using the data from around 1980 yields that $F^{14}C_{\text{shallow waters}}$ is to $\sim 80\%$ represented by the atmospheric curve ($F^{14}C_{\text{atmospheric}}$) and to $\sim 20\%$ represented by the modelled marine curve ($F^{14}C_{\text{marine-modelled}}$), i.e.

$$F^{14}C_{\text{shallow waters}} \approx 0.8 \cdot F^{14}C_{\text{atmospheric}} + 0.2 \cdot F^{14}C_{\text{marine-modelled}}$$

The estimated excess $F^{14}C$ in Särðal *Fucus* (defined as $F^{14}C_{\text{Särðal}} - F^{14}C_{\text{shallow waters}}$) is shown in Figure 19. Also shown in the figure is the sum of the liquid discharge rates of ^{14}C from La Hague and Sellafield including dilution factors and delay times representative for Särðal [8, 10] (see also Figure 18). Since the end of the 1990ies, the excess $F^{14}C$ has been between 0.030 and 0.063, with an average of ~ 0.047 (corresponding to an excess specific activity of ~ 11 Bq per kg C).

The sum of the liquid discharge rates of ^{14}C from La Hague and Sellafield including dilution factors and delay times representative for Särðal (blue line in Figure 19) corresponds rather well with the measured excess $F^{14}C$ in *Fucus* spp. Fluctuating water currents, various degrees of runoff from land and upwelling as well as other sources of ^{14}C may contribute to differences in the patterns of the two lines in Figure 19.

For environmental monitoring of ^{14}C at NPPs, the temporal variability of ^{14}C due to influences from La Hague and Sellafield need to be considered, as evident from Figure 17 and Figure 19. This is further demonstrated in the upcoming section 6.4.

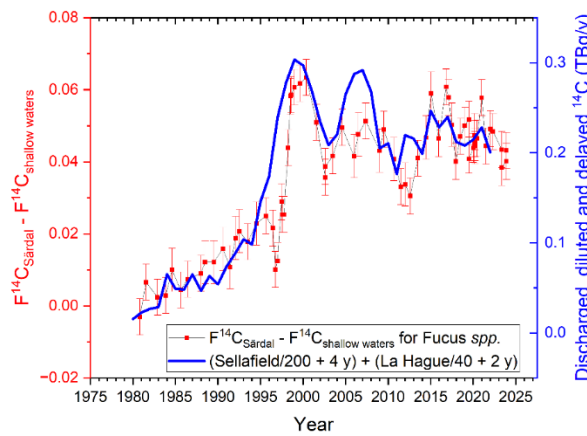


Figure 19 Excess $F^{14}C$ ($F^{14}C_{\text{Särðal}} - F^{14}C_{\text{shallow waters}}$) in *Fucus* spp. collected at Särðal for 1980-2023, and sum of discharged ^{14}C from Sellafield and La Hague taking dilution factors and delay times from [8] into account.

6.4. Observed spatial and temporal variations of ^{14}C at the Swedish west coast

The spatial and temporal variations in $F^{14}\text{C}$ in *Fucus* spp. (representative of DIC) and in grass collected between 2020 and 2024 are shown in Figure 20 [8, 9, 11]. The *Fucus* spp. samples from Svinesund (site 52), Saltbacken (site 53) and Strömstad (site 1) collected in spring 2024 showed decreasing $F^{14}\text{C}$ upstream towards the Halden research reactor. Hence, influence from any ^{14}C discharges from the Halden reactor on the $F^{14}\text{C}$ values in *Fucus* spp. on the Swedish west coast was considered unlikely [11].

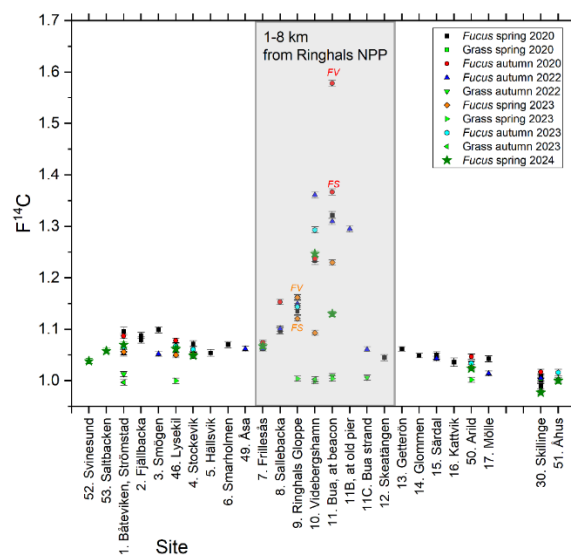


Figure 20 $F^{14}\text{C}$ in *Fucus* spp. and grass collected at the marine sites from 2020 to 2024. For Skagerrak and Kattegat, the sites are sorted according to longitude from north to south. Sites 30 (Skillinge) and 51 (Åhus) serve as reference sites in the Baltic Sea. Data from spring 2020 is published in Eriksson Stenström and Mattsson [8], data from Särödal in Eriksson Stenström and Mattsson [8] and Mattsson *et al.* [10]. Data from Svinesund (site 52) and Saltbacken (site 53) are published in Bjarheim *et al.* [11]. The uncertainty bars represent 1σ , resulting from repeated measurement of the same sample. FV – *Fucus vesiculosus*; FS – *Fucus serratus*. Adapted from [9].

A more detailed analysis of the data is presented in Eriksson Stenström *et al.* [9]. $F^{14}\text{C}$ in *Fucus* spp. at sites that have been sampled on several occasions in 2020–2024 is shown in Figure 21 (the Särödal data are excluded as these samples were collected on other dates). As described in [8, 9], and as visualised Figure 20 and Figure 21, the general trends are that:

1. $F^{14}\text{C}$ varies considerably spatially as well as temporally in the marine environment.
2. Skagerrak has higher $F^{14}\text{C}$ in *Fucus* spp. than southern Kattegat, which is attributed to increasing dilution of ^{14}C from La Hague and Sellafield towards the south of the Swedish west coast.

3. variations in the annual liquid ^{14}C discharges from La Hague and Sellafield may contribute to the temporal pattern in Figure 21.
4. both Skagerrak and Kattegat show higher $F^{14}\text{C}$ than the Baltic Sea (up to ~10% higher in northern Skagerrak than in the Baltic Sea).
5. the data from 2020 and 2024 shows an increase in $F^{14}\text{C}$ with increasing latitude for Skagerrak, whereas the data from 2022 and 2023 does not.
6. the local marine environment of Ringhals NPP is clearly affected from liquid discharges from the NPP.
7. $F^{14}\text{C}$ in the terrestrial environment has low spatial and temporal variability.

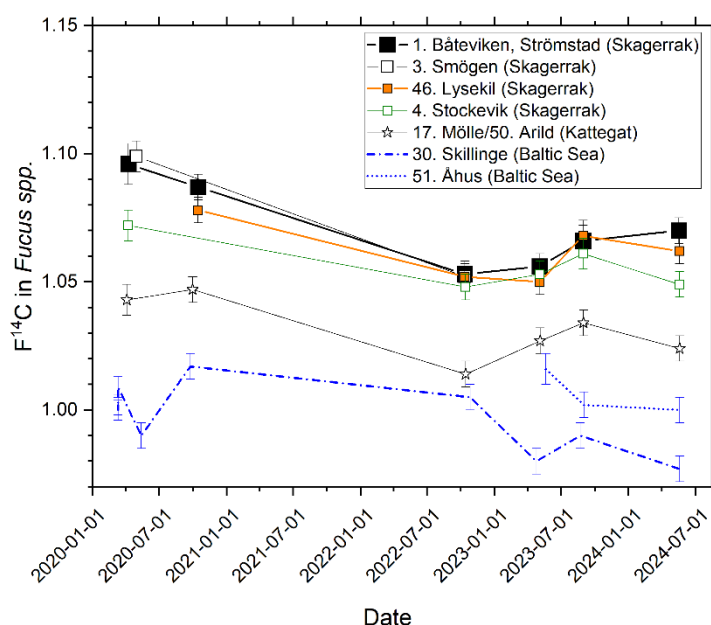


Figure 21 $F^{14}\text{C}$ at sites in Skagerrak and Kattegat on the Swedish west coast (date given as YYYY-MM-DD), and at two reference sites in the Baltic Sea for 2020-2024 [9]. The sites at Skagerrak and Kattegat are ranked from north to south in the legend. The uncertainty bars represent 1σ , resulting from repeated measurement of the same sample. From [9].

6.5. Carbon-14 reference level for Ringhals NPP 2020-2024

As seen in Figure 8, the Ringhals site is located almost at half the distance between site 4 Stockevik and site 15 Särödal (84 km from Ringhals to Stockevik and 64 km from Ringhals to Särödal). The two sites may possibly be used to establish an approximate reference value for the Ringhals site. Figure 22 shows linear regressions of the $F^{14}C$ data for site 4 Stockevik and site 15 Särödal for 2020 to 2024. The solid thick line is the average of the two regression lines, and may serve as an approximate reference level for the Ringhals site. A refined reference curve, also visualizing wiggles e.g. due to varying input from the foreign fuel reprocessing plants, could be obtained if samples were collected more frequent and at the same occasion (in the present study, the Särödal samples were collected independently of the other samples).

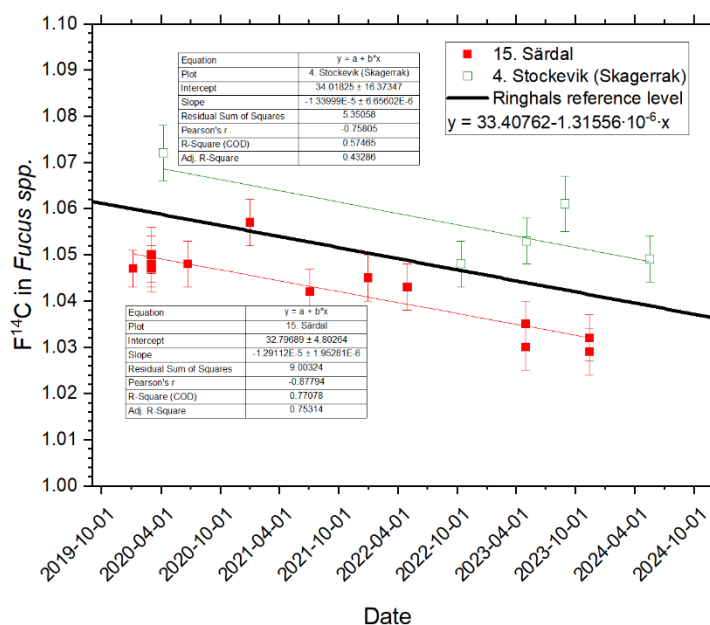


Figure 22 Estimated $F^{14}C$ reference value for the Ringhals site for 2020-2024. The estimated level is the average of linear regressions of $F^{14}C$ data from site 4 Stockevik and site 15 Särödal.

6.6. Mussel shells for retrospective ^{14}C -DIC analysis

In the study of the potential of using shells of *Mytilus edulis* for retrospective analysis is DIC in the marine environment of nuclear power plants [11] a thermal separation method was developed to extract the fibrous layer of annual bands *M. edulis* prior to ^{14}C analysis. The paper also [11] discusses challenges in correct identification of the year of formation of the annual bands, as well as the potential limitations of using mussels, which as semi-sessile, as bioindicators for retrospective assessments. The data also offers comparison between dietary carbon and shell DIC-derived carbon for *M. edulis*.

6.6.1. Shell annual bands versus *Fucus vesiculosus* for reference sites

To test the applicability of the method, F^{14}C in annual bands of *M. edulis* were compared with data of F^{14}C in *Fucus* spp. (both are built up of DIC, or at least mainly built up of DIC for *M. edulis* shells). The Särödal *Fucus* spp. series was used as part of this testing of the method. Not only *Fucus* spp. have been collected at Särödal over the past 6 decades: also samples of *M. edulis* (shells and dried soft tissue) collected in 1978 are available in the biobank. Two of these shells were subjected to the thermal separation method and analysed for its ^{14}C content. The main results are described below.

Särödal

1. For one of two analysed shells from Särödal (representing 1974–1978), F^{14}C in *Fucus* spp. and mussel annual bands agreed very well.
2. For the other shell (1972–1978), F^{14}C for some of the earlier years were to 6% lower than in *Fucus* spp. The lower F^{14}C values for the earlier years of shell 2 may indicate that this particular mussel has changed habitat, moving from an environment with lower F^{14}C in DIC (e.g. close to the mouth of a creek bringing ^{14}C -depleted carbon into coastal waters [61]) to one with higher F^{14}C .

Another more northern site was also investigated, Båteviken at Strömstad close to the border of Norway (site 1), which has *F. vesiculosus* F^{14}C data for years 2020 (sampled in April and October), 2022 (October) and 2023 (May and August). Two shells from *M. edulis* collected in October 2022 were tested. For one of the shell samples 6 annual bands were analysed (representing 2017–2022) and for the other shell 2 year were analysed (2020 and 2021). The main findings from the analysis of the Båteviken samples are described below (see also Figure 23).

Båteviken

1. For the shell with 6 annual bands analysed (shell 2 in Figure 23), F^{14}C in *M. edulis* agreed well with F^{14}C in *F. vesiculosus*.
2. The trend in F^{14}C of the shell with 6 annual bands analysed (shell 2 in Figure 23) may be correlated to liquid ^{14}C discharges from La Hague

and Sellafield. As stated in [11], the peak in the shell data for 2020 may possibly be attributed to a peak in liquid discharges reported from La Hague in the year before (2019). This observation is supported by previous studies showing that the transport time from La Hague to Särddal is approximately 2 years (see [8] and references therein).

3. For the second shell (shell 1 in Figure 23), the obtained $F^{14}C$ data for 2020 overlaps within 1σ with shell 2, and for 2021 the overlap between the $F^{14}C$ data of the two shells is within 3σ .

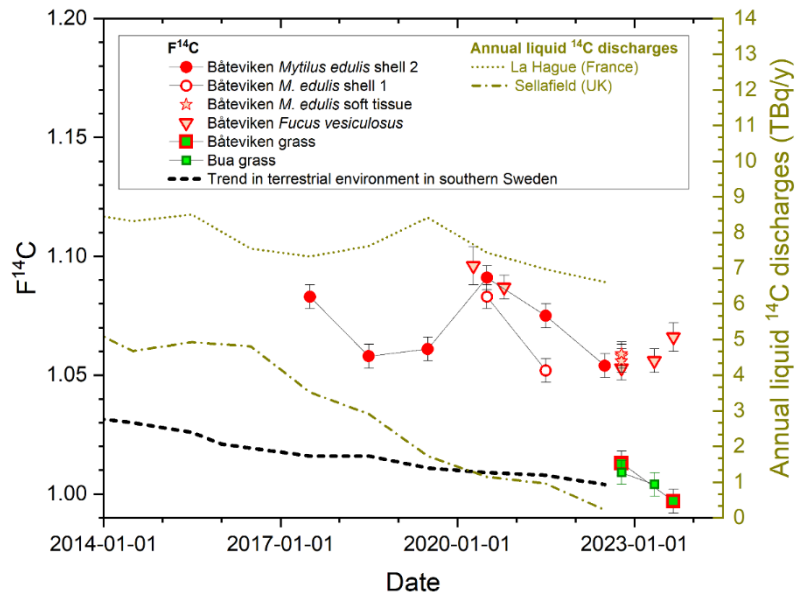


Figure 23 $F^{14}C$ in annual bands from shells of *Mytilus edulis*, in soft tissue of *M. edulis* and in *Fucus vesiculosus* collected at Båteviken (site 1). The $F^{14}C$ *F. vesiculosus* data is plotted at the collection date. The average formation season is plotted as summer for the *M. edulis* shell structures. The terrestrial environment is represented by grass samples from the Båteviken (site 1) and Bua (site 11) (plotted at collection date). A trendline of $F^{14}C$ in the terrestrial environment of southern Sweden is also included (data from [44, 55]). Uncertainty bars represent the analytical uncertainties (1σ). The right y axis displays annual liquid discharges from La Hague (France) and Sellafield (United Kingdom) [27]. From [11].

6.6.2. DIC versus dietary carbon of *M. edulis* at reference sites

Apart from investigating the potential of shells of *M. edulis* for retrospective ^{14}C -DIC assessment, the comparison of $F^{14}C$ in the outer (most recent) annual bands of *M. edulis* with that of the soft tissue of *M. edulis* and to *Fucus* spp. is of interest due to the origin of carbon in these sample types. *Fucus* spp. represent DIC, mussel shells mainly represent DIC (a minor fraction of dietary carbon may be incorporated in the shell), whereas the mussel soft tissue is representative of dietary carbon. The main results of the study from Särddal (site 15) and Båteviken (site 1) were:

Särddal

1. $F^{14}C$ in soft tissue (representing dietary carbon) of *M. edulis* collected in 1978 overlapped within 2σ with $F^{14}C$ in *Fucus* spp. from 1978 and in the

outer annual bands (most recent annual bands, representing 1978) of both shells investigated. Hence, dietary carbon for *M. edulis* appears to have been in equilibrium with DIC in 1978 at Särödal.

Båteviken

2. $F^{14}C$ values of soft tissue (dietary carbon) of 3 individuals of *M. edulis* collected in 2022 overlapped within 1σ with $F^{14}C$ in *F. vesiculosus* collected at the same site in 2022, and with $F^{14}C$ in the outer (most recent, 2022) annual band of one of the shells analysed (in the other shell year 2022 was not analysed). Equilibrium between DIC and dietary carbon of *M. edulis* is hence indicated at Båteviken in 2022.

6.6.3. Shell annual bands versus *Fucus vesiculosus* at Ringhals NPP

As reported in [11], two shells collected at site SLU5b (Bua lighthouse, close to site 11, see Figure 10) in the vicinity of Ringhals NPP) in May 2023 were subjected to thermal separation of the annual bands followed by ^{14}C analysis. One shell covered the period 2014–2022 and the other 2016–2022. Soft tissue of three individuals of *M. edulis* were also analysed. *Fucus vesiculosus* from April and October 2020, October 2022, May 2023 and August 2023 were used for comparison with $F^{14}C$ obtained from *M. edulis*.

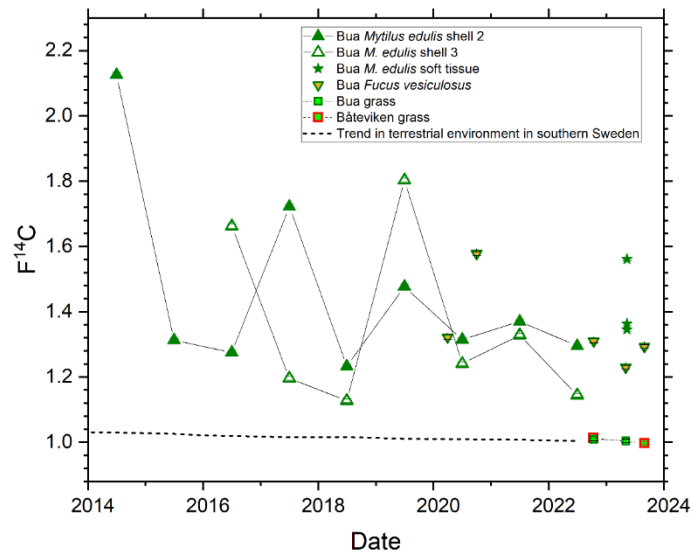


Figure 24 $F^{14}C$ in annual bands of shells of *Mytilus edulis*, in soft tissue of *M. edulis* and in *Fucus vesiculosus* collected at SLU5b Bua lighthouse (close to Ringhals NPP). The *F. vesiculosus* and *M. edulis* soft tissue data is plotted at the collection date. The average formation season is plotted as summer for the *M. edulis* shell annual bands. $F^{14}C$ in the terrestrial environment is represented by grass samples from Bua (site 11) and Båteviken (site 1) (plotted at collection date). A trendline of $F^{14}C$ in the terrestrial environment of southern Sweden is included (data from [44, 55])). Error bars represent the analytical uncertainties (1σ). From [11].

The results from Bua are presented in Figure 24. The increased $F^{14}C$ levels in *M. edulis* and *F. vesiculosus* at Ringhals NPP compared to Båteviken (see above) unequivocally originates from the NPP. The most important observations are:

1. $F^{14}C$ in the annual bands in *M. edulis* from the vicinity of Ringhals NPP had higher average $F^{14}C$ and a pronounced temporal variability compared to the samples from Båteviken:
 - Bua (site SLU5b) 2014–2022: $F^{14}C_{\text{average}} = 1.427 \pm 0.268$ (1 σ)
 - Bua (site SLU5b) 2017–2022: $F^{14}C_{\text{average}} = 1.348 \pm 0.207$ (1 σ)
 - Båteviken (site 1) 2017–2022: $F^{14}C_{\text{average}} = 1.070 \pm 0.015$ (1 σ)
2. Physical factors, such as varying discharge rates of ^{14}C from the NPP and different temporal characteristics of the effluent plume of discharged cooling water, may partly explain the high temporal variability in the shells of *M. edulis*. The observed temporal variability in $F^{14}C$ in *F. vesiculosus* supports this hypothesis.
3. Biological factors related to *M. edulis* may also contribute to the large variability in $F^{14}C$ in the shell annual band. Individual (not equal) dietary preferences, differences in the time of shell formation, and the possibility to change of habitat are such factors.
4. There may also be analytical factors partly explaining differences in $F^{14}C$ for annual band from the same year. Misidentification of annual bands is one possibility (see [11] for a further discussion). Another risk is that the samples taken to ^{14}C analysis are not representative of the full growing season due to varying degrees of removal of shell material during the acid treatment following the thermal separation process. The degree of material removal in the acid treatment process (acid fraction removal, AFR) varied between 6% and 29%, see

5. Table 11 (data from Supplementary material of [11]). For each year, the absolute difference between the ARFs ($\Delta\text{ARF} = \text{abs}(\text{ARF}_{\text{shell 2}} - \text{ARF}_{\text{shell 3}})$) and the absolute difference between their F^{14}C values ($\Delta\text{F}^{14}\text{C} = \text{abs}(\text{F}^{14}\text{C}_{\text{shell 2}} - \text{F}^{14}\text{C}_{\text{shell 3}})$) were calculated. The largest difference in F^{14}C for the cut annual samples of two shells from Bua is for 2017 ($\Delta\text{F}^{14}\text{C} = 0.526 \pm 0.009$). This year also has the largest difference in weight removal ($\Delta\text{ARF} = 23\%$). The opposite is valid for 2021: equal weight removals ($\Delta\text{ARF} = 0\%$) correspond to a low $\Delta\text{F}^{14}\text{C}$ (0.042 ± 0.008). The data is not conclusive but should be seen as an indication that the acid treatment may skew the results. However, the acid treatment procedure may not be necessary when preceded by the heating step.

Table 11 Data related to acid treatment of the annual bands of the two shells collected at Bua. The acid removal fraction (AFR) has been calculated from data in Supplementary materials of [11]. $\Delta\text{AFR} = \text{abs}(\text{AFR}_{\text{shell 2}} - \text{AFR}_{\text{shell 3}})$ and $\Delta\text{F}^{14}\text{C} = \text{abs}(\text{F}^{14}\text{C}_{\text{shell 2}} - \text{F}^{14}\text{C}_{\text{shell 3}})$

Year	AFR _{shell 2}	F ¹⁴ C _{shell 2}	AFR _{shell 3}	F ¹⁴ C _{shell 3}	ΔAFR	ΔF ¹⁴ C
2016	13%	1.275 ± 0.006	8%	1.662 ± 0.007	5%	0.387 ± 0.009
2017	29%	1.722 ± 0.007	6%	1.196 ± 0.005	23%	0.526 ± 0.009
2018	27%	1.233 ± 0.005	8%	1.127 ± 0.005	20%	0.106 ± 0.009
2019	25%	1.477 ± 0.007	27%	1.803 ± 0.005	2%	0.326 ± 0.009
2020	28%	1.315 ± 0.006	27%	1.241 ± 0.005	2%	0.074 ± 0.008
2021	28%	1.370 ± 0.006	28%	1.328 ± 0.006	0%	0.042 ± 0.008
2022	28%	1.295 ± 0.006	10%	1.144 ± 0.005	18%	0.151 ± 0.008

6. F¹⁴C in soft tissue of the three *M. edulis* individuals (representing dietary carbon of *M. edulis*) is significantly higher for one of the individuals (F¹⁴C = 1.561 ± 0.005) than for the other two (F¹⁴C = 1.363 ± 0.006 and F¹⁴C = 1.345 ± 0.006). Individual dietary preferences, changes of habitat and individual variations in the turnover rate of carbon in the tissue may contribute to the differences.
7. F¹⁴C in soft tissue of the three *M. edulis* individuals (representing dietary carbon of *M. edulis*; range in F¹⁴C: 1.345-1.561) appear higher than F¹⁴C in three samples of *F. vesiculosus* collected in 2022 and 2023 (representing DIC; range in F¹⁴C: 1.230-1.310). For the mussel with the highest F¹⁴C in the soft tissue (Mussel 2 from Bua in Supplementary materials of [11], F¹⁴C = 1.561 ± 0.005) none of the five most recent annual bands analysed (2018-2022) have as high, or higher, F¹⁴C. F¹⁴C values in the annual bands from 2017 and 2014 do exceed the soft tissue F¹⁴C (1.722 ± 0.007 and 2.126 ± 0.008), but it seems unlikely that the turnover of carbon in mussel soft tissue would be slow enough to generate the observed soft tissue F¹⁴C. A more plausible explanation would be that F¹⁴C in the dietary carbon of *M. edulis* is higher than in DIC at the site, as a result of organic ¹⁴C discharges from Ringhals NPP or due to a delay in the food chain from primary producers feeding on DIC to diet of *M. edulis* (e.g. from 2014 or 2017).

6.7. Carbon-14 in *Fucus* spp. at Ringhals 2020-2024 [9]

For sites close to Ringhals NPP, the $F^{14}C$ data for *Fucus* spp. from Figure 20 are presented in more detail in Figure 25.

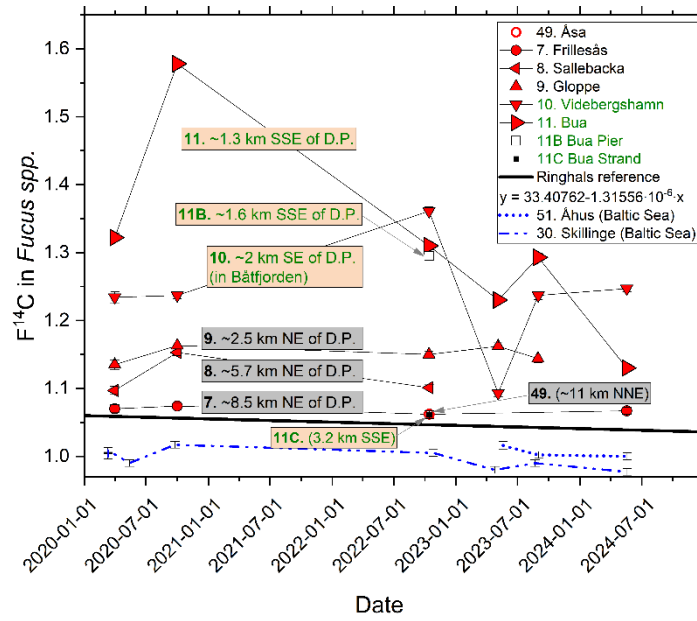


Figure 25 $F^{14}C$ in *Fucus* spp. at sites close to Ringhals NPP, and at two reference sites in the Baltic Sea (blue text and lines) for 2020-2024 (date given as YYYY-MM-DD). The sites at Ringhals NPP are ranged from north to south in the legend. Sites north of the discharge point (D.P.) of liquid effluents from the NPP are in black text, and sites south of the D.P. are in green text. The uncertainty bars represent 1σ , resulting from repeated measurement of the same sample. The thick line is the estimated Ringhals reference level (Figure 22).

The results are discussed in detail in [9], and the main findings can be summarized as:

1. The highest $F^{14}C$ is observed south of the discharge point (see Figure 10, the discharge point is referred to as “Outlet of cooling water”). This is expected since the cooling water at the outlet is directed towards the south.
2. Bua (site 11), located ~1.3 km SSE of the discharge point and south of the fjord Båtfjorden, has highest observed $F^{14}C$, corresponding to an excess in $F^{14}C$ of about 50% compared to the estimated Ringhals reference level (Figure 22).
3. Videbergshamn (site 10), located in the fjord Båtfjorden south of the discharge point, has the highest $F^{14}C$ at two sampling occasions (up to about 30% higher than the estimated Ringhals reference level).
4. *Fucus* spp. collected at Bua (site 11) and Videbergshamn (site 10) show significant temporal variations in $F^{14}C$. Varying dispersion direction of

the cooling water plume [103] in combination with fluctuating discharge rates of ^{14}C are likely to be responsible for this phenomenon.

5. At Bua strand (site 11C), located ~3.2 km SSE of the discharge point and facing open sea, sampling was performed only once (in October 2022). $F^{14}\text{C}$ in this sample overlap within 3σ with the estimated Ringhals reference level.
6. Gloppe (site 9), located ~2.5 km NE of the discharge point and close to the cooling water inlets of Ringhals NPP, has the third highest $F^{14}\text{C}$ (up to ~10% excess compared to the estimated Ringhals reference level). The cooling water is let out toward the south, but as observed by Notter [103], the plume of the discharged cooling water is frequently turned in the northerly direction due to the prevailing water currents in the area. Recirculation of discharged radionuclides in the cooling water system is thus likely to occur.
7. Sallebacka (site 8), located ~5.7 km NE of the discharge point, has up to about ~9% higher $F^{14}\text{C}$ than the estimated Ringhals reference level.
8. For Frillesås (site 7), located ~8.5 km NE of the discharge point, $F^{14}\text{C}$ is <1.8% above the estimated Ringhals reference level. For Åsa (site 49), located ~11 km NNE of the discharge point, $F^{14}\text{C}$ overlaps within 2σ with the estimated Ringhals reference level.

6.8. Carbon-14 in *Mytilus edulis* versus *Fucus vesiculosus* at Ringhals NPP in 2022

Prior to the one-year study and prior to the study resulting in paper [11], some preliminary analyses were performed of soft tissue of *M. edulis* and of *F. vesiculosus* collected in October 2022 in the area close to Ringhals NPP (see Figure 26). The more remote sites from Ringhals NPP (7. Frillesås and 8. Sallesbacka) show lower $F^{14}C$ than the sites located closer to the NPP (11. Bua, 11B. Bua Pier).

For all four sites $F^{14}C$ in soft tissue of *M. edulis* was higher than *F. vesiculosus* at the same site (see Figure 26). The highest observed value in *M. edulis* was found at Bua (site 11) with $F^{14}C = 1.892 \pm 0.007$. This is ~80% higher than in *F. vesiculosus* at site 7. Frillesås (the lowest $F^{14}C$ in Figure 26). Furthermore, individual variations in $F^{14}C$ were considerable (e.g., $F^{14}C$ varies from 1.396 ± 0.006 to 1.892 ± 0.007 at site 11. Bua). No correlation between $F^{14}C$ and age of the mussels were found. These observations support the observation (point 6 above) $F^{14}C$ in dietary carbon of *M. edulis* is higher than in DIC, possibly due to organic ^{14}C discharges from Ringhals NPP.

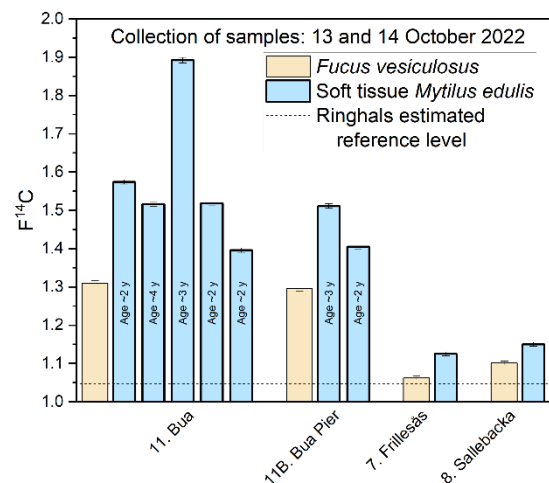


Figure 26 $F^{14}C$ in *Fucus vesiculosus* and *Mytilus edulis* collected in October 2022 at four sites in the vicinity of Ringhals NPP. The estimated Ringhals reference level (Figure 22) at the time was $F^{14}C = 1.047$.

6.9. One-year study of ^{14}C at Ringhals 2023-2024

The data from the one-year study is presented in detail in Appendix D.

Biofouling plates

The $F^{14}\text{C}$ values of organic matter collected from the biofouling plates are shown in Table 12. Material collected from biofouling plate 1 in March 2024 shows the highest $F^{14}\text{C}$ in the entire study: 8.250 ± 0.023 . The obtained values demonstrate that the liquid ^{14}C discharges from Ringhals NPP are not negligible, and that marine biota in the waters off Ringhals NPP may exhibit significant excess in ^{14}C compared to unaffected reference sites. If comparing the maximum excess in $F^{14}\text{C}$ to *F. vesiculosus* collected in Öresund and the southern Baltic Sea in 2023-2024, the typical $F^{14}\text{C}$ in *F. vesiculosus* is $\sim 1.0^3$. Särda (site 15), has $F^{14}\text{C}$ of ~ 1.03 in 2023. Hence maximum observed $F^{14}\text{C}$ in the biofouling plates is ~ 8 times the reference value.

Table 12 $F^{14}\text{C}$ in biofouling plates located close to the discharge point of cooling water at Ringhals NPP. The specific activity (A/m) has been calculated using $\delta^{13}\text{C} = -15\text{‰}$ (see Appendix A and Appendix E).

Date (YYYY-MM-DD)	Sample	$F^{14}\text{C}$	Uncertainty (1 σ)	A/m (Bq/kg carbon)
2023-12-11	Biofouling plate 1	3.494	0.011	799 ± 3
2024-01-02	Biofouling plate 2	1.897	0.007	343 ± 2
2024-03-04	Biofouling plate 1	8.250	0.023	$1.89 \cdot 10^3 \pm 5$
2024-03-04	Biofouling plate 2	3.835	0.011	877 ± 3

Marine organisms – overall results

Figure 27, Figure 28, Figure 29 and Figure 30 show all $F^{14}\text{C}$ data in the investigated marine organisms based on season. For comparison, grass (representing $F^{14}\text{C}$ in atmospheric CO_2) is also included for a few sites, as well as *F. vesiculosus* and grass for a reference site in the Baltic Sea. Several interesting observations emerge from

Firstly, considering the magnitude of the measured $F^{14}\text{C}$:

1. The fish *S. melops* has the highest $F^{14}\text{C}$ values, up to $F^{14}\text{C} = 5.058 \pm 0.017$ for one individual caught in August 2023.
2. *Fucus vesiculosus* is often lowest in $F^{14}\text{C}$ for each site.

³ *Fucus vesiculosus* from Öresund and Baltic Sea in 2023: $F^{14}\text{C} = 1.000$ (N=4), σ 0.009, SUM 0.004 51. C. Bernhardsson, K. Eriksson Stenström and G. Pédehontaa-Hiaa. *Radiological environmental monitoring at the ESS facility - annual report 2023*. BAR-2025-01. Lund University. 2025.; 2024 $F^{14}\text{C} = 0.995$ (N=5), σ 0.005, SUM 0.002; 56. C. Bernhardsson, K. Eriksson Stenström and G. Pédehontaa-Hiaa. *Radiological environmental monitoring at the ESS facility - annual report 2024*. BAR-2025-03. 2025.

3. *Fucus vesiculosus* and *M. gigas* show similar $F^{14}C$ (the number of samples of *M. gigas* is however limited, making this statement rather weak).
4. $F^{14}C$ in *M. edulis* is generally higher than in *F. vesiculosus* and *M. gigas*.
5. *Cancer pagurus* appears to have somewhat higher $F^{14}C$ than *F. vesiculosus*.

Secondly, considering variation in $F^{14}C$ within species:

1. $F^{14}C$ varies significantly for different individuals of *S. melops*, even for individuals collected at the same site and at the same time (e.g. at SLU3/22 $F^{14}C$ varies between 2.443 ± 0.008 to 5.058 ± 0.017 for samples collected in summer/autumn 2023, see Figure 28). These variations, which are more pronounced for *S. melops* than for any of the other species collected, may be a result of the relatively large size of the habitat of this fish and different dietary preferences between individuals.
2. For *M. edulis* soft tissue $F^{14}C$ varies between individuals collected at the same site. For spring 2023, the highest $F^{14}C$ value ($F^{14}C = 1.561 \pm 0.005$) of a *M. edulis* individual collected at site SLU5b Bua lighthouse is 16% higher than for the individual with the lowest $F^{14}C$ ($F^{14}C = 1.345 \pm 0.005$). For the *M. edulis* samples collected at 11. Bua in 2022 the corresponding ratio was 36%, see Figure 26.
3. Also *M. gigas* show interindividual variations in $F^{14}C$ (samples only collected at site SLU3/22).

Thirdly, considering variation in $F^{14}C$ between sites:

1. The highest $F^{14}C$ values in *F. vesiculosus* and *M. edulis* are observed at the site closest to the outlet of cooling water (site SLU3/22).
2. For *F. vesiculosus* which is most abundantly collected sample type at the different sites, the $F^{14}C$ values reflect the pattern of the dispersed cooling water plume. Apart from site SLU3/22 (at the cooling water outlet), the site SLU 5b Bua lighthouse (~1.4 km SSE of the cooling water outlet) is the most affected site followed by SLU8 Gyltan (~1.0 km SW of the outlet). Differences in $F^{14}C$ for the sites located further away from the cooling water outlet are discussed below.
3. For *S. melops*, the highest $F^{14}C$ in spring 2023 was found at site SLU7 N Horten (~3.6 km S of the cooling water outlet), and for autumn/winter it was found at SLU3/22 (at the cooling water outlet).

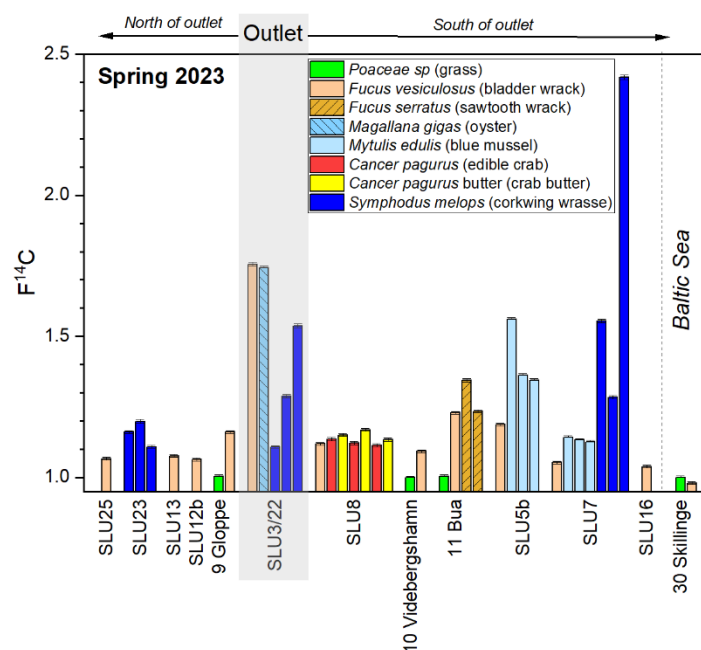


Figure 27 $F^{14}C$ in marine organisms and terrestrial grass collected in the Ringhals area and at the Skillinge reference site in the Baltic Sea in spring 2023.

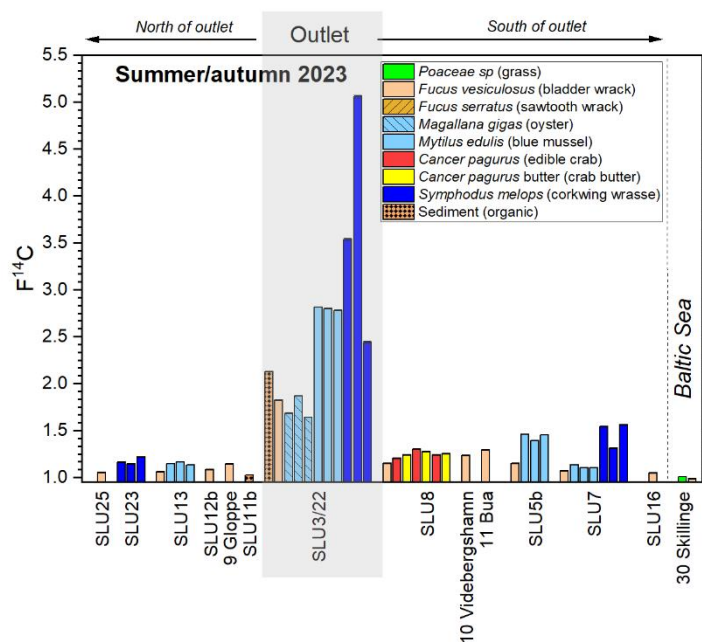


Figure 28 $F^{14}C$ in marine organisms and terrestrial grass collected in the Ringhals area and at the Skillinge reference site in the Baltic Sea in summer/autumn 2023.

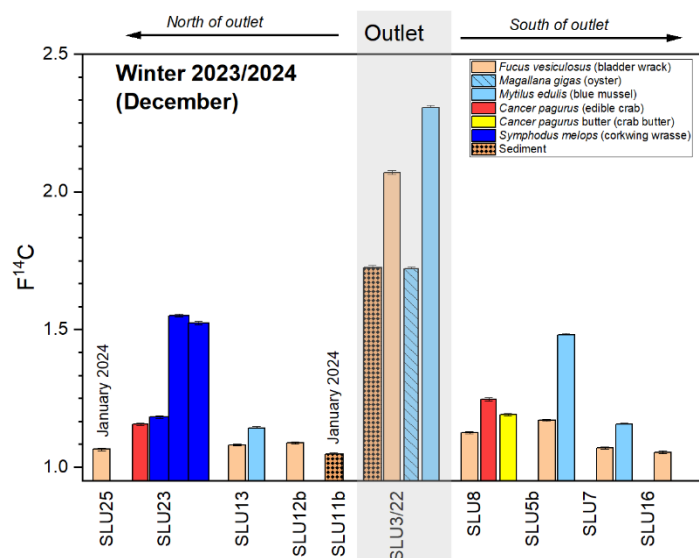


Figure 29 F¹⁴C in marine organisms and terrestrial grass collected in the Ringhals area and at the Skillinge reference site in the Baltic Sea in winter 2023/2024. All samples except the *Symphodus melops* samples at site SLU23 are pooled samples containing 3 individuals.

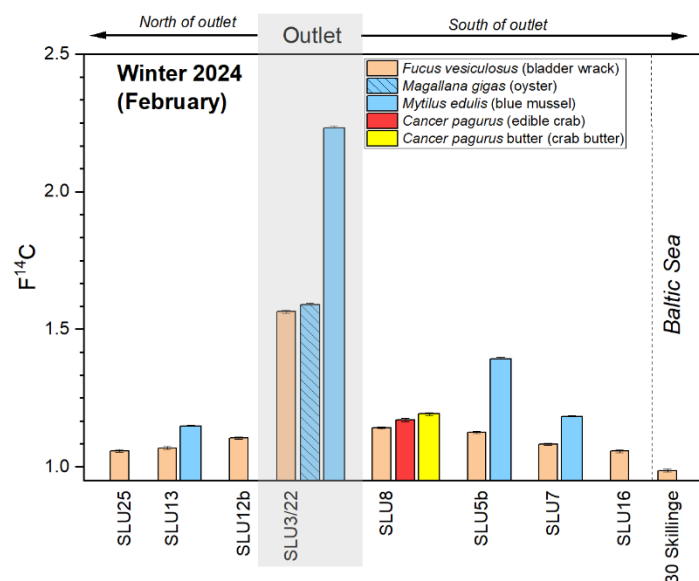


Figure 30 F¹⁴C in marine organisms and terrestrial grass collected in the Ringhals area and at the Skillinge reference site in the Baltic Sea in winter 2024 February. All samples are pooled samples containing 3 individuals. Corkwing wrasse was not available.

Marine organisms – detailed observations

Algae - *Fucus vesiculosus*

The $F^{14}C$ values of *F. vesiculosus* as a function of collection date for the different sites in the one-year study are presented in Figure 31. The shaded lower part of the upper figure is enlarged in the lower figure. $F^{14}C$ is as expected highest at site SLU3/22 which is located near the discharge point and in the flow direction of the discharged water. $F^{14}C$ varies over the year, and for the investigated period the maximum value was in winter (13 December 2023; $F^{14}C = 2.070 \pm 0.007$, i.e. ~twice the reference level). The lowest value at the discharge point (13 February 2024; $F^{14}C = 1.564 \pm 0.006$, i.e. ~50% above the reference level).

Figure 31 also shows if the sites are located in north or south of the outlet. The two sites showing the second and third highest $F^{14}C$ values (all below $F^{14}C = 1.2$) are located south of the discharge point: SLU5b (Bua at lighthouse, ~1-4 km SSE of the discharge point) and SLU8 (Gyltan, ~1.0 km SW of the discharge point). The pattern of how $F^{14}C$ varies over the year is not the same for the 3 sites with the highest $F^{14}C$ values. This is likely due to changes in currents over the year, as observed in previous studies (see section 4.2.3).

The effect of the northern direction of the Baltic current, twisting the dispersed cooling water plume towards the north, is seen when comparing $F^{14}C$ of the rest of the sites in Figure 31 (SLU7 N Horten, SLU16 Knarrskär, SLU12b Stavder, SLU13 Ustö and SLU25 Näsbykrok). The northernmost site (SLU25 Näsbykrok, located ~9.3 km N of the discharge point) appears more affected than the southernmost site SLU16 Knarrskär, located ~7.7 S of the discharge point). However, $F^{14}C$ in the southernmost site SLU16 may be affected (lowered) by the outflow of river Viskan in Klosterfjorden (see Figure 10).

Examining the lowest part of Figure 31, there seems to be a trend of increasing $F^{14}C$ over time. The same trend is seen during this period in Skagerrak in Figure 21. Excess ^{14}C from Ringhals NPP is therefore hence added on top of the ^{14}C from La Hague and Sellafield. Future environmental monitoring of ^{14}C in the marine environment around Ringhals NPP should preferably include sites located further from the discharge point than those shown in Figure 31 (both to the north and south), in order to obtain relevant reference values.

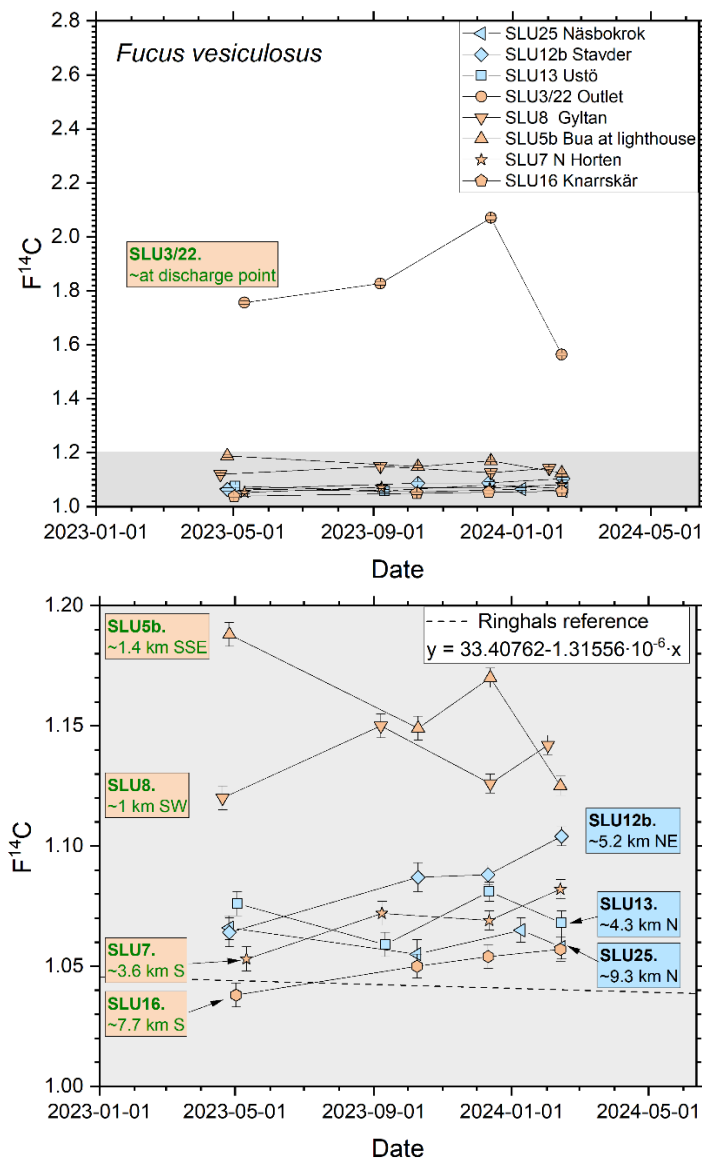


Figure 31 $F^{14}C$ in *Fucus vesiculosus* as a function of collection date for various sites close to Ringhals NPP. Approximate distances from the release point of liquid discharges are listed. The lower figure is an enlargement of the lower shaded part in the upper figure.

Molluscs – *Mytilus edulis* and *Magallana gigas*

The results of $F^{14}C$ over one year in soft tissue of *M. edulis*, which were collected at four sites, are shown in Figure 32. Three individuals from each site were analysed separately for the samplings in spring and summer/autumn 2023, to study the homogeneity of $F^{14}C$ in the mussel population. For the other two sampling occasions, three individuals were pooled into one sample at each site. For the outlet (site SLU3/22), *M. edulis* displayed the highest values in summer/autumn 2023. This is in not as seen in *F. vesiculosus* (Figure 31), for which $F^{14}C$ peaked in winter 2023/2024. These differences may not be surprising since *F. vesiculosus* reflects ^{14}C in DIC and *M. edulis* mirrors ^{14}C in dietary carbon of this species.

SLU5b (Bua lighthouse, ~1-4 km SSE of the discharge point) has the second highest values for the sites where *M. edulis* was collected (in agreement with what observed for *F. vesiculosus*, see Figure 31). As seen in Figure 32 (and in Figure 27 and Figure 28), the variation in $F^{14}C$ is most pronounced at SLU5b (Bua lighthouse). SLU7 (N Horten, ~3.4 km south of the outlet) and SLU13 (Ustö, ~4.3 km N of the outlet) display similar values in $F^{14}C$ for all seasons. As described above, $F^{14}C$ in *M. edulis* is elevated (4-9% higher) compared to *F. vesiculosus* also for these sites. This observed excess stems from the NPP, in view of the results found at Särödal and Båtevik (see section 6.6.2) where ^{14}C in *Fucus* spp. overlapped with $F^{14}C$ in *M. edulis* soft tissue.

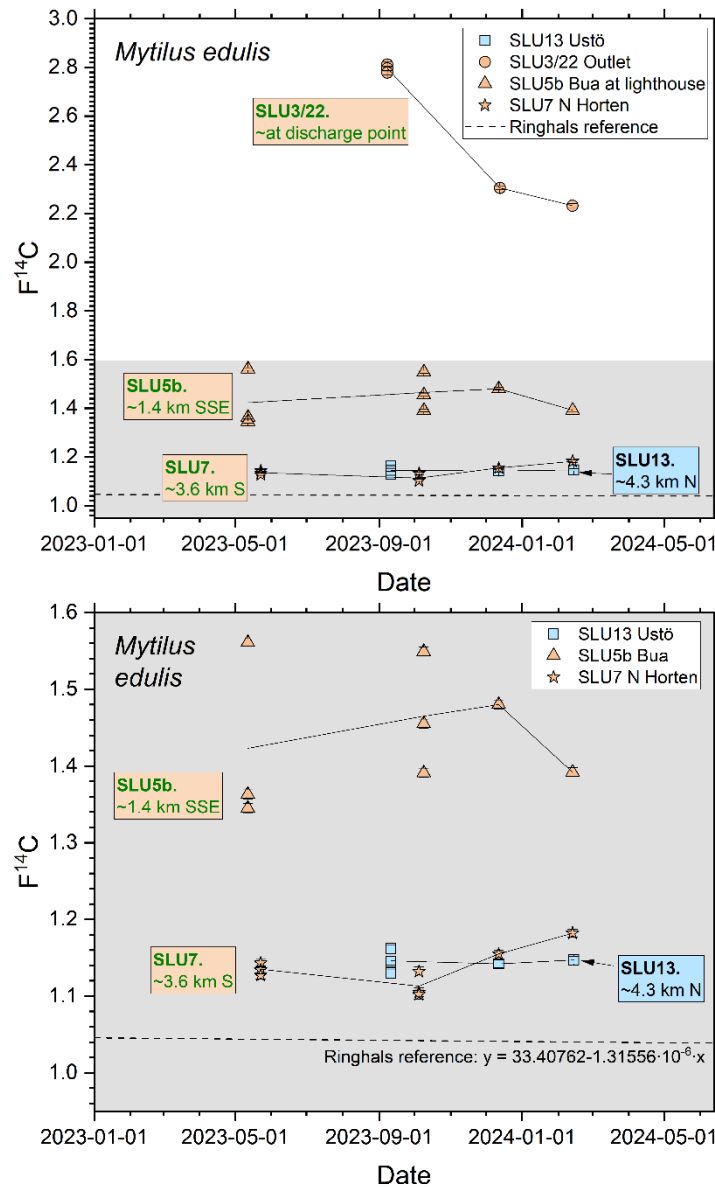


Figure 32 $F^{14}C$ in soft tissue of *Mytilus edulis* as a function of collection date for various sites close to Ringhals NPP. Approximate distances from the release point of liquid discharges are listed. The lower figure is an enlargement of the lower shaded part in the upper figure. For data from winter 2023/2024 and in winter 2024, $F^{14}C$ is measured in pooled samples containing three individuals.

$F^{14}C$ in *M. gigas* collected at the four different seasons at the outlet of cooling water (site SLU3/22) is shown in Figure 33. As for *M. edulis*, $F^{14}C$ appears slightly lower at the fourth season (winter 2024) than at the third (winter 2023/2024). However, due to the large intra-individual variations in $F^{14}C$, such trends must be considered speculative.

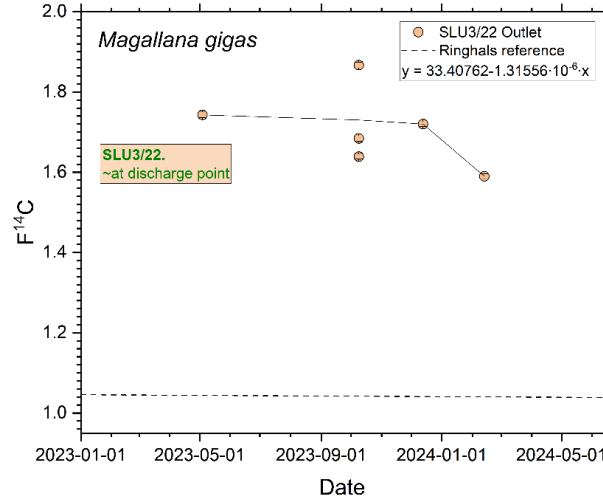


Figure 33 $F^{14}C$ in soft tissue of *Magallana gigas* as a function of collection date for site SLU3/22 (at the outlet of cooling water). Approximate distances from the release point of liquid discharges are listed. The data from spring 2023 is from one single individual. For data from winter 2023/2024 and in winter 2024, $F^{14}C$ is measured in pooled samples containing three individuals.

Arthropods – *Cancer pagurus*

The results of $F^{14}C$ over one year in soft tissue and butter of *C. pagurus*, which were collected at site SLU8 at all four seasons, are shown in Figure 34. For the first two sampling occasions (spring 2023 and summer/autumn 2023) three individuals were analysed separately. For the two other samplings (winter 2023/2023 and February 2024) three individuals were pooled into one prior to ^{14}C analysis. The highest values were seen in summer/autumn 2023.

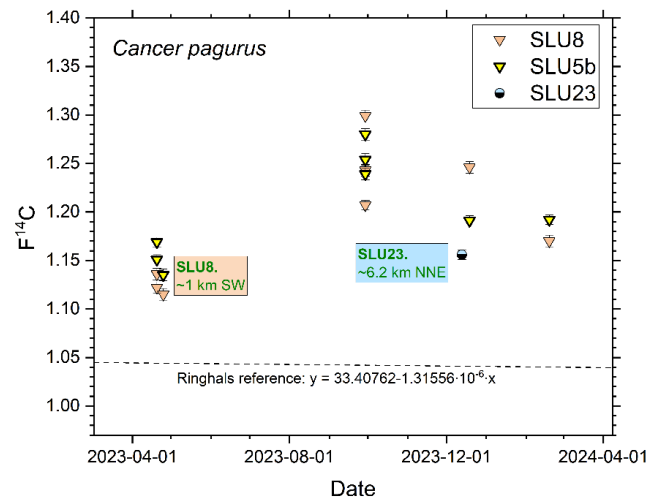


Figure 34 $F^{14}C$ in soft tissue of *Cancer pagurus* as a function of collection date for site SLU8 and SLU23. Approximate distances from the release point of liquid discharges are listed. The data from spring 2023 is from one single individual. For data from winter 2023/2024 and in winter 2024, $F^{14}C$ is measured in pooled samples containing three individuals.

Fish – Symphodus melops

Figure 35 shows $F^{14}C$ in fillet of single individuals of *Symphodus melops*, collected at three seasons at the outlet (SLU3/22) and at SLU23 and SLU7. The highest values are seen in summer/autumn 2023 at the outlet.

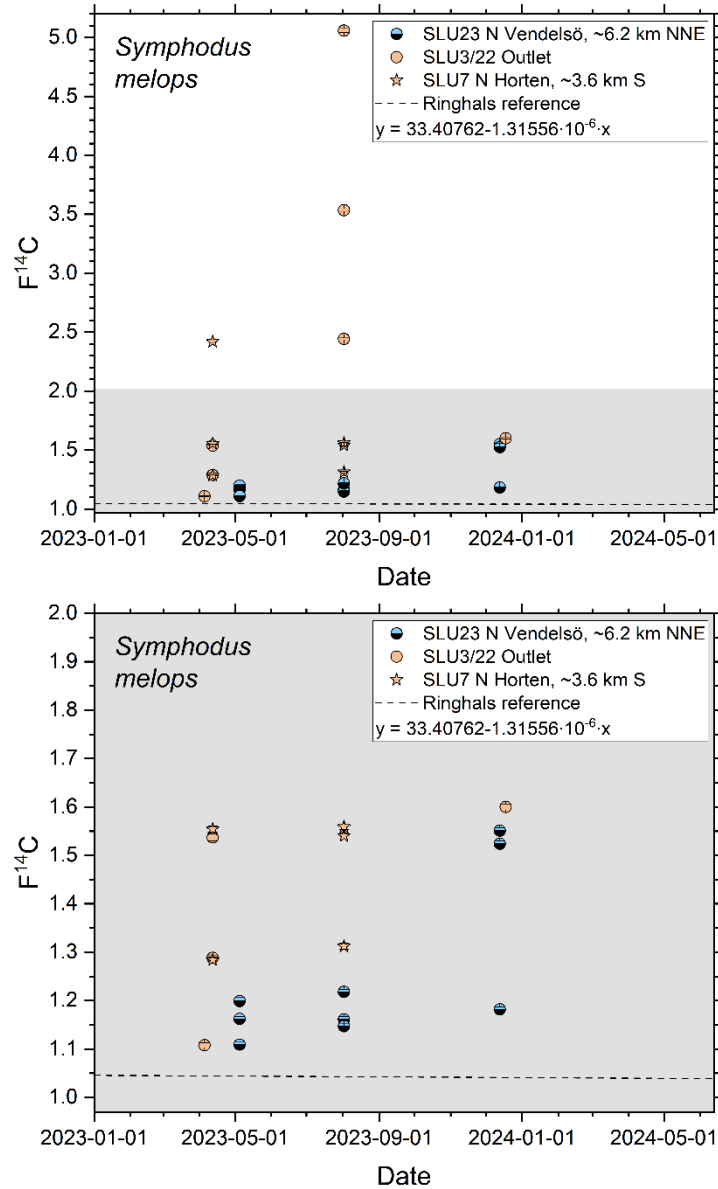


Figure 35 $F^{14}C$ in soft tissue of *Symphodus melops* as a function of collection date for site SLU23, SLU3/22 and SLU7. The lower figure is an enlargement of the lower shaded part in the upper figure. Approximate distances from the release point of liquid discharges are listed.

6.10. Sediments

F¹⁴C in sediments collected between 30 August and 1 September 2023 for a number of sites in Skagerrak and Kattegat and for a reference site in the Baltic Sea are shown in Table 13. Since the sediments were pretreated with AAA, removing carbonates, F¹⁴C should represent the organic fraction of the sediments.

Table 13 F¹⁴C in sediments.

Site	Date (YYYY-MM-DD)	LuS	F ¹⁴ C	Unc (1 σ)
SLU11b Södra Ledskär	2023-07-05	LuS 19631	1.022	0.005
	2024-01-02	LuS 20093	1.048	0.005
SLU3/22 Outlet	2023-07-05	LuS 19632	2.128	0.008
	2023-12-11	LuS 20086	1.725	0.007
1. Båteviken	2023-08-30	LuS 19625	1.011	0.005
46. Lysekil	2023-08-30	LuS 19629	1.035	0.005
4. Stockevåg	2023-08-30	Lus 19626	1.004	0.005
9. Ringhals Gloppe	2023-08-30	Not enough carbon		
10. Videbergshamn	2023-08-31	LuS 19627	1.435	0.006
11. Bua	2023-08-31	LuS 19628	1.743	0.010
50. Arild	2023-08-31	Not enough carbon		
51. Åhus	2023-09-01	LuS 19630	0.913	0.005

Some observations:

- F¹⁴C in sediments from SLU11b (Södra Ledskär) are low compared to sediments from SLU3/22 (Outlet).
- Higher F¹⁴C values have been found in *S. melops* and *M. edulis* than in sediments from SLU3/22 (Outlet) (compare Table 13 and Figure 28).
- Higher F¹⁴C values were found in 10 Videbergshamn, close to Ringhals NPP, than at sites remote from the NPP (samples collected 2023-08-30 and 2023-08-31 in Table 13).

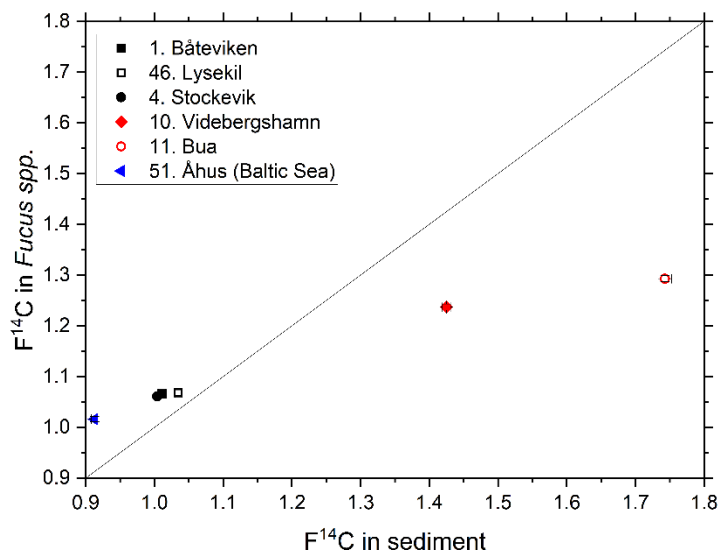


Figure 36 F¹⁴C in sediments collected 30 August to 1 September 2023 at sites in Skagerrak and Kattegat on the Swedish west coast, and at one reference sites in the Baltic Sea. The solid line represents a 1:1 ratio. Uncertainty bars represent 1 σ , resulting from repeated measurement of the same sample.

In Figure 36, F¹⁴C has been plotted for the organic fraction of sediments and *F. vesiculosus* for samples collected at the same occasion. For the sites 2 Båteviken, 46 Lysekil, 4 Stockevik and 51 Åhus (Baltic Sea), F¹⁴C is slightly lower in the organic fraction of sediments than in *F. vesiculosus*. This may possibly indicate that a fraction of the sediments (which were collected close to shore) is of terrestrial origin (see e.g. Figure 17 or Figure 23, demonstrating that F¹⁴C in marine organic matter is higher than F¹⁴C in the terrestrial biota). For site 10 Videbergshamn and 11 Bua close to Ringhals NPP F¹⁴C in sediment is higher than for *F. vesiculosus* collected at the same occasion. This could reflect that organic marine material other than *F. vesiculosus* has higher F¹⁴C than *F. vesiculosus* (as seen e.g. in Figure 28).

6.11. Particulate carbon

Particulate carbon has been collected in the beginning of 2024 at three different sites: the Baltic Sea reference site 30 Skillinge, site 46 Lysekil and site 10 Videbergshamn close to Ringhals NPP.

F¹⁴C in particulate carbon from site 30 Skillinge is shown in Figure 37 together with F¹⁴C in *F. vesiculosus* and terrestrial grass from the same site. Particulate carbon is significantly lower in F¹⁴C than in *F. vesiculosus* and terrestrial grass. One speculation is that the low values are due to influence from the large amounts of oil released from ship Marco Polo, which ran aground at Pukavik 22 October 2023 (~75 km NNE of Skillinge), releasing 150 ton of bunker oil (HFO, RMG380) [114].

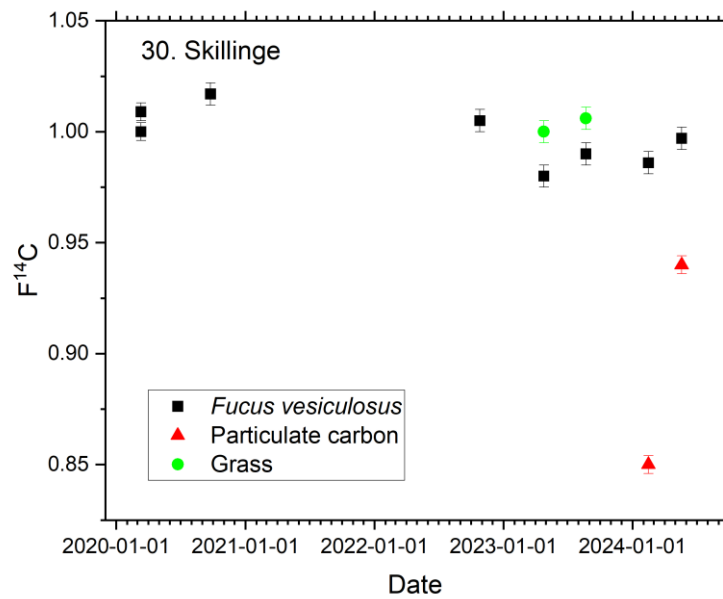


Figure 37 Particulate carbon collected at site 30 Skillinge compared to *Fucus vesiculosus* and terrestrial grass collected at the same site.

At site 46 Lysekil (see Figure 38), particulate carbon is lower than *Fucus* spp., but higher than terrestrial grass. Sediments and particulate carbon show similar F¹⁴C values.

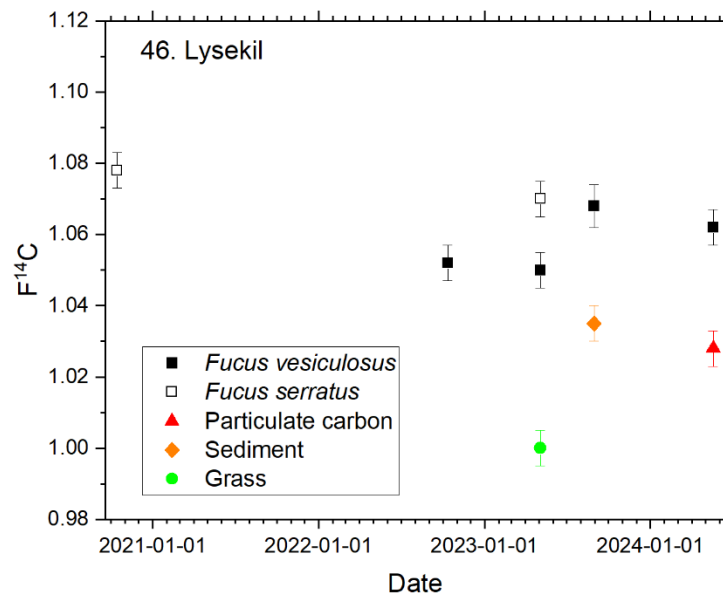


Figure 38 Particulate carbon collected at site 46 Lysekil compared to *Fucus* spp., sediment and terrestrial grass collected at the same site.

For the site close to Ringhals NPP – site 10 Videbergshamn – F¹⁴C values in particulate carbon, sediment, *F. vesiculosus* and terrestrial grass are shown in Figure 39. From this single measurement it is indicated that F¹⁴C in particulate

carbon is significantly higher than in *F. vesiculosus* (representative of DIC) as well as in sediment and terrestrial grass. It must be noted that the particulate carbon sample is a grab sample, whereas the other sample types represent longer time periods. Still, this observation may support the observations in e.g. Figure 28, that filter feeders such as *M. edulis*, feeding on particulate carbon, have higher $F^{14}C$ values than observed in DIC.

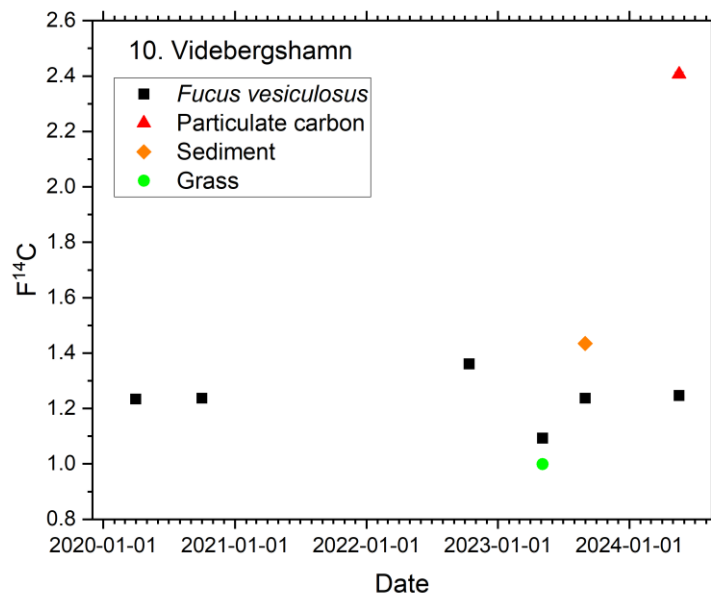


Figure 39 Particulate carbon collected at site 10. Videbergshamn compared to *Fucus* spp., sediment and terrestrial grass collected at the same site.

6.12. Trophic levels and carbon content

The results of the EA-IRMS measurements of some samples of *F. vesiculosus*, *M. edulis* (soft tissue), *S. melops* (soft tissue), *M. gigas* (soft tissue), and *C. pagurus* (soft tissue and butter) are presented in Appendix E. This information is e.g. of interest for conversion of $F^{14}C$ to Bq/kg d.w.

6.13. Technetium-99

The ^{99}Tc concentration in *Fucus* spp. from Särda (2002–2024) and Ringhals (2023) are shown in Figure 40, and the reported liquid discharges of ^{99}Tc from Sellafield and La Hague are presented in Figure 41 [10]. The ^{99}Tc concentrations in *F. vesiculosus* collected at Ringhals (SLU3 at cooling water outlet and SLU 7 located ~3.5 km south of the cooling water outlet) overlap with the Särda results. Hence, there is no evidence of liquid ^{99}Tc discharges from Ringhals NPP.

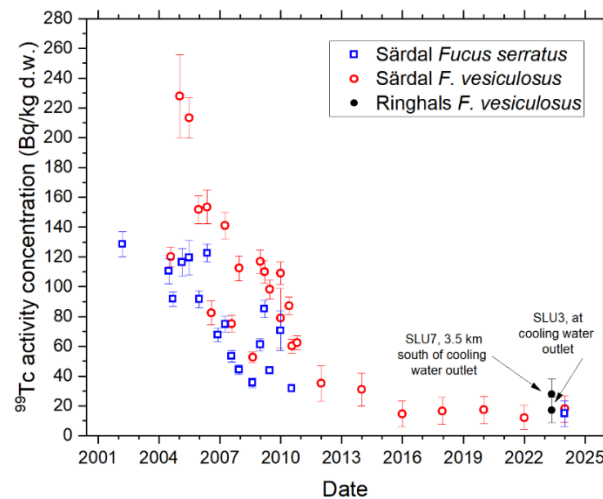


Figure 40 Technetium-99 in *Fucus* spp. at Särda and at two samples from Ringhals NPP. Sampling rate of the Ringhals samples: 11 May 2023.

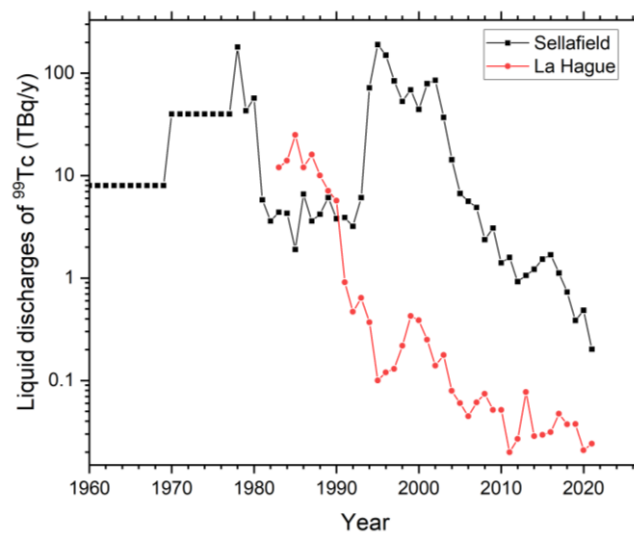


Figure 41 Reported releases of ^{99}Tc from the reprocessing facilities at Sellafield and La Hague [27, 115, 116].

6.14. Radioecological discussion

The results of this study are reported as $F^{14}\text{C}$, which is the specific activity of carbon in a sample, normalized to $\delta^{13}\text{C} = -25\text{‰}$. If all organisms in the marine compartment were in equilibrium with DIC, $F^{14}\text{C}$ would have been identical for all organisms, and the same as in DIC. This most simple form of the specific activity approach, assuming that ^{14}C is discharged only as DIC from Ringhals NPP and $F^{14}\text{C}$ is identical in all marine compartments, is – as expected from previous studies (e.g. [21, 22, 117]) – not applicable for marine biota in the Ringhals area.

The general trend seen at Ringhals NPP (see e.g. Figure 28) is that *F. vesiculosus* (representative of DIC in the seawater) has the lowest $F^{14}\text{C}$ of the different sample types and marine species investigated. Mussels (filter-feeders) generally have higher $F^{14}\text{C}$ than *Fucus* spp. collected at the same site. The highest $F^{14}\text{C}$ values have been observed in muscle tissue of the omnivorous fish *S. melops*. Several previous studies observing similar patterns associate these differences to species-specific feeding habits and various turnover of carbon in the organism. However, we believe, as suggested by [71, 72], that liquid discharges of water-soluble organic compounds play a significant role.

The liquid ^{14}C discharges from Ringhals NPP are expected to mainly consist of DIC. However, as seen in Table 6, previous measurements of 5 samples from R3 and R4 showed that the organic fractions of the wastewater (DOC) at the Ringhals PWRs were 19%, 29%, 34% and 90% in the four samples with measurable ^{14}C activities [82]. These numbers regard fractions of the ^{14}C activity per kg of water. However, for uptake of carbon into living organisms, the stable carbon isotopes also need to be considered.

Seawater at Ringhals NPP has a natural DIC concentration of about 100 mg/L through the main part of the year, according to Engdal [42]. The specific activity of DIC in seawater resulting from ^{14}C -DIC discharges from the NPP, thus depends not only on the amount of discharged ^{14}C , but also on the DIC concentration in the seawater. The organic carbon fraction in the seawater is normally much lower than DIC. The total organic carbon is typically only a few mg/L [42], mainly constituting of DOC and only to a minor fraction of POC. Any organic liquid ^{14}C discharges from the NPP will hence not be diluted to the same extent as discharged ^{14}C -DIC.

The chemical speciation of the organic ^{14}C -releases is not known, but as stated above, it may be in the form of acetate or formate [7]. The report [82] points out that organic compounds may be converted into inorganic compounds and vice versa in both wastewater tanks and sampling bottles by e.g. microbial activity. Despite these uncertainties, it is reasonable to assume that organic compounds are discharged from R3 and R4 with the wastewater in fractions that are not negligible.

In general, uptake of organic molecules in marine biota may occur as a direct transfer from seawater to the organism (bioconcentration through respiration) or be bioaccumulated in the organism through all possible pathways, including contact, respiration and ingestion. Biomagnification may possibly also occur when organic compounds are transferred to higher trophic levels, resulting in higher concentrations compared to the source. In particular, fatty tissues of marine biota such as fish can accumulate organic compounds. These

mechanisms may account for the observations that $F^{14}\text{C}$ is higher in mussels (*M. edulis*) and fish (*S. melops*) than in *F. vesiculosus* (given that the latter only absorbs ^{14}C in the more diluted form of DIC). It can also be speculated if parts of the organic compounds can be transferred to POC by microbial absorption of acetate [118, 119] already in the liquid waste storage tanks of the NPP prior to discharge to the sea.

Only one sample of Particulate Carbon (POC + PIC) was sampled close to Ringhals NPP at site 10 Videbergshamn (sampling date 18 May 2024). The $F^{14}\text{C}$ value, 2.407 ± 0.008 , was significantly higher than in any of the 6 samples of *F. vesiculosus* collected at the same site between March 2020 and May 2024 (range 1.093 ± 0.005 to 1.361 ± 0.006). The Particulate Carbon $F^{14}\text{C}$ was also considerably higher than in the single sediment sample collected at the same site ($F^{14}\text{C} = 1.435 \pm 0.006$, sampled in August 2023). It should however be noted that the sediment sample was subjected to the acid-alkali-acid pretreatment (removing carbonates and organic acids, and extracting organic solid material), whereas the Particulate Carbon sample did not undergo this pretreatment. Hence, the excess $F^{14}\text{C}$ in the Particulate Carbon sample may possibly be related to organic acids or other organic forms attaching to particulate matter.

The results of the sediment samples do not indicate that the solid organic component of sediments is a major source of ^{14}C re-entering the marine POC or PIC pool.

The radioecological transfers of ^{14}C in the marine environment at Ringhals NPP may thus be represented by Figure 42.

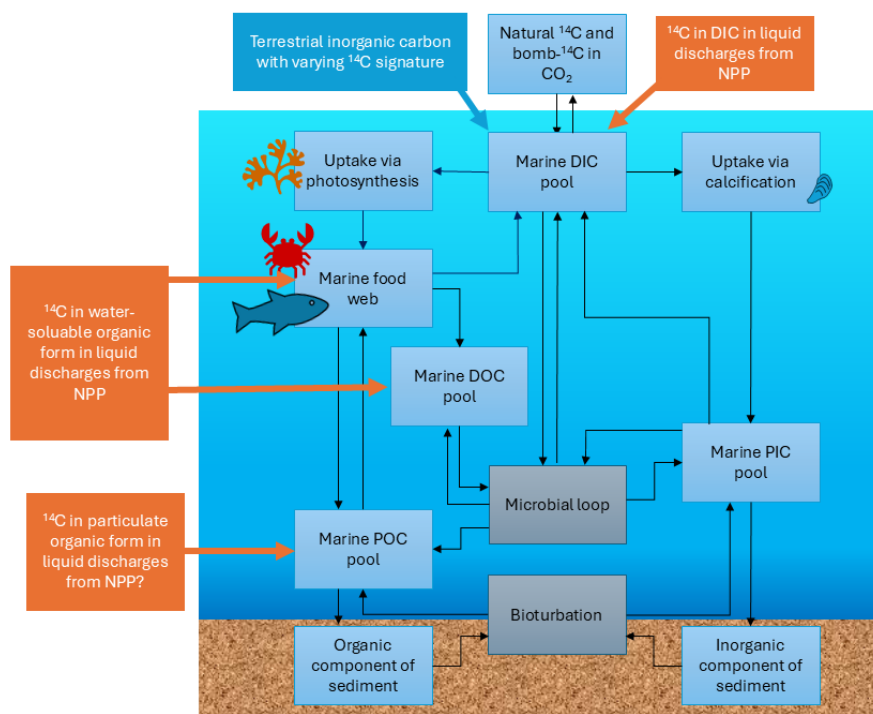


Figure 42 Updated transfer of ^{14}C from the atmosphere to and in the marine environment. DIC – dissolved inorganic carbon, PIC – particulate inorganic carbon, DOC – dissolved organic carbon, POC – particulate organic carbon. Adapted from [22].

The present study cannot evaluate the generic concentration factors listed in Table 4, or produce site-specific concentration factors, since ^{14}C was not measured in water samples. Since the Ringhals area is characterized by fluctuating water current that change direction frequently, such investigations are difficult to perform, since grab samples may not be representative of the average ^{14}C concentration of the different carbon-containing fractions. However, for dose assessment purposes, environmental concentrations in biota, which are provided in this report, are more useful than concentration factors.

7. Summary and conclusions

A one-year study has been conducted on ^{14}C in the marine environment of Ringhals NPP to evaluate the radioecological fate of liquid ^{14}C discharges from the NPP. In contrast to airborne ^{14}C releases, the discharge of ^{14}C to the marine environment is not monitored at Swedish NPPs. Neither is ^{14}C analysis included in the regular environmental monitoring programmes of Swedish NPPs. The amounts of ^{14}C discharged to water has previously been assessed, based on a few measurements to be significantly less ($<0.5\%$) than the airborne releases from Ringhals NPP [7]. In total, Ringhals AB estimates the total ^{14}C liquid discharges from the two operational PWRs to be 9 and 8 GBq per year in 2022 and 2023, respectively [4, 5]. Regarding the chemical form of the liquid ^{14}C discharges in terms of inorganic and organic carbon, only a few measurements have been done in the past (in 2006) on water in the wastewater tanks [82]. In 3 of the 4 samples analysed from the waste water tanks of the PWRs the inorganic form dominated (the organic fraction being 19%, 29% and 34%), and for the fourth sample the organic form dominated (90% organic) [82]. The chemical form of the organic ^{14}C -releases is not known, but may be acetate or formate [7].

To evaluate the impact of ^{14}C discharged from Ringhals NPP it is necessary to establish a reference level, corresponding to the ^{14}C levels in the marine environment in the hypothetical absence of the NPP. Carbon-14 concentrations in the marine environment are influenced by several sources and phenomena giving temporal variations in the relevant reference levels. Marine coastal sites that are not influenced by any anthropogenic ^{14}C discharges, and that are not affected by influence from ^{14}C -depleted DIC from rivers or upwelling of old bottom water, currently (2025) have a $F^{14}\text{C}$ of ~ 1.0 (approximately the same as in the contemporary atmosphere). This is not the case for Ringhals NPP, nor for the entire Swedish west coast, in particular for Skagerrak and Kattegat. Carbon-14 discharged to water from the reprocessing plants for spent nuclear fuel in France (La Hague) and Great Britain (Sellafield) reach the Swedish west-coast via water currents from the North Sea. We have seen in samples of *F. vesiculosus* (absorbing DIC from the surrounding seawater) sampled between 2020 and 2024 that $F^{14}\text{C}$ increases towards the north of the west coast, and that northernmost Skagerrak have up to $\sim 10\%$ higher $F^{14}\text{C}$ values than at Swedish coastal Baltic Sea sites in southern Sweden. In the Särödal *Fucus* spp. series, beginning in 1967, we see a correlation between annual discharged amounts from the reprocessing facilities and $F^{14}\text{C}$ in *Fucus* spp. at Särödal. Since the end of the 1990ies, we estimate that the excess $F^{14}\text{C}$ in *Fucus* spp. at Särödal has been between 0.030 and 0.063, with an average of ~ 0.047 (corresponding to an excess specific activity of ~ 11 Bq per kg C). For the observations we have seen during studies of $F^{14}\text{C}$ in *Fucus* spp. collected at various sites along the Swedish coast, we conclude that appropriate choice of reference sites is fundamental, and that the current geographical area covered in the regular environmental monitoring programme would need to be extended, to the north as well as to the south of the NPP.

In the present one-year study of ^{14}C in the marine environment of Ringhals NPP, sampling sites were selected from the regular environmental monitoring programme at Ringhals NPP. The sampling sites were located close to the coast up to ~ 9 km north and 8 km south of the NPP's cooling water outlet. The sample

types and organisms were biofouling plates, *Fucus vesiculosus* (bladderwrack), *Symphodus melops* (corkwing wrasse), *Mytilus edulis* (blue mussel), *Magallana gigas* (pacific oyster), *Cancer pagurus* (crab), sediment and particulate carbon. The different sample types represent various compartments in the marine ecology. The biofouling plates are located in the eutrophic zone to allow photosynthetic growth of e.g. diatoms and filamentous green algae. *Fucus vesiculosus* is a sessile species that absorbs ^{14}C in the form of DIC through photosynthesis from the surrounding water. *Mytilus edulis* (semi-sessile) and *M. gigas* (sessile) are two different types of filter-feeding molluscs (which may not have identical diets). Non-migratory males of *C. pagurus* are used as representative of arthropods, and feed on various animals in the benthic environment. *Symphodus melops*, the representative of fish, is a non-migratory omnivorous opportunist living close to the seafloor. Sediments represent organic carbon from the recent past, and particulate matter collected on filters represents carbon in particulate form in the seawater.

The highest concentrations of ^{14}C (up to $F^{14}\text{C} = 8.250 \pm 0.023$, i.e. ~700% above the contemporary reference levels of $F^{14}\text{C} \approx 1$) were found in organisms residing on a biofouling plate located close to the cooling water outlet of the NPP (sampling in March 2024). The second highest specific activity of carbon (up to $F^{14}\text{C} = 5.058 \pm 0.017$, i.e. approximately 400% above the contemporary reference level) was found in soft tissue of the fish *S. melops* (corkwing wrasse) caught close to the cooling water outlet in August 2023. For all *S. melops* samples analysed, collected at the cooling water outlet SLU3 (7 samples), at SLU23 N. Vendelsö (~6.2 km NNE of the discharge point, 9 samples) and SLU7 N Horten (~3.6 km S of the discharge point, 6 samples), $F^{14}\text{C}$ varies between 1.108 ± 0.017 and 5.058 ± 0.017 with a median $F^{14}\text{C}$ of 1.418 and a mean of 1.704.

The general trend is that *F. vesiculosus*, representative of DIC, is often lowest in $F^{14}\text{C}$ for each site. *Symphodus melops* has the highest ^{14}C specific activity followed by soft tissue of *M. edulis*. *Magallana gigas* (soft tissue) has usually lower $F^{14}\text{C}$ than *M. edulis*, and show $F^{14}\text{C}$ values similar to *F. vesiculosus*. *Cancer pagurus* appears to have somewhat higher $F^{14}\text{C}$ than *F. vesiculosus*. In one single sample of Particulate Carbon (POC and PIC) collected at site 10 Videbergshamn in Båtfjorden, $F^{14}\text{C}$ was significantly (77-120%) higher than in any of the *F. vesiculosus* samples collected at the same site. We believe that liquid discharges of water-soluble organic compounds play a significant role in the observed excess in $F^{14}\text{C}$ in the Particulate Carbon sample, and also in e.g. *S. melops* and *M. edulis*. Bioconcentration of organic compounds through respiration, or bioaccumulation through contact, respiration and ingestion may be involved for the fish and mussels. It can also be speculated if the organic compounds discharged from the NPP can accumulate in fatty tissues of fish.

The spatial variability in marine $F^{14}\text{C}$ at Ringhals NPP is best reflected in the most frequent sample type, *F. vesiculosus*. The highest $F^{14}\text{C}$ value is shown at the outlet, and south of the outlet (SLU5b Bua at lighthouse, ~1-4 km SSE of the discharge point, and SLU8 Gyltan, ~1.0 km SW of the discharge point), which is consistent with the fact that the cooling water is discharged in southerly direction. $F^{14}\text{C}$ in *F. vesiculosus* samples also demonstrates how the Baltic current twists the dispersed cooling water plume towards the north. The northernmost site, SLU25 Näsbykrok (~9.3 km N of the discharge point), appears more affected than the southernmost site SLU16 Knarrskär (~7.7 S of the discharge point). However, $F^{14}\text{C}$ at SLU16 may be affected (lowered) by the outflow of river Viskan in Klosterfjorden.

Temporal variability in $F^{14}\text{C}$ was seen during the one-year study, in particular at the site close to the cooling water outlet. No obvious overlap was seen for the temporal variation in $F^{14}\text{C}$ for the different species. This may be related to the variations in $F^{14}\text{C}$ between different individuals of the same species collected at the same time and place. E.g., three individuals of *S. melops* caught at the outlet in August 2023 had $F^{14}\text{C}$ of 5.058 ± 0.017 , 3.535 ± 0.011 and 2.443 ± 0.008 , respectively. Being an omnivorous opportunist with a relatively wide range of habitat compared to the other organisms in the study may explain the individual variability. For *M. edulis*, *M. gigas* and *C. pagurus* the variability between individuals of the same species and collected at the same site was less, but not inconsiderable. Different feeding patterns may explain this phenomenon.

The $F^{14}\text{C}$ levels observed in the marine environment of Ringhals NPP is significantly higher than what expected in the terrestrial environment. In the current study we report on measurements of ^{14}C in grass collected in the terrestrial environment of Ringhals NPP and at other sites in southern Sweden. None of the samples can be considered to have deviating $F^{14}\text{C}$ the atmospheric reference level. However, the operational PWRs at Ringhals mainly release ^{14}C as hydrocarbons, which are not accessible to vegetation by photosynthetic absorption. It should be noted that the grass samples collected at Ringhals NPP were not located in the main downwind direction of the NPP. These circumstances, in combination with an effective dilution of ^{14}C (released as CO_2) from its upward release through the 45 m high stacks to the ground level and its vegetation, account for the absence of observed ^{14}C in the grass samples from Ringhals NPP. From the literature it has been seen that light-water reactors typically give a maximum excess in the terrestrial environment of ~10% above the reference level within a few km of the power plant [82]. In the marine environment we have seen excess in $F^{14}\text{C}$ of up to 700%.

Since no previous data exist on past marine levels of ^{14}C in the Ringhals area we have evaluated the potential use of annual structures of *M. edulis* shells to estimate past liquid discharges of ^{14}C -DIC. A method was developed to extract the fibrous layer that forms visible annual structures in the shells. The approach has proven to be promising.

8. Outlook

The results of this report demonstrate that even though the liquid discharges are small compared to the total ^{14}C operational releases, the increase in $F^{14}\text{C}$ in marine biota can be substantial and much higher than in terrestrial biota. To obtain a more detailed understanding of the radioecological fate of the ^{14}C discharges from Ringhals NPP, knowledge of the various chemical and physical ^{14}C -containing fractions of the source term is fundamental. Hence, we suggest time-resolved studies to characterize ^{14}C in the discharge water. Simultaneous complementary studies of ^{14}C in various compartments of the marine environment, tentatively at the cooling water outlet (SLU3/SLU22) and at a reference site, would form a basis for a radioecological marine model for ^{14}C at Ringhals NPP. Plankton should be added to the species used in the current study, as well as analysis of the various biogeochemical fractions of seawater.

Of particular interest is to further investigate ^{14}C on the biofouling plates at the cooling water outlet. One purpose of the biofouling plates is to indicate the bioavailability of the discharges. Time-resolved measurements of ^{14}C in the discharges and of ^{14}C from the biofouling plates would reveal how well the biofouling plates reflect the actual discharges.

We also suggest further investigations of the distribution of ^{14}C in edible fish. Additional investigations are also needed to understand the differences in ^{14}C uptake in *M. edulis* and *M. gigas*. Such studies could be basis for realistic dose estimates not only to man but also to biota.

In the present study only the solid organic fraction of sediments was analysed for ^{14}C . We suggest further analysis of other biogeochemical fractions of sediments to obtain a more comprehensive description of the marine radioecology at Ringhals NPP.

Due to the relative importance of ^{14}C in dose assessments to the public, we strongly recommend that analysis of ^{14}C is included in the regular environmental monitoring programmes of Swedish NPPs. At Ringhals NPP, this is of particular importance in view of ongoing decommissioning of R1 and R2 and potential expansion of nuclear power at the Ringhals site. We also recommend that ^{14}C analysis of liquid effluents should be included in the source monitoring of Swedish NPPs.

9. Acknowledgement

This study was financed by the Swedish Radiation Safety Authority SSM (SSM2022-4035). The authors wish to thank the Radiocarbon Dating Laboratory in Lund for advice regarding sample pretreatments and for the excellent quality of the AMS-analyses. We also thank staff at the Swedish NPPs for providing data on ^{14}C releases from Swedish NPPs. We also thank staff at SLU Väröbacka for their assistance in the project, both regarding planning and sampling.

10. References

1. UNSCEAR. *UNSCEAR 2016 Report—Sources, Effects and Risks of Ionizing Radiation*. Report to the General Assembly. Scientific Annexes A, B, C, and D. United Nations Scientific Committee on the Effects of Atomic Radiation. 2016.
2. K. Aquilonius and B. Hallberg. *Process-oriented dose assessment model for ^{14}C due to releases during normal operation of a nuclear power plant*. Journal of Environmental Radioactivity, 82(3): 267-283, 2005.
3. Å. Magnusson. *^{14}C produced by nuclear power reactors - generation and characterization of gaseous, liquid and solid waste*. PhD thesis. Lund University. PhD thesis. ISBN 978-91-628-7248-9. 2007.
4. Vattenfall. *Ringhals utsläppsrappport över radioaktiva ämnen 2022*. Vattenfall 2559093 / 2.0. In Swedish. Ringhals AB, 2559093 / 2.0. (In Swedish). 2023.
5. Vattenfall. *Ringhals utsläppsrappport över radioaktiva ämnen 2023*. Ringhals AB, 2583029 / 3.0. In Swedish. Ringhals AB, 2583029 / 3.0. (In Swedish). 2024.
6. International Atomic Energy Agency. *Management of waste containing tritium and carbon-14*. Technical report series no 421, 2004.
7. Å. Magnusson, P. O. Aronsson, K. Lundgren and K. Stenström. *Characterization of ^{14}C in Swedish light water reactors*. Health Physics, 95 Suppl 2: S110-21, 2008.
8. K. Eriksson Stenström and S. Mattsson. *Spatial and temporal variations of ^{14}C in *Fucus* spp. in Swedish coastal waters*. Journal of Environmental Radioactivity, 242: 106794, 2022.
9. K. Eriksson Stenström and S. Mattsson. *Current trends in radiocarbon in Skagerrak and Kattegat assessed by brown algae from Swedish coastal waters*. Radiation protection dosimetry, <https://doi.org/10.1093/rpd/ncaf032>, 2025.
10. S. Mattsson, K. Eriksson Stenström, G. Pedehontaa-Hiaa, C. Bernhardsson, M. Jönsson, J. M. López-Gutiérrez, V. Lérída-Toro and E. Chamizo Calvo. *Radionuclides in algae from Swedish coastal waters for over half a century*. Accepted for publication in Radiation Protection Dosimetry, 2025.
11. S. Bjarheim, K. Eriksson Stenström, A. Lindskog, M. Olsson, P. Carlsson and S. Mattsson. *The potential of shells of *Mytilus edulis* for retrospective analysis of marine ^{14}C discharges from nuclear power plants*. Accepted for publication in Radiocarbon, 2025.
12. UNSCEAR. *UNSCEAR 2008 Report—Sources, Effects and Risks of Ionizing Radiation. Volume 1. Annex B. Exposures of the public and workers from various sources of radiation*. 2008.
13. K. Eriksson Stenström, G. Skog, E. Georgiadou, J. Genberg and A. Johansson. *A guide to radiocarbon units and calculations*. LUNFD6(NFFR-3111)/1-17/(2011). Lund University. Dep of Physics. Div of Nuclear Physics. <http://lup.lub.lu.se/search/ws/files/5555659/2173661.pdf>, 2011.

14. P. J. Reimer, T. A. Brown and R. W. Reimer. *Discussion: Reporting and calibration of post-bomb ^{14}C data*. Radiocarbon, 46(3): 1299-1304, 2004.
15. I. Levin and B. Kromer. *The tropospheric $^{14}\text{CO}_2$ level in mid latitudes of the Northern Hemisphere (1959-2003)*. Radiocarbon, 46: 1261-1271, 2004.
16. I. Levin, B. Kromer and S. Hammer. *Atmospheric $\Delta^{14}\text{CO}_2$ trend in Western European background air from 2000 to 2012*. Tellus B: Chemical and Physical Meteorology, 65(1): 20092, 2013.
17. S. Hammer and I. Levin. Monthly mean atmospheric D^{14}CO_2 at Jungfrauoch and Schauinsland from 1986 to 2016. . heiDATA: Heidelberg Research Data Repository [Distributor] V2 [Version]. <http://dx.doi.org/10.11588/data/10100>; www.calibomb.org. 2017.
18. F. Conen, L. Emmenegger, M. Leuenberger, D. Steger and M. Steinbacher. "ICOS RI, 2020. ICOS ATC 14C Release, Jungfrauoch (10.0 m), 2016-01-04_2019-08-12". <https://hdl.handle.net/11676/X-IXPKZIO4DWX7wnesLQ7akY>; <http://calib.org/CALIBomb/>. 2019.
19. M. Heliasz and T. Biermann. ICOS ATC/CAL 14C Release, Hyltemossa (150.0 m), 2015-09-23–2022-12-08, ICOS RI. <https://data.icos-cp.eu/portal/>. ICOS_ATC_L2_L2-2023.1_HTM_150.0_779.14C. ICOS DATA is licensed under CC4BY (<http://creativecommons.org/licenses/by/4.0/>). 2024.
20. P. J. Reimer, M. G. Baillie, E. Bard, A. Bayliss, J. W. Beck, P. G. Blackwell, C. B. Ramsey, C. E. Buck, G. S. Burr and R. L. Edwards. *IntCal09 and Marine09 radiocarbon age calibration curves, 0–50,000 years cal BP*. Radiocarbon, 51(4): 1111-1150, 2009.
21. F. Begg, G. Cook, M. Baxter, E. Scott and M. McCartney. *Anthropogenic radiocarbon in the eastern Irish Sea and Scottish coastal waters*. Radiocarbon, 34(3): 707-716, 1992.
22. K. M. Tierney. *Marine ecosystem uptake of nuclear reprocessing derived radiocarbon (^{14}C)*. PhD thesis. University of Glasgow. 2017.
23. M. Castrillejo, C. A. Richardson, R. Witbaard, R. Dekker, C. Welte, L. Wacker, C. Yeman, N. Casacuberta, H.-A. Synal and M. Christl. *Sea shells record large biases from the marine bomb- ^{14}C curve in NW European seawater between the late 1960s and 2019*. EGU General Assembly 2020. <https://ui.adsabs.harvard.edu/abs/2020EGUGA..22.1495C>, 2020.
24. G. Zazzeri, E. A. Yeomans and H. Graven. *Global and regional emissions of radiocarbon from nuclear power plants from 1972 to 2016*. Radiocarbon, 60(4): 1067-1081, 2018.
25. S. Brandt and F. Öhrlund. *^{14}C and ^3H discharges from Pressurized Water Reactors and Boiling Water Reactors*. Report BAR 2025/01. Lund University. <https://portal.research.lu.se/en/publications/14c-and-3h-discharges-from-pressurized-water-reactors-and-boiling>, 2025.
26. I. Svetlik, M. Fejgl, P. Povinec, T. Kořínková, L. Tomášková, J. Pospíchal, M. Kurfírt, R. Striegler and M. Kaufmanová. *Determination of chemical forms of ^{14}C in*

liquid discharges from nuclear power plants. Journal of Environmental Radioactivity, 177: 256-260, 2017.

27. OSPAR Commission. OSPAR Liquid Discharges from Nuclear Installations 2014-2021. <https://www.ospar.org/work-areas/rsc>. Accessed: 2024-08-30. 2024.

28. G. Cook, E. Scott, A. MacKenzie, F. Naysmith, K. Isogai, P. Kershaw, R. Anderson and P. Naysmith. *Reconstructing the history of ^{14}C discharges from Sellafield*. Journal of Radioanalytical and Nuclear Chemistry, 260(2): 239-247, 2004.

29. P. Gulliver, G. Cook, A. MacKenzie, P. Naysmith and R. Anderson. *Sources of anthropogenic ^{14}C to the North Sea*. Radiocarbon, 46(2): 869-875, 2004.

30. S. M. Keogh, E. J. McGee and D. Gallagher. *Spatial and temporal impacts of ^{14}C releases from the Sellafield nuclear complex on the Irish coastline*. Radiocarbon, 46(2): 885-892, 2004.

31. S. Keogh, S. Cournane, L. L. Vintró, E. McGee and P. Mitchell. *Modelling the biological half-life and seasonality of ^{14}C in *Fucus vesiculosus* from the east coast of Ireland: Implications for the estimation of future trends*. Marine pollution bulletin, 62(4): 696-700, 2011.

32. E. Douville, B. Fiévet, P. Germain and M. Fournier. *Radiocarbon behaviour in seawater and the brown algae *Fucus serratus* in the vicinity of the COGEMA La Hague spent fuel reprocessing plant (Goury)—France*. Journal of Environmental Radioactivity, 77(3): 355-368, 2004.

33. B. Fiévet, P. B. Du Bois and C. Voiseux. *Concentration factors and biological half-lives for the dynamic modelling of radionuclide transfers to marine biota in the English Channel*. Sci Total Environ, 791: 148193, 2021.

34. M. Castrillejo, R. Witbaard, C. A. Richardson, R. Dekker, C. Welte, L. Wacker and M. Christl. *Impact of nuclear fuel reprocessing on the temporal evolution of marine radiocarbon*. Science of The Total Environment, 738: 139700, 2020.

35. Å. Magnusson and K. Stenström. *^{14}C produced in Swedish nuclear reactors - measurements on spent ion exchange resins, various process water systems and ejector off-gas*. SKB R-05-78. 2005.

36. Å. Magnusson and K. Stenström. *^{14}C Produced in Swedish Nuclear Power Reactors: Measurements on Spent Ion Exchange Resins, Various Process Water Systems and Ejector Off-gas*. Report to SKB. SKB. 2006.

37. Å. Magnusson, K. Stenström and P.-O. Aronsson. *^{14}C in Swedish PWRs and BWRs - Measurements on spent ion exchange resins and processwater and estimation of the ^{14}C inventory in the Swedish waste repository*. Conference proceedings of EPRI International Low-Level Waste Conference & Exhibit Show – June 27-29, 2006, Albuquerque, New Mexico., 2007 Published.

38. Å. Magnusson, K. Stenström and P. Aronsson. *^{14}C in spent ion-exchange resins and process water from nuclear reactors: a method for quantitative determination of organic and inorganic fractions*. Journal of Radioanalytical and Nuclear Chemistry, 275(2): 261-273, 2008.

39. R. P. Bush, G. M. Smith and I. F. White. *Carbon-14 waste management*. Nuclear Science and Technology, Rep. EUR 8749, Office for Official Publications of the European Communities, Luxembourg. 1984.
40. C. J. H. P. Kunz. *Carbon-14 discharge at three light-water reactors*. Health Physics, 49(1): 25-35, 1985.
41. A. Molnár, M. Molnár, M. Veres, A. Czébely, L. Rinyu, P. Rozmanitz and R. Janovics. *Determination of the total ^{14}C concentration of water samples using the COD method and AMS*. Radiocarbon, 64(5): 1065-1074, 2022.
42. A. Engdahl. *Data report – sampling of sea water and marine organisms outside Ringhals NPP*. SSM2022:18. 2022.
43. A. Molnár, M. Veres, T. Varga, P. Turza, A. J. T. Jull, R. Janovics and M. Molnár. *Novel dissolved organic ^{14}C analyses method applied in a case study at a LILW waste repository*. Radiocarbon: 1-14, 2024.
44. K. Eriksson Stenström, G. Skog, C. Bernhardsson, S. Mattsson, A. B. Nielsen, M. Rundgren, R. Muscheler, H. Linderson, G. Pédehontaa-Hiaa and C. Rääf. *Environmental levels of radiocarbon in Lund, Sweden, prior to the start of the European Spallation Source*. Radiocarbon, 64(1): 51-67, 2022.
45. K. Stenström, G. Skog, C. M. Nilsson, R. Hellborg, S. Leide-Svegborn, E. Georgiadou and S. Mattsson. *Local variations in ^{14}C – How is bomb-pulse dating of human tissues and cells affected?* Nuclear Instruments and Methods in Physics Research Section B: Beam Interactions with Materials and Atoms, 268(7–8): 1299-1302, 2010.
46. K. Stenström, I. Unkel, C. M. Nilsson, C. Raaf and S. Mattsson. *The use of hair as an indicator of occupational ^{14}C contamination*. Radiat Environ Biophys, 49(1): 97-107, 2010.
47. H. Oeschger, U. Siegenthaler, U. Schotterer and A. Gugelmann. *A box diffusion model to study the carbon dioxide exchange in nature*. Tellus, 27(2): 168-192, 1975.
48. S. Pawełczyk and A. J. R. Pazdur. *Carbon isotopic composition of tree rings as a tool for biomonitoring CO_2 level*. 46(2): 701-719, 2004.
49. A. Rakowski, T. Kuc, T. Nakamura and A. Pazdur. *Radiocarbon Concentration in the Atmosphere and Modern Tree Rings in the Kraków Area, Southern Poland*. Radiocarbon, 46(2): 911-916, 2004.
50. A. Pasquier-Cardin, P. Allard, T. Ferreira, C. Hatte, R. Coutinho, M. Fontugne, M. J. J. o. V. Jaudon and G. Research. *Magma-derived CO_2 emissions recorded in ^{14}C and ^{13}C content of plants growing in Furnas caldera, Azores*. 92(1-2): 195-207, 1999.
51. C. Bernhardsson, K. Eriksson Stenström and G. Pédehontaa-Hiaa. *Radiological environmental monitoring at the ESS facility - annual report 2023*. BAR-2025-01. Lund University. 2025.
52. L. Emmenegger, M. Leuenberger and M. Steinbacher. *ICOS ATC/CAL ^{14}C Release, Jungfraujoch (5.0 m), 2015-09-21–2022-08-22, ICOS RI*. <https://data.icos->

cp.eu/portal/. ICOS_ATC_L2_L2-2023.1_JFJ_13.9_779.14C. ICOS DATA is licensed under CC4BY (<http://creativecommons.org/licenses/by/4.0/>). 2024.

53. I. Levin, S. Hammer, B. Kromer and F. Meinhardt. *Radiocarbon observations in atmospheric CO₂: determining fossil fuel CO₂ over Europe using Jungfraujoch observations as background*. Science of The Total Environment, 391(2-3): 211-216, 2008.
54. C. Bernhardsson, K. Eriksson Stenström, M. Jönsson and G. Pedehontaa-Hiaa. *Radiological environmental monitoring at the ESS facility – Annual report 2021*. Report MA RADFYS 2022:01, Report BAR-2022/01. <https://portal.research.lu.se/en/publications/radiological-environmental-monitoring-at-the-ess-facility-annual--4>, 2022.
55. C. Bernhardsson, K. Eriksson Stenström, M. Jönsson, C. Nilsson and G. Pedehontaa-Hiaa. *Radiological environmental monitoring at the ESS facility - Annual report 2022*. MA RADFYS 2023:91, BAR-2023-01. MA RADFYS 2023:91, BAR-2023-01. Lund University. 2023.
56. C. Bernhardsson, K. Eriksson Stenström and G. Pédehontaa-Hiaa. *Radiological environmental monitoring at the ESS facility - annual report 2024*. BAR-2025-03. 2025.
57. E. Q. Alves, K. Macario, P. Ascough and C. Bronk Ramsey. *The worldwide marine radiocarbon reservoir effect: definitions, mechanisms, and prospects*. Reviews of Geophysics, 56(1): 278-305, 2018.
58. B. L. Ingram and J. R. Southon. *Reservoir ages in Eastern Pacific coastal and estuarine waters*. Radiocarbon, 38(3): 573-582, 1996.
59. J. D. Scourse, A. D. Wanamaker, C. Weidman, J. Heinemeier, P. J. Reimer, P. G. Butler, R. Witbaard and C. A. Richardson. *The marine radiocarbon bomb pulse across the temperate North Atlantic: A compilation of $\Delta^{14}\text{C}$ time histories from Arctica islandica growth increments*. Radiocarbon, 54(2): 165-186, 2012.
60. E. A. Gómez, C. M. Borel, M. L. Aguirre and D. E. Martínez. *Radiocarbon reservoir ages and hardwater effect for the northeastern coastal waters of Argentina*. Radiocarbon, 50(1): 119-129, 2008.
61. B. C. Loughheed, H. L. Filipsson and I. Snowball. *Large spatial variations in coastal ^{14}C reservoir age – a case study from the Baltic Sea*. Climate of the Past, 9(3): 1015-1028, 2013.
62. International Atomic Energy Agency (IAEA). *Sediment distribution coefficients and concentration factors for biota in the marine environment*. IAEA Technical Report Series No. 422., 2004.
63. A. Souloumiac, V. Camilleri, I. Cavalié, P. Ciffroy and F. Alonzo. *Short-term accumulation and elimination of carbon-14 in the common carp *Cyprinus carpio* under laboratory conditions*. Journal of Environmental Radioactivity, 233: 106585, 2021.
64. M. Thorne, A. Ikonen and K. Smith. *Transport of C-14 in terrestrial and aquatic environments. BIOPROTA project report*. TR-23-24. 2023.

65. M. Thorne, K. Smith, I. Kovalets, R. Avila and R. Walke. *Terrestrial model-data comparisons and review of carbon uptake by fish*. QRS-1769B-1, Version 2.0. 2018.
66. S. C. Sheppard, P. Ciffroy, F. Siclet, C. Damois, M. I. Sheppard and M. Stephenson. *Conceptual approaches for the development of dynamic specific activity models of ^{14}C transfer from surface water to humans*. Journal of Environmental Radioactivity, 87(1): 32-51, 2006.
67. N. Bodereau, F. Eyrolle, Y. Copard, J.-P. Dumoulin, H. Lepage, F. Giner, D. Mourier and R. Gurriaran. *Carbon-14 cycling in a nuclearized river: A first study in the downstream part of the Rhône River (France)*. Science of The Total Environment, 954: 176502, 2024.
68. J. P. Dumoulin, C. Rabouille, S. Pourtout, B. Bombled, B. Lansard, I. Caffy, S. Hain, M. Perron, M. Sieudat, B. Thellier, E. Delqué-Količ, C. Moreau and L. Beck. *Identification in pore waters of recycles sediment organic matter using the dual isotopic composition of carbon ($\delta^{13}\text{C}$ and $\Delta^{14}\text{C}$): new data from the continental shelf influenced by the Rhône river*. Radiocarbon, 64(6): 1617-1627, 2022.
69. F. Eyrolle, O. Radakovitch, Y. Copard, H. Lepage, N. Bodereau, P. Raimbault, A. Dabrin, V. Lagadec, C. J. J. o. S. Le Corre and Sediments. *Tritium and ^{14}C dependencies upon particulate organic matter within the nuclearized Rhone River (France)*. 22(7): 2076-2093, 2022.
70. Y. Copard, F. Eyrolle, C. Grosbois, H. Lepage, L. Ducros, A. Morereau, N. Bodereau, C. Cossonnet and M. Desmet. *The unravelling of radiocarbon composition of organic carbon in river sediments to document past anthropogenic impacts on river systems*. Science of The Total Environment, 806: 150890, 2022.
71. R. Barisevičiūtė, J. Mažeika, E. Maceika, L. Juodis, V. Rakauskas, O. Jefanova, Ž. Ežerinskis, J. Šapolaitė, L. Butkus and V. Remeikis. *What cooling pond sediments can reveal about ^{14}C in nuclear power plant liquid effluents: Case study Lake Drūkšiai, Ignalina nuclear power plant cooling pond*. PloS one, 18(10): e0285531, 2023.
72. R. Barisevičiūtė, E. Maceika, Ž. Ežerinskis, J. Šapolaitė, L. Butkus, J. Mažeika, V. Rakauskas, L. Juodis, A. Steponėnas and R. Druteikienė. *Distribution of radiocarbon in sediments of the cooling pond of RBMK type Ignalina Nuclear Power Plant in Lithuania*. PloS one, 15(8): e0237605, 2020.
73. G. Cook, A. MacKenzie, P. Naysmith and R. Anderson. *Natural and anthropogenic ^{14}C in the UK coastal marine environment*. Journal of Environmental Radioactivity, 40(1): 89-111, 1998.
74. G. K. Muir, K. M. Tierney, G. T. Cook, G. MacKinnon, J. A. Howe, J. J. Heymans, D. J. Hughes and S. Xu. *Ecosystem uptake and transfer of Sellafield-derived radiocarbon (^{14}C). Part 1. The Irish Sea*. Marine pollution bulletin, 114(2): 792-804, 2017.
75. K. M. Tierney, G. K. Muir, G. T. Cook, G. MacKinnon, J. A. Howe, J. J. Heymans, D. J. Hughes and S. Xu. *Ecosystem uptake and transfer of Sellafield-derived radiocarbon (^{14}C) part 2: The West of Scotland*. Marine pollution bulletin, 115(1-2): 57-66, 2017.

76. H. Ren, Y. Cao and P. Wang. *Radioactivity of organically bound tritium and carbon-14 in sea food from waters near nuclear power plant and committed effective dose of exposed people in Zhejiang province, 2020*. Journal of Chinese Journal of Public Health, 39(5): 622-626, 2023.
77. P. Lagerkvist and A. Tovedal. *Bestämning av ^{14}C i marin biota under en årscykel*. FOI-R--4861--SE, ISSN 1650-1942, Swedish Defence Research Agency. 2019.
78. X. Ma, Y. Cao, T. Zheng, S. Yu, H. Zou, X. Gong, Y. Cao and H. Ren. *Determination and human health risk assessment of TFWT, OBT and carbon-14 in seafood around Qinshan Nuclear Power Plant*. Journal of Food Chemistry, 22: 101243, 2024.
79. Vattenfall. "Luft och Vattenutsläpp 1974_2023", Ringhals document id:2604829. 2024.
80. K. Stenström, B. Erlandsson, R. Hellborg, A. Wiebert, S. Skog, R. Vesanen, M. Alpsten and B. Bjurman. *A one-year study of the total air-borne ^{14}C effluents from two Swedish light-water reactors, one boiling water-and one pressurized water reactor*. Journal of Radioanalytical and Nuclear Chemistry, 198(1): 203-213, 1995.
81. M. Notter. *Radioactivity in sediments at Ringhals nuclear power plant 1988*. National Swedish Environment Protection Board. 1990. National Swedish Environment Protection Board. 1990.
82. K. Stenström, S. Leide Svegborn, Å. Magnusson, G. Skog, M. Zakaria and S. Mattsson. *Analysis of ^{14}C at nuclear facilities, industries and laboratories. Final report for project SSI P 1378*. LUNFD6(NFFR-3101)1-47/(2006). 2006.
83. J. Qiao, K. Andersson and S. Nielsen. *A 40-year marine record of ^{137}Cs and ^{99}Tc transported into the Danish Straits: Significance for oceanic tracer studies*. Journal of Chemosphere, 244: 125595, 2020.
84. J. Qiao, H. Zhang, P. Steier, K. Hain, X. Hou, V.-P. Varti, G. M. Henderson, M. Eriksson, A. Aldahan, G. Possnert and R. Golser. *An unknown source of reactor radionuclides in the Baltic Sea revealed by multi-isotope fingerprints*. Nature Communications, 12(1): 823, 2021.
85. D. P. Gillikin, A. Lorrain, S. Bouillon, P. Willenz and F. J. O. G. Dehairs. *Stable carbon isotopic composition of *Mytilus edulis* shells: relation to metabolism, salinity, $\delta^{13}\text{C}$ DIC and phytoplankton*. Journal of Organic Geochemistry, 37(10): 1371-1382, 2006.
86. Ringhals AB. *Ringhals delprogram för övervakning av radioaktiva ämnen i miljön*. Vattenfall. Report 2497823 / 2.0. 2021.
87. Strålsäkerhetsmyndigheten (SSM). *Strålsäkerhetsmyndighetens föreskrifter och allmänna råd om drift av kärnkraftsreaktorer SSMFS 2021:6*. 2021.
88. T. K. Rees. *A note on the longevity of certain species of the Fucaceae*. Annals of Botany, 46(184): 1062-1064, 1932.

89. M. Knight and M. Parke. *A biological study of Fucus vesiculosus L. and F. serratus L.* Journal of the Marine Biological Association of the United Kingdom, 29(2): 439-514, 1950.
90. L. Kautsky, S. Qvarfordt and E. Schagerström. *Fucus vesiculosus adapted to a life in the Baltic Sea: impacts on recruitment, growth, re-establishment and restoration.* Botanica Marina, 62(1): 17-30, 2019.
91. SLU Artdatabanken. Blåstång *Fucus vesiculosus* L. <https://artfakta.se/taxa/232759/information>. 2025.
92. Havforskningsinstituttet. Tema: Blåskjell. (in Norwegian). <https://www.hi.no/hi/temasider/arter/blaskjell>. 2024.
93. C. Lehane and J. Davenport. *A 15-month study of zooplankton ingestion by farmed mussels (Mytilus edulis) in Bantry Bay, Southwest Ireland.* Journal of Estuarine, Coastal Shelf Science, 67(4): 645-652, 2006.
94. K. Troost. *Causes and effects of a highly successful marine invasion: case-study of the introduced Pacific oyster Crassostrea gigas in continental NW European estuaries.* Journal of Sea Research, 64(3): 145-165, 2010.
95. O. Lindahl, R. Hart, B. Hernroth, S. Kollberg, L.-O. Loo, L. Olrog, A.-S. Rehnstam-Holm, J. Svensson, S. Svensson and U. Syversen. *Improving marine water quality by mussel farming: a profitable solution for Swedish society.* AMBIO: A Journal of the Human Environment, 34(2): 131-138, 2005.
96. A. Hawkins. *Relationships between the synthesis and breakdown of protein, dietary absorption and turnovers of nitrogen and carbon in the blue mussel, Mytilus edulis L.* Oecologia, 66(1): 42-49, 1985.
97. A.-L. Wrangé, J. Valero, L. S. Harkestad, Ø. Strand, S. Lindegarth, H. T. Christensen, P. Dolmer, P. S. Kristensen and S. J. B. I. Mortensen. *Massive settlements of the Pacific oyster, Crassostrea gigas, in Scandinavia.* 12: 1145-1152, 2010.
98. Nordiska ministerrådet. *Policy Brief: Stillahavsstron – en ny nordisk livsmedelsresurs och underlag för turism.* 2019.
99. S. Bougrier, A. Hawkins and M. Héral. *Preingestive selection of different microalgal mixtures in Crassostrea gigas and Mytilus edulis, analysed by flow cytometry.* J Aquaculture, 150(1-2): 123-134, 1997.
100. M. Sayer, R. N. Gibson and R. Atkinson. *Growth, diet and condition of cormorant wrasse and rock cod on the west coast of Scotland.* Journal of Fish Biology, 49(1): 76-94, 1996.
101. P.-O. Skoglund and C. Peterson. *Ringhals - Kylvattenutsläpp i havet. Slutrapport från oceanografiska undersökningar utför Ringhals kärnkraftverk med fyra aggregat i drift.* SMHI Oceanografi, Nr 25. 1988.
102. U. Ehlin, S. Lindahl, E. Neuman, O. Sandström and J. Svensson. *Miljöeffekter av stora kylvattenutsläpp. Erfarenheter från de svenska kärnkraftverken.* Elforsk rapport nr 98:79 (In Swedish). 2009.

103. M. Notter. *Radionuklider i sediment utanför Ringhals kärnkraftverk 1984*. 9162031031. (In Swedish). Statens naturvårdsverk. 1986.
104. F. Käll, A. Falk, J. Sjöholm, W. J. Langert and N. Nykvist. *Biologisk recipientkontroll för Ringhals kärnkraftverk. Årsrapport för 2022*. SLU. Aqua reports 2023:2 (in Swedish). 2023.
105. W. J. Langert, J. Sjöholm and F. Käll. *Biologisk recipientkontroll för Ringhals kärnkraftverk. Årsrapport för 2023*. SLU. Aqua notes 2024:9 (in Swedish). 2024.
106. U. Grimaas, A. Jacobsson and E. Neuman. *Biological and radioecological investigations at the Ringhals nuclear power station, 1968-1987*. National Swedish Environmental Protection Board. 1989.
107. S. Mattsson, K. Eriksson Stenström and G. Pédehontaa-Hiaa. *Long-time variations of radionuclides and metals in the marine environment of the Swedish west-coast studied using brown algae (*Fucus serratus* and *Fucus vesiculosus*)*. Swedish Radiation Authority (SSM). Report 2022:13.
<https://www.stralsakerhetsmyndigheten.se/publikationer/rapporter/stralskydd/2022/202213/>, 2022.
108. K. E. Stenström, C. Nilsson, M. Olsson, C. Bernhardsson and M. Jönsson. *Assessment of sediment sampling techniques for ESS environmental monitoring programme*. Report MA RADFYS 2023:02, Report BAR-2023/02.
<https://portal.research.lu.se/sv/publications/assessment-of-sediment-sampling-techniques-for-ess-environmental->, 2023.
109. L. Wacker, M. Němec and J. Bourquin. *A revolutionary graphitisation system: Fully automated, compact and simple*. Nuclear Instruments and Methods in Physics Research Section B: Beam Interactions with Materials and Atoms, 268(7): 931-934, 2010.
110. G. Skog. *The single stage AMS machine at Lund University: Status report*. Nuclear Instruments and Methods in Physics Research Section B: Beam Interactions with Materials and Atoms, 259(1): 1-6, 2007.
111. G. Skog, M. Rundgren and P. Sköld. *Status of the Single Stage AMS machine at Lund University after 4 years of operation*. Nuclear Instruments and Methods in Physics Research Section B: Beam Interactions with Materials and Atoms, 268(7-8): 895-897, 2010.
112. C. Bernhardsson, K. Eriksson Stenström, M. Jönsson, G. Pedehontaa-Hiaa and S. Mattsson. *Radiological environmental monitoring at the ESS facility – Annual report 2020*. Report MA RADFYS 2021:01, Report BAR 2021/01.
<https://portal.research.lu.se/en/publications/radiological-environmental-monitoring-at-the-ess-facility-annual--3>, 2021.
113. K. Eriksson Stenström and S. Mattsson. *Project SSM2019-5225: “Marine ¹⁴C levels around the Swedish coast” – Additional gamma spectrometry measurements and ICP-MS analysis of brown algae (*Fucus* spp.)*. BAR 2021/02. MA RADFYS 2021/02. <https://portal.research.lu.se/en/publications/project-ssm2019-5225-marine-14c-levels-around-the-swedish-coast-a>, 2021.

114. M. Granberg and G. Gustavsson. *Miljöundersökning efter oljespill från Marco Polo. Analyser av oljerelaterade miljögiftshalter i blåmusslor, sediment, vatten och oljeprov* Reprt number C856. IVL Svenska Miljöinstitutet. 2024.
115. D. Jackson, B. Lambers and J. Gray. *Radiation doses to members of the public near to Sellafield, Cumbria, from liquid discharges 1952-98*. Journal of Radiological Protection, 20(2): 139, 2000.
116. Groupe radioecologie Nord_Cetentin. *GT1. Rapport final detaille. Juilliet 1999. Invetaire de rejets. Radioactifs des installations nucleaire*. http://www.gep-nucleaire.org/norcot/gepnc/sections/travauxgep/premiere_mission5339/volume_1_publication/en/downloadFile/file/GT1.pdf?nocache=1284989908.32, 1999.
117. G. T. Cook, F. H. Begg, P. Naysmith, E. M. Scott and M. McCartney. *Anthropogenic ¹⁴C marine geochemistry in the vicinity of a nuclear fuel reprocessing plant*. Radiocarbon, 37(2): 459-467, 1995.
118. G. Gong, B. Wu, L. Liu, J. Li, Q. Zhu, M. He and G. Hu. *Metabolic engineering using acetate as a promising building block for the production of bio-based chemicals*. Engineering Microbiology, 2(4): 100036, 2022.
119. P. M. Stanley and J. T. Staley. *Acetate uptake by aquatic bacterial communities measured by autoradiography and filterable radioactivity I*. Limnology Oceanography, 22(1): 26-37, 1977.

Appendix A – Units for ^{14}C

Concentrations of ^{14}C in the environment may be expressed in a variety of quantities and units [1], often depending of the analytical technique used for the ^{14}C measurement, and on the purpose of the measurement. In the present study we use the unitless quantity $F^{14}\text{C}$ (fraction Modern) for reasons explained below.

One common quantity is specific activity of carbon, $\frac{A}{m_C}$, with the unit Bq per kg of total carbon. This unit is a convenient choice when decay counting methods are used for the ^{14}C analysis. The specific activity of carbon can easily be converted to (or from) activity concentration of dry material ($\frac{A}{m_{d.w.}}$), given that the carbon content of the sample ($\frac{m_C}{m_{d.w.}}$) is known:

$$\frac{A}{m_{d.w.}} = \frac{A}{m_C} \cdot \frac{m_C}{m_{d.w.}}$$

The activity concentration of fresh material ($\frac{A}{m_{w.w.}}$) can be calculated provided that the ratio of dry weight to wet weight ($\frac{m_{d.w.}}{m_{w.w.}}$) is known:

$$\frac{A}{m_{w.w.}} = \frac{A}{m_{d.w.}} \cdot \frac{m_{d.w.}}{m_{w.w.}}$$

However, activity concentrations of ^{14}C of dry or wet material have limited use when comparing species with different carbon and water content. To assess possible excess of ^{14}C in biota in the surroundings of a nuclear facility, specific activity of carbon is a better choice, however with some limitations, since it usually does not take isotope fractionation into account. When carbon is transferred from one environmental compartment to another, the mass difference between the carbon isotopes leads to a discrimination of some isotopes compared to others, resulting in small changes in the isotopic ratios. This phenomenon, known as isotope fractionation, occurs for all elements, but is more pronounced for the lighter elements, due to the relatively higher mass difference between isotopes of light elements than heavy elements. The isotope fractionation of carbon is defined as the relative deviation of the $^{13}\text{C}/^{12}\text{C}$ ratio of the sample compared to that of a standard material, VPDB (Vienna Pee Dee Belemnite), expressed in ‰ (see [1]). Typical values of $\delta^{13}\text{C}$ range from about 0‰ for marine carbonates, -9‰ for atmospheric CO_2 , -15‰ for marine organisms and -27‰ for tree leaves [2].

As an example of the effect on isotope fractionation of specific activity of carbon, consider the transfer of dissolved inorganic carbon (DIC) in water to seaweed (*Fucus* spp.). Due to the isotope fractionation, the specific activity of seaweed will not be identical to that in DIC. A unitless quantity that removes the effect of isotope fractionation is $F^{14}\text{C}$, also known as Fraction Modern [1, 3]. It is commonly used in accelerator mass spectrometry measurements of samples from the 1950s and onwards (the bomb-peak era). In principle, $F^{14}\text{C}$ is the ratio between the specific activity (or ^{14}C to ^{12}C ratio) of the sample, normalized to $\delta^{13}\text{C} = -25$ ‰, and the specific activity (or ^{14}C to ^{12}C ratio) of a standard (see [1, 3]). The normalization removes the effect of isotope fractionation and makes the ^{14}C content in different sample types directly comparable. In source apportionment of ^{14}C related to nuclear facilities, and in dose assessments, the

effect of isotope fractionation can often be ignored due to its low impact. However, the $\delta^{13}\text{C}$ value itself, and the corresponding value for nitrogen, $\delta^{15}\text{N}$, may provide useful information e.g. on trophic levels of various organisms and of various environmental conditions, such as temperature.

Another feature of $F^{14}\text{C}$ is its independence of the year of measurement. The relation between specific activity of carbon, $\frac{A}{m_c}$, at the year of measurement, y , and $F^{14}\text{C}$ is given by [1]:

$$\frac{A}{m_c} = F^{14}\text{C} \cdot \left(\frac{1 + \frac{\delta^{13}\text{C}}{1000}}{0.975} \right)^2 \cdot e^{\frac{(1950-y)}{8267}} \cdot 226 \frac{\text{Bq}}{\text{kg C}}$$

Several other quantities of expressing ^{14}C concentrations exist, e.g. Δ , $\Delta^{14}\text{C}$, D^{14}C and pMC [1]. The unit $\Delta^{14}\text{C}$ (unit ‰) is often used [1]. Its relation to $F^{14}\text{C}$ is:

$$F^{14}\text{C} = \left(\frac{\Delta^{14}\text{C}}{1000} + 1 \right) e^{(y-1950)/8267}$$

where y is the year of measurement. The reader is referred to [1] for a summary of definitions and interconversions of other ways of expressing ^{14}C concentrations.

Figure A1 attempts to illustrate the relation between the quantities and units commonly used in literature regarding ^{14}C in the environment of nuclear installations.

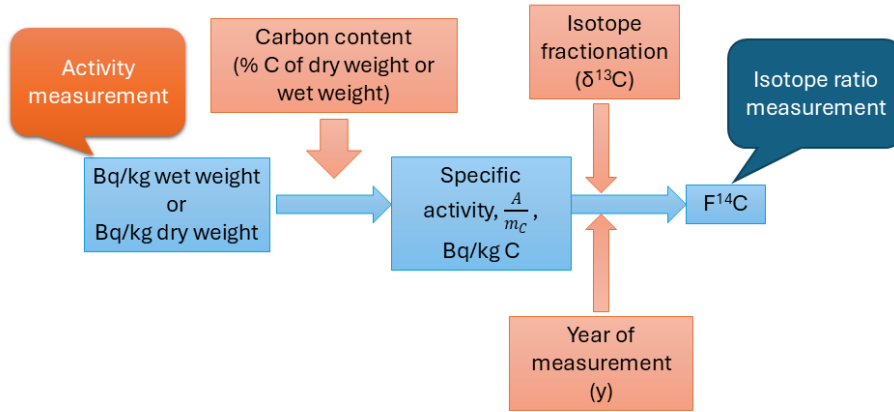


Figure A1 Common quantities and units used in studies of ^{14}C in the vicinity of nuclear installations

References

1. K. Eriksson Stenström, G. Skog, E. Georgiadou, J. Genberg and A. Johansson. *A guide to radiocarbon units and calculations*. LUNFD6(NFFR-3111)/1-17/(2011). Lund University. Dep of Physics. Div of Nuclear Physics. <http://lup.lub.lu.se/search/ws/files/5555659/2173661.pdf>, 2011.
2. M. Stuiver and H. A. Polach. *Discussion reporting of ^{14}C data*. Radiocarbon, 19(3): 355-363, 1977.
3. P. J. Reimer, T. A. Brown and R. W. Reimer. *Discussion: Reporting and calibration of post-bomb ^{14}C data*. Radiocarbon, 46(3): 1299-1304, 2004.

Appendix B – Examples of methods for ^{14}C analysis of water

Compiled by Anne Birgitte Nielsen and Kristina Eriksson Stenström

The present study we have analysed PIC and POC in a few water samples. Below is a brief summary of methods that can be used to extract and measure other biogeochemical fractions of seawater.

PIC and POC

The particulate carbon fractions (PIC and POC) can be separated from the dissolved fractions through filtration on glass fibre filters, usually at the time when the water samples are collected. Reported filter sizes range from 0.7 to 45 μm (using e.g. GF/F filters). Carbon dioxide from the PIC fraction can be released through acid hydrolysis using HCl. The remaining POC fraction can be dried and combusted. For further information, see e.g. [1].

DIC

The DIC pool is usually the largest in sea water, and often the most enriched in radiocarbon from nuclear facilities. Therefore, there may be enough to use LSC methods, whereas the other carbon pools almost always require AMS-based methods.

For example, Douville et al [2] used LSC after benzene synthesis to measure the radioactivity in the DIC of seawater near La Hague. They extracted DIC from 120 litre samples, filtered through a 0.45 μm filter and trapped CO_2 released by acidification in sodium hydroxide solution followed by precipitation to barium carbonate.

At SUERC [1], a method has been developed to extract DIC from water for AMS analysis, by acidifying relatively small amounts of waters (100-300 ml) in 500 ml syringes with HCl, and injecting the released CO_2 through a hydrophobic filter directly into the graphitisation line, similar to the one illustrated in Macchia et al [3]. By keeping the HCl concentration sufficiently low, oxidation of the DOC component is avoided.

DOC

DOC can be extracted after filtration and DIC removal, commonly through combustion of dried salts or by wet oxidation methods [4, 5]. Molnar et al present a wet-oxidation method that should be easy to use for determination of total dissolved carbon in water samples, but also for the DIC and DOC fractions (for AMS measurements) [6, 7]. Organic carbon can also be liberated from water samples, after removal of the DIC fraction, for AMS measurements e.g. through the following methods:

1. UV oxidation [8, 9]
2. solid phase extraction [10]
3. ultrafiltration methods [11]

Total Dissolved Carbon (TDC)

Molnár et al [6] describe a method used for determining ^{14}C in total dissolved (TDC) for environmental monitoring of groundwater at Paks nuclear power plant (Hungary) using AMS. The wet oxidation method involves sulphuric acid, potassium-dichromate and silver-sulphate.

Table B1 contains examples of methods to extract ^{14}C from various biogeochemical fractions of water.

Table B1 Examples of methods to extract ^{14}C from various biogeochemical fractions of water.

Study	Fraction	LSC/AMS	Volume (L)	Filter (μm)	Water treatment	Particle treatment	CO_2 capture
Wolstenholme et al 1998 [12]	DIC	AMS	0.5	0.7	Sealed in CO_2 -free environment		Acidified, purged with N_2 , trapped using liquid N_2
	DOC	AMS					
	PIC	AMS	200-700	0.7		2 M HCl	Trapped using liquid N_2
	POC	AMS	200-700	0.7		Remainder from PIC cleaned with water and dried	
Bregg 1992 [13]	DIC	LSC	200	yes	acidification and nitrogen bubbling etc.		
	DOC	AMS	25	yes	Macro-porous non-ionic XAD resins		
	PIC	AMS		yes	Hydro-lysing with 50% H_3PO_4 to release PIC		
	POC	AMS		yes	hydrolysing with 50% H_3PO_4 to remove PIC		
Bauer et al 2001 [14]	DIC	AMS	0.5	0.8	Poisoned with HgCl_2 . DIC removed with phosphoric acid		
	DOC	AMS	12 (1)	0.8	Frozen immediately		Oxidised with high energy UV
	POC	AMS	12 (1)	0.8		Filter frozen immediately	
Gulliver et al 2001 [15]	DIC	LSC	80	0.7	4M HCl		Cryogenically captured and converted to Benzene (Barker 1953)
	DOC	AMS	200 (0.5)	0.7	freeze drying		Oxygen added under vacuum, combusted, graphitised
	PIC	AMS	200	0.7		4M HCl to filter	Cryogenically captured and reduced to graphite
	POC	AMS	200	0.7		Residual from PIC on filter rinsed, dried, combusted and graphitised	
Cook et al 2004 [16]	DIC	LSC	100	0.7			
	DOC	LSC	100	0.7	poisoned with mercuric chloride and stored in the dark at 4 °C		
	PIC	LSC	100	0.7			
	POC	LSC	100	0.7			
Douville et al 2004 [2]	DIC	LSC	120	45	acidification and nitrogen bubbling		Sodium hydroxide molar solution before being precipitated as barium carbonate.
	PIC	AMS	200	45		2 M HCl	Recovered in carbonate form, and then precipitated (BaCO_3).
	POC	AMS	200	45		Highly oxidising attack (chromic acid, potassium dichromate)	Recovered in carbonate form, and then precipitated (BaCO_3).
Ahad et al 2006 [17]	DOC	AMS	25	0.7	Tangential flow UF, acidified, frozen, lyophilised, decarbonated with HCl, dried		
Tierney 2017 [1]	DIC	AMS	160	0.7	Orthophosphoric acid	85%	
	DOC				Vacuum drying, combustion		
	PIC				Acid hydrolysis of filters	1 M HCl	
	POC				Combustion of filters remaining after PIC removal		
Povinec et al 2023 [18]	DIC	AMS	1 (25 ml)	45	85% phosphoric acid, heating		Cryogenically captured and reduced to graphite
Molnar et al 2022 and 2024 [6, 7]				0.45 μm cellulose-acetate syringe filter			
	DIC	AMS	20		85% phosphoric acid, heating		
	TDC	AMS	10		Ag_2SO_4 and a $\text{K}_2\text{Cr}_2\text{O}_7\text{-H}_2\text{SO}_4$ solution, heating		
	DOC	AMS	400-800	0.7 μm glass filter	After removal of DIC, Ag_2SO_4 and a $\text{K}_2\text{Cr}_2\text{O}_7\text{-H}_2\text{SO}_4$ solution, heating		

References

1. K. M. Tierney. *Marine ecosystem uptake of nuclear reprocessing derived radiocarbon (^{14}C)*. PhD thesis. University of Glasgow. 2017.
2. E. Douville, B. Fiévet, P. Germain and M. Fournier. *Radiocarbon behaviour in seawater and the brown algae *Fucus serratus* in the vicinity of the COGEMA La Hague spent fuel reprocessing plant (Goury)—France*. Journal of Environmental Radioactivity, 77(3): 355-368, 2004.
3. M. Macchia, M. D'Elia, G. Quarta, V. Gaballo, E. Braione, L. Maruccio, L. Calcagnile, G. Ciceri, V. Martinotti and L. Wacker. *Extraction of Dissolved Inorganic Carbon (DIC) from Seawater Samples at CEDAD: results of an intercomparison exercise on samples from Adriatic Sea shallow water*. Radiocarbon, 55(2): 579-584, 2013.
4. G. S. Burr, J. Thomas, D. Reines, D. Jeffrey, C. Courtney, A. T. Jull and T. Lange. *Sample preparation of dissolved organic carbon in groundwater for AMS ^{14}C analysis*. Radiocarbon, 43(2A): 183-190, 2001.
5. A. Leonard, S. Castle, G. S. Burr, T. Lange and J. Thomas. *A wet oxidation method for AMS radiocarbon analysis of dissolved organic carbon in water*. Radiocarbon, 55(2): 545-552, 2013.
6. A. Molnár, M. Molnár, M. Veres, A. Czébely, L. Rinyu, P. Rozmanitz and R. Janovics. *Determination of the total ^{14}C concentration of water samples using the COD method and AMS*. Radiocarbon, 64(5): 1065-1074, 2022.
7. A. Molnár, M. Veres, T. Varga, P. Turza, A. J. T. Jull, R. Janovics and M. Molnár. *Novel dissolved organic ^{14}C analyses method applied in a case study at a LILW waste repository*. Radiocarbon: 1-14, 2024.
8. S. Q. Lang, C. P. McIntyre, S. M. Bernasconi, G. L. Früh-Green, B. M. Voss, T. I. Eglinton and L. Wacker. *Rapid ^{14}C analysis of dissolved organic carbon in non-saline waters*. Radiocarbon, 58(3): 505-515, 2016.
9. L. Xu, M. L. Roberts, K. L. Elder, R. L. Hansman, A. R. Gagnon and M. D. Kurz. *Radiocarbon in dissolved organic carbon by UV oxidation: An update of procedures and blank characterization at NOSAMS*. Radiocarbon, 64(1): 195-199, 2022.
10. T. Dittmar, B. Koch, N. Hertkorn and G. Kattner. *A simple and efficient method for the solid-phase extraction of dissolved organic matter (SPE-DOM) from seawater*. Limnology Oceanography: Methods, 6(6): 230-235, 2008.
11. R. Benner, B. Benitez-Nelson, K. Kaiser and R. M. Amon. *Export of young terrigenous dissolved organic carbon from rivers to the Arctic Ocean*. Geophysical research letters, 31(5), 2004.
12. A. Wolstenholme, G. Cook, A. MacKenzie, P. Naysmith, P. Meadows and P. McDonald. *The behavior of Sellafield-derived ^{14}C in the Northeast Irish Sea*. Radiocarbon, 40(1): 447-458, 1997.
13. F. Begg, G. Cook, M. Baxter, E. Scott and M. McCartney. *Anthropogenic radiocarbon in the eastern Irish Sea and Scottish coastal waters*. Radiocarbon, 34(3): 707-716, 1992.

14. J. E. Bauer, E. R. Druffel, D. M. Wolgast and S. Griffin. *Sources and cycling of dissolved and particulate organic radiocarbon in the northwest Atlantic continental margin*. Global Biogeochemical Cycles, 15(3): 615-636, 2001.
15. P. Gulliver, G. Cook, A. MacKenzie, P. Naysmith and R. Anderson. *Sources of anthropogenic ^{14}C to the North Sea*. Radiocarbon, 46(2): 869-875, 2004.
16. G. Cook, A. MacKenzie, G. Muir, G. Mackie and P. Gulliver. *Sellafield-derived anthropogenic ^{14}C in the marine intertidal environment of the NE Irish Sea*. Radiocarbon, 46(2): 877-883, 2004.
17. J. M. Ahad, R. S. Ganeshram, R. G. Spencer, G. Uher, P. Gulliver and C. L. Bryant. *Evidence for anthropogenic ^{14}C -enrichment in estuarine waters adjacent to the North Sea*. Geophysical research letters, 33(8), 2006.
18. P. Povinec, V. Papadopoulos, G. Krokos, Y. Abualnaja, A. Pavlidou, I. Kontuľ, J. Kaizer, A. Cherkinsky, A. Molnár and M. J. J. o. E. R. Molnár. *Tritium and radiocarbon in the water column of the Red Sea*. 256: 107051, 2023.

Appendix C – Sites

Table C1 Sampling sites along the coast

Sea	Site number	Site name	Latitude	Longitude	Reference
Skagerrak	52	Svinesund	59.10N	11.27E	
	53	Saltbacken	59.08N	11.23E	
	1	Båteviken, Strömstad	58.95N	11.13E	
	2	Fjällbacka, Sälvik	58.59N	11.28E	Data in [1]
	3	Smögen, Kleven	58.35N	11.22E	
	46	Lysekil	58.27N	11.42E	
	4	Stockevik, Tjörn	57.96N	11.55E	
Kattegat	5	Hällsvik	57.70N	11.74E	Data in [1]
	6	Smarholmens badplats	57.43N	11.92E	Data in [1]
	49	Åsa	57.35N	12.12E	
	7	Frillesås	57.31N	12.15E	
	8	Sallebacka	57.28N	12.14E	
	9	Gloppe	57.27N	12.11E	
	10	Videbergshamn	57.25N	12.11E	
	11	Bua, at beacon	57.242N	12.099E	
	11B	Bua, at old pier	57.242N	12.103E	
	11C	Bua strand	57.229N	12.108E	
	12	Skeatången, Ånäshalvön	57.20N	12.17E	Data in [1]
	13	Getterön	57.12N	12.21E	Data in [1]
	14	Glommen	56.94N	12.36E	Data in [1]
	15	Särdal	56.76N	12.63E	Data in [1] [2]
	16	Kattvik	56.46N	12.75E	Data in [1]
	50	Arild	56.27N	12.58E	
	17	Mölle	56.28N	12.50E	
Baltic Sea	30	Skillinge	55.47N	14.28E	
	51	Åhus	55.91N	14.30E	

[1] Eriksson Stenström K, Mattsson S. 2022. Spatial and temporal variations of ^{14}C in *Fucus* spp. in Swedish coastal waters. *Journal of Environmental Radioactivity* Volume 242, February 2022, 106794.

[2] Mattsson et al 2024. Radionuclides in algae from Swedish coastal waters for over half a century. Accepted for publication in *Radiation Protection Dosimetry*.

Table C2 Sampling sites in the vicinity of Ringhals NPP. LU: Lund University. SLU: Swedish Agricultural University Väröbacka. Samples are organized from north to south in the table (for each sampling organization. Distances from outlet are approximate.

Sampling organ- isation	Site number	Site name	Latitude	Longitude	Approx. distance from outlet (km)	Direction from outlet
LU	49	Åsa	57.35N	12.12E	12	N
	7	Frillesås	57.31N	12.15E	8.5	N
	8	Sallebacka	57.28N	12.14E	5.7	N
	9	Gloppe	57.27N	12.11E	2.5	N
	10	Videbergshamn	57.25N	12.11E	2.2	S
	11	Bua, at lighthouse	57.242N	12.099E	1.3	S
	11B	Bua, at old pier	57.242N	12.103E	1.6	S
	11C	Bua strand	57.229N	12.108E	3.2	S
	12	Skeatången, Årnäshalvön	57.20N	12.17E	8.4	S
SLU	SLU25	Näsbokrok	57.335N	12.077E	9.3	N
	SLU23	N Vendelsö	57.307N	12.107E	6.2	NNE
	SLU12b	Stavder	57.282N	12.137E	5.2	NE
	SLU13	Ustö	57.291N	12.083E	4.3	N
	SLU11b	Södra Ledskär	57.268N	12.081E	1.8	N
	SLU3	Outlet	57.252N	12.088E	0.1	S
	SLU22	Stora o Lilla Halsbåden	57.252N	12.088E	0.1	S
	SLU8	Gyltan	57.245N	12.081E	1.0	SW
	SLU5b	Bua at lighthouse	57.242N	12.108E	1.4	SSE
	SLU5b.1	Bua at lighthouse.1	57.241N	12.097E	1.4	SSE
	SLU7	N Horten	57.221N	12.091E	3.6	S
	SLU16	Knarrskär	57.192N	12.148E	7.7	SSE

Appendix D – Results

Table D1 $F^{14}C$ in *Fucus* spp. collected at Särö (56.76N, 12.63E), 1967-2023. Uncertainties in $F^{14}C$ represent the analytical uncertainty (one standard deviation), resulting from repeated measurements of the same sample. N.D. – No data. FV – *Fucus vesiculosus*. FS – *Fucus serratus*. V.A. – Vesicles and above.

Date	Sample number	Species	SSAMS sample code	$F^{14}C$	$\delta^{13}C$ (‰)
1967-07-15	V759	<i>Fucus vesiculosus</i>	LuS 15390	1.407 ± 0.007	-13.5
1967-07-15	V760	<i>Fucus vesiculosus</i>	LuS 15391	1.397 ± 0.007	-14.3
1970-08-23	T70		LuS 18475	1.354 ± 0.005	
1972-08-18	T72		LuS 18476	1.329 ± 0.005	
1973-08-15	T73		LuS 18477	1.329 ± 0.005	
1974-08-16	T74		LuS 18478	1.315 ± 0.005	
1975-08-20	T75		LuS 18479	1.312 ± 0.005	
1976-12-31	V2109	<i>Fucus serratus</i>	LuS 18480	1.287 ± 0.005	
1977-06-20	V2027		LuS 18481	1.279 ± 0.005	
1978-06-26	V2070		LuS 18482	1.273 ± 0.005	
1979-09-09	V2226		LuS 19 071	1.249 ± 0.006	
1980-10-26	V2554		LuS 18483	1.236 ± 0.005	
1981-07-24	V2782	<i>Fucus vesiculosus</i>	LuS 19811	1.235 ± 0.005	
1982-11-27	V3315		LuS 19812	1.213 ± 0.005	
1983-11-12	V3557		LuS 18484	1.202 ± 0.005	
1984-08-05	V763	<i>Fucus serratus</i>	LuS 15382	1.201 ± 0.006	-12.5
1985-08-24		<i>Fucus vesiculosus</i>	LuS 19813	1.185 ± 0.005	
1986-06-07			LuS 18485	1.180 ± 0.005	
1987-12-24			LuS 18486	1.168 ± 0.005	
1988-06-26		<i>Fucus serratus</i>	LuS 15383	1.167 ± 0.006	-13.5
1989-07-08			LuS 18487	1.159 ± 0.006	
1990-07-30			LuS 18488	1.155 ± 0.006	
1991-06-09			LuS 18489	1.144 ± 0.006	
1992-01-19		<i>Fucus serratus</i>	LuS 15384	1.148 ± 0.006	-13.9
1992-07-04		<i>Fucus serratus</i>	LuS 15385	1.147 ± 0.006	-12.5
1993-06-25			LuS 18490	1.138 ± 0.005	
1994-07-09		<i>Fucus serratus</i>	LuS 15386	1.137 ± 0.006	-13.8
1995-08-12			LuS 18491	1.133 ± 0.005	
1996-06-16			LuS 18492	1.125 ± 0.005	
1996-09-29		<i>Fucus serratus</i>	LuS 19072	1.112 ± 0.005	
1997-01-03		<i>Fucus serratus</i>	LuS 19073	1.113 ± 0.005	
1997-06-21		<i>Fucus serratus</i>	LuS 19074	1.127 ± 0.005	
1997-07-21		<i>Fucus serratus</i>	LuS 19075	1.123 ± 0.005	
1997-09-28		<i>Fucus serratus</i>	LuS 19076	1.122 ± 0.005	
1998-03-30		<i>Fucus serratus</i>	LuS 19077	1.138 ± 0.005	
1998-07-03		<i>Fucus serratus</i>	LuS 19078	1.151 ± 0.005	
1998-08-03			LuS 18 493	1.151 ± 0.005	
1999-01-01		<i>Fucus serratus</i>	LuS 19 079	1.151 ± 0.005	
1999-08-14			LuS 19494	1.149 ± 0.005	
2000-05-20			LuS 18495	1.147 ± 0.005	
2001-07-28			LuS 18496	1.129 ± 0.005	
2002-08-08			LuS 19814	1.109 ± 0.005	
2002-08-08			LuS 19815	1.112 ± 0.005	
2003-06-26		<i>Fucus vesiculosus</i>	LuS 18497	1.111 ± 0.005	
2004-08-03		<i>Fucus serratus</i>	LuS 18498	1.114 ± 0.005	
2005-12-29		<i>Fucus serratus</i>	LuS 14569	1.100 ± 0.006	-15.4
2006-06-25		<i>Fucus serratus</i>	LuS 14570	1.104 ± 0.006	-15.1
2007-05-12			LuS 18499	1.104 ± 0.005	
2008-12-31		<i>Fucus serratus</i>	LuS 14571	1.089 ± 0.006	-12.8
2009-06-21			LuS 18500	1.093 ± 0.005	
2010-08-29		<i>Fucus serratus</i>	LuS 19 080	1.080 ± 0.006	
2011-06-26		<i>Fucus serratus</i>	LuS 14572	1.069 ± 0.005	-14.8
2011-12-30		<i>Fucus serratus</i>	LuS 14573	1.067 ± 0.006	-13.9
2012-08-05	M29	<i>Fucus serratus</i>	LuS 19816	1.062 ± 0.005	
2013-06-23	M188	<i>Fucus serratus</i>	LuS 19817	1.069 ± 0.005	
2014-06-20	M330	<i>Fucus serratus</i>	LuS 14574	1.071 ± 0.006	-15.6
2015-01-19	M342	<i>Fucus serratus</i>	LuS 14575	1.081 ± 0.006	-14.5
2015-12-26	M490		LuS 19818	1.065 ± 0.005	
2016-10-02	M504		LuS 18501	1.076 ± 0.005	
2017-02-06	M509	<i>Fucus serratus</i>	LuS 13899	1.072 ± 0.005	
2017-06-22	M527	<i>Fucus serratus</i>	LuS 15387	1.063 ± 0.006	-14.9
2017-12-17	M537	<i>Fucus serratus</i>	LuS 13901	1.051 ± 0.005	
2018-06-23	M552	<i>Fucus serratus</i>	LuS 13902	1.056 ± 0.005	
2018-12-31	M571	<i>Fucus serratus</i>	LuS 15388	1.057 ± 0.005	-15.3
2019-06-23	M587	<i>Fucus serratus</i>	LuS 15389	1.057 ± 0.005	-16.3
2019-06-23	M587	<i>Fucus serratus</i>	LuS 15780	1.046 ± 0.004	-15.6
2020-01-06	M606	<i>Fucus serratus</i>	LuS 15781	1.047 ± 0.004	-17.2
2020-03-03	M611	<i>Fucus serratus</i>	LuS 15782	1.048 ± 0.004	-16.1
2020-03-03	M612 (whole plants)	<i>Fucus vesiculosus</i>	LuS 15783	1.047 ± 0.004	-16.4
2020-03-03	M612 (vesicles and above (part A), ~10 cm)	<i>Fucus vesiculosus</i>	LuS 15827	1.048 ± 0.006	
2020-03-03	M612 (top part of part A, youngest 6 cm)	<i>Fucus vesiculosus</i>	LuS 15828	1.050 ± 0.006	
2020-03-03	M613	<i>Fucus spiralis</i>	LuS 15785	1.050 ± 0.004	-18.2
2020-06-23	M676	<i>Fucus serratus</i>	LuS 18 034	1.048 ± 0.005	
2021-01-01	M734	<i>Fucus serratus</i>	LuS 18 035	1.057 ± 0.005	
2021-07-04	M747	<i>Fucus serratus</i>	LuS 18 036	1.042 ± 0.005	
2021-12-31	M802	<i>Fucus serratus</i>	LuS 18 037	1.045 ± 0.005	
2022-05-01	M814	<i>Fucus serratus</i>	LuS 18 038	1.043 ± 0.005	
2023-05-01	M960	<i>Fucus serratus</i>	LuS 19 081	1.035 ± 0.005	
2023-05-01	M961	<i>Fucus vesiculosus</i>	LuS 19 082	1.030 ± 0.005	
2023-11-13	M1003	<i>Fucus serratus</i>	LuS 19819	1.029 ± 0.005	
2023-11-13	M1004	<i>Fucus vesiculosus</i>	LuS 19820	1.032 ± 0.005	

Table D2 $F^{14}C$ in samples collected close to Ringhals nuclear power plant. FV – *Fucus vesiculosus*, SM – *Symphodus melops*, CP – *Cancer pagurus*, ME – *Mytilus edulis*, MG – *Magallana gigas*.

Site name	Site	Sampling date	Water temp (°C)	Salinity (%)	Species	Sample name	SSAMS code	$F^{14}C$	Unc (1 σ)
Näsbykrok	SLU 25	2023-04-26	11.60	1.61	FV	FV_SLU25_2023-04-26	LuS 19187	1.066	0.005
		2023-10-09	12.70	2.30	FV	FV_SLU25_2023-10-09	LuS 19679	1.055	0.006
		SLU25.1 2024-01-09	0.10	2.50	FV	FV_SLU25_2024-01-09	LuS 20041	1.065	0.005
		SLU25.1 2024-02-14	2.50	2.09	FV	FV_SLU25_2024-02-14	LuS 20042	1.058	0.005
N Vendelsö	SLU23	2023-05-05	9.40	1.96	SM	SM_SLU23_2023-05-05_ind1	LuS 19194	1.162	0.005
		2023-05-05	9.60	1.96	SM	SM_SLU23_2023-05-05_ind2	LuS 19195	1.199	0.007
		2023-05-05	9.60	1.96	SM	SM_SLU22_2023-05-05_ind3	LuS 19196	1.109	0.005
		2023-08-02	18.30	2.06	SM	SM_SLU23_2023-08-02_ind1	LuS 19472	1.161	0.006
					SM	SM_SLU23_2023-08-02_ind2	LuS 20103	1.147	0.005
					SM	SM_SLU23_2023-08-02_ind3	LuS 20104	1.218	0.005
	SLU23.1	2023-12-13	9.20	3.13	SM	SM_SLU23_2023-12-13_ind1	LuS 20105	1.182	0.005
	SLU23.1	2023-12-13	9.20	3.13	SM	SM_SLU23_2023-12-13_ind2	LuS 20106	1.551	0.006
	SLU23.2	2023-12-13	9.20	3.51	SM	SM_SLU23_2023-12-13_ind3	LuS 20107	1.524	0.006
	SLU23.2	2023-12-13	9.20	3.51	CP. soft tissue	CP_SLU23-2_2023-12-13_muskel_ind1	LuS 20040	1.156	0.005
					CP. soft tissue	CP_SLU23-2_2023-12-13_muskel_ind2			
					CP. soft tissue	CP_SLU23-2_2023-12-13_muskel_ind3			
Stavder	SLU12b	2023-04-26	10.70	1.53	FV	FV_SLU12b_2023-04-26	LuS 19184	1.064	0.006
		2023-10-10	14.00	2.24	FV	FV_SLU12b_2023-10-10	LuS 19677	1.087	0.006
		2023-12-11	2.50	2.06	FV	FV_SLU12b_2023-12-11	LuS 20032	1.088	0.004
		2024-02-14	3.60	1.99	FV	FV_SLU12b_2024-02-14	LuS 20033	1.104	0.004
Ustö	SLU13	2023-05-03	10.50	1.95	FV	FV_SLU13_2023-05-03	LuS 19185	1.076	0.005
		2023-09-11	18.9	1.64	FV	FV_SLU13_2023-09-11	LuS 19458	1.059	0.005
		2023-12-12	2.0	2.24	FV	FV_SLU13.2_2023-12-12	LuS 20034	1.081	0.004
		2024-02-14	2.7	1.98	FV	FV_SLU13.2_2024-02-14	LuS 20035	1.068	0.005
		2023-09-11	18.8	1.88	ME	Mussla1_SLU13_2023-09-11	LuS 19462	1.145	0.005
					ME	Mussla2_SLU13_2023-09-11	LuS 19463	1.162	0.005
					ME	Mussla3_SLU13_2023-09-11	LuS 19464	1.130	0.005
		2023-12-12	2	2.24	ME	Mussla1_SLU13.2_2023-12-12	LuS 20094	1.142	0.005
					ME	Mussla2_SLU13.2_2023-12-12			
					ME	Mussla3_SLU13.21_2023-12-12			
		2024-02-14	2.7	1.98	ME	Mussla1_SLU13.2_2024-02-14	LuS 20095	1.147	0.005
					ME	Mussla2_SLU13.2_2024-02-14			
					ME	Mussla3_SLU13.2_2024-02-14			
Södra Ledskär	SLU11b	2023-07-05	ND	ND	Sediment	SED_SLU11b_2023-07-05	LuS 19632	1.022	0.005
		2024-01-09	4.5	2.71	Sediment	Sed_SLU11b_2024-01-09	LuS 20093	1.048	0.005

Table D2 cont. F¹⁴C in samples collected close to Ringhals nuclear power plant. FV – *Fucus vesiculosus*, SM – *Symphodus melops*, CP – *Cancer pagurus*, ME – *Mytilus edulis*, MG – *Magallana gigas*. N.D. – No data.

Site name	Site	Sampling date	Water temp (°C)	Salinity (‰)	Species	Sample name	SSAMS code	F ¹⁴ C	Unc (1 σ)
Outlet	SLU3	2023-05-11	16.1	1.79	FV	FV_SLU3_230511	LuS 19180	1.756	0.007
		2023-09-07	24.3	1.67	FV	FV_SLU3_230907	LuS 19456	1.827	0.007
Stora o Lilla Halsbåden	SLU22	2023-12-13	4.4	2.24	FV	FV_SLU22_2023-12-13	LuS 20038	2.070	0.007
		2024-02-13	10	2.16	FV	FV_SLU22_2024-02-13	LuS 20038	1.564	0.006
	SLU3	2023-09-08	17	2.05	ME	Mussla1_SLU3_2023-09-08	LuS 19468	2.812	0.010
					ME	Mussla2_SLU3_2023-09-08	LuS 19469	2.795	0.010
					ME	Mussla3_SLU3_2023-09-08	LuS 19470	2.778	0.009
	SLU22	2023-12-13	4.4	2.24	ME	Mussla1_SLU22_2023-12-13	LuS 20100	2.305	0.008
					ME	Mussla2_SLU22_2023-12-13			
					ME	Mussla3_SLU22_2022-12-13			
	SLU22	2024-02-13	10	2.16	ME	Mussla1_SLU22_2024-02-13	LuS 20101	2.232	0.008
					ME	Mussla2_SLU22_2024-02-13			
					ME	Mussla3_SLU22_2024-02-13			
	SLU22	2023-05-11	15.1	1.78	MG	MG_SLU22_2023-05-11_ind1_muskel	LuS 19762	1.743	0.007
	SLU22	2023-10-09	15.8	2.27	MG	MG_SLU22_2023-10-09_ind1_muskel	LuS 19673	1.684	0.007
		2023-10-09			MG	MG_SLU22_2023-10-09_ind2_muskel	LuS 19674	1.867	0.007
		2023-10-09			MG	MG_SLU22_2023-10-09_ind3_muskel	LuS 19675	1.639	0.006
	SLU22	2023-12-13	4.4	2.24	MG	MG1_SLU22_2023-12-13	LuS 20098	1.720	0.006
					MG	MG2_SLU22_2023-12-13			
					MG	MG3_SLU22_2023-12-13			
	SLU22	2024-02-13	10	2.16	MG	MG_SLU22_2024-02-13_ind1	LuS 20099	1.590	0.006
					MG	MG_SLU22_2024-02-13_ind2			
					MG	MG_SLU22_2024-02-13_ind3			
	SLU22	2023-04-05	8.90	2.03	SM	SM_SLU22_2023-04-05_ind1	LuS 19191	1.108	0.005
		2023-04-12	10.20	1.45	SM	SM_SLU22_2023-04-12_ind2	LuS 19192	1.288	0.006
		2023-04-12	10.60	1.46	SM	SM_SLU22_2023-04-12_ind3	LuS 19193	1.537	0.007
	SLU22	2023-08-02	19.1	2.15	SM	SM_SLU22_2023-08-02_ind1	LuS 19471	3.535	0.011
		2023-08-02	19.1	2.15	SM	SM_SLU22_2023-08-02_ind2	LuS 20096	5.058	0.017
		2023-08-02	19.1	2.15	SM	SM_SLU22_2023-08-02_ind3	LuS 20097	2.443	0.008
	SLU22.53	2023-12-18	7.4	3.19	SM	SM_SLU22.53_2023-12-18_ind1	LuS 20102	1.600	0.006
	SLU3	2023-07-05	N.D.	N.D.	Sediment	SED_SLU3_2023-07-05	LuS 19631	2.128	0.008
		2023-12-11	4.1	2.21	Sediment	Sed_SLU3_2023-12-11	LuS 20086	1.725	0.007
		2023-12-11	6.9	2.25	Biofouling plate 1	Påväxtplatta 1_2023-12-11	LuS 20018	3.494	0.011
		2024-01-02	12.9	2.5	Biofouling plate 2	Påväxtplatta 2_2024-01-02	LuS 20020	1.897	0.007
		2024-03-04	N.D.	N.D.	Biofouling plate 1	Påväxtplatta 1_2024-03-04	LuS 20019	8.250	0.023
		2024-03-04	N.D.	N.D.	Biofouling plate 2	Påväxtplatta 2_2024-03-04	LuS 20021	3.835	0.011

Table D2 cont. F¹⁴C in samples collected close to Ringhals nuclear power plant. FV – *Fucus vesiculosus*, SM – *Symphodus melops*, CP – *Cancer pagurus*, ME – *Mytilus edulis*, MG – *Magallana gigas*.

Site name	Site	Sampling date	Water temp (°C)	Salinity (%)	Species	Sample name	SSAMS code	F ¹⁴ C	Unc (1 σ)
Gyltan	SLU8	2023-04-20	6.10	2.20	FV	FV_SLU8_2023-05-04	LuS 19183	1.120	0.005
		2023-09-07	18.10	1.75	FV	FV_SLU8_2023-09-07	LuS 19455	1.150	0.005
		2023-12-13	2.60	2.32	FV	FV_SLU8_2023-12-13	LuS 20026	1.126	0.004
		2024-02-02	2.50	2.22	FV	FV_SLU8_2024-02-12	LuS 20027	1.142	0.004
		2023-04-20	6.10	2.20	CP, soft tissue	CP_SLU8_2023-04-20_ind1_muskel	LuS 19197	1.136	0.006
					CP, butter	CP_SLU8_2023-04-20_ind1_smör	LuS 19200	1.151	0.005
		2023-04-20	6.10	3.02	CP, soft tissue	CP_SLU8_2023-04-20_ind2_muskel	LuS 19198	1.122	0.006
					CP, butter	CP_SLU8_2023-04-20_ind2_smör	LuS 19201	1.169	0.005
		2023-04-25	6.10	3.35	CP, soft tissue	CP_SLU8_2023-04-25_ind3_muskel	LuS 19199	1.115	0.006
					CP, butter	CP_SLU8_2023-04-25_ind3_smör	LuS 19202	1.135	0.006
		2023-09-29	15.6	3.07	CP, soft tissue	CP_SLU8_2023-09-29_ind1_muskel	LuS 19666	1.207	0.005
					CP, butter	CP_SLU8_2023-09-29_ind1_smör	LuS 19667	1.239	0.006
		2023-09-29	14.8	3.22	CP, soft tissue	CP_SLU8_2023-09-29_ind2_muskel	LuS 19668	1.299	0.006
					CP, butter	CP_SLU8_2023-09-29_ind2_smör	LuS 19669	1.280	0.006
		2023-09-29	14.8	3.22	CP, soft tissue	CP_SLU8_2023-09-29_ind3_muskel	LuS 19670	1.243	0.006
					CP, butter	CP_SLU8_2023-0929_ind3_smör	LuS 19671	1.254	0.006
		2023-12-19	8.9	3.47	CP, soft tissue	CP_SLU8.4_2023-12-19_muskel_ind1	LuS 20030	1.246	0.006
						CP_SLU8.4_2023-12-19_muskel_ind2			
						CP_SLU8.4_2023-12-19_muskel_ind3			
		2023-12-19	8.9	3.47	CP, butter	CP_SLU8.4_2023-12-19_smör_ind1	LuS 20031	1.191	0.005
						CP_SLU8.4_2023-12-19_smör_ind2			
						CP_SLU8.4_2023-12-19_smör_ind3			
		2024-02-19	4.7	3.32	CP, soft tissue	CP_SLU8.2_2024-02-19_muskel_ind1	LuS 20028	1.170	0.006
						CP_SLU8.2_2024-02-19_muskel_ind2			
						CP_SLU8.2_2024-02-19_muskel_ind3			
		2024-02-19	4.7	3.32	CP, butter	CP_SLU8.2_2024-02-19_smör_ind1	LuS 20029	1.192	0.005
						CP_SLU8.2_2024-02-19_smör_ind2			
						CP_SLU8.2_2024-02-19_smör_ind3			

Table D2 cont. F¹⁴C in samples collected close to Ringhals nuclear power plant. FV – *Fucus vesiculosus*, SM – *Symphodus melops*, CP – *Cancer pagurus*, ME – *Mytilus edulis*, MG – *Magallana gigas*.

Site name	Site	Sampling date	Water temp (°C)	Salinity (%)	Species	Sample name	SSAMS code	F ¹⁴ C	Unc (1 σ)
Bua at lighthouse	SLU5b	2023-04-26	11.4	1.55	FV	FV_SLU5b_2023-04-26	LuS 19181	1.188	0.005
		2023-10-10	14.7	1.94	FV	FV_SLU5b_2023-10-10	LuS 19676	1.149	0.005
		2023-12-13	1.6	2.26	FV	FV_SLU5b_2023-12-13	LuS 20022	1.170	0.004
		2024-02-13	3.1	2.01	FV	FV_SLU5b_2024-02-13	LuS 20023	1.125	0.004
		2023-05-12	13.3	1.76	ME	Mussla2_SLU5b_2023-05-12	LuS 19459	1.561	0.005
		2023-05-12	13.3	1.76	ME	Mussla3_SLU5b_2023-05-12	LuS 19460	1.363	0.006
		2023-05-12	13.3	1.76	ME	Mussla4_SLU5b_2023-05-12	LuS 19461	1.345	0.006
		2023-10-09	18.2	2.21	ME	Mussla1_SLU5b_2023-10-09	LuS 19660	1.549	0.006
		2023-10-09	18.2	2.21	ME	Mussla2_SLU5b_2023-10-09	LuS 19661	1.391	0.006
		2023-10-09	18.2	2.21	ME	Mussla3_SLU5b_2023-10-09	LuS 19662	1.455	0.006
		2023-12-12	1.2	2.21	ME	Mussla1_SLU5.1_2023-12-12	LuS 20087	1.480	0.006
					ME	Mussla2_SLU5.1_2023-12-12			
					ME	Mussla3_SLU5.1_2023-12-12			
		2024-02-13	3.4	1.89	ME	Mussla1_SLU5.1_2024-02-13	LuS 20088	1.392	0.006
					ME	Mussla2_SLU5.1_2024-02-13			
					ME	Mussla3_SLU5.1_2024-02-13			
N Horten	SLU7	2023-05-11	11.1	1.71	FV	FV_SLU7.66_230511	LuS 19182	1.053	0.005
		2023-09-08	18.6	1.62	FV	FV_SLU7_230908	LuS 19456	1.072	0.005
		2023-12-12	2.8	2.21	FV	FV_SLU7_2023-12-12	LuS 20024	1.069	0.004
		2024-02-13	2.5	2.03	FV	FV_SLU7_2024-02-13	LuS 20025	1.082	0.004
		2023-05-23	13.7	1.95	ME	Mussla1_SLU7_2023-05-23	LuS 19465	1.143	0.005
		2023-05-23	13.7	1.95	ME	Mussla2_SLU7_2023-05-23	LuS 19466	1.134	0.005
		2023-05-23	13.7	1.95	ME	Mussla3_SLU7_2023-05-23	LuS 19467	1.127	0.005
		2023-10-05	15.8	2.26	ME	Mussla1_SLU7_2023-10-05	LuS 19663	1.132	0.006
		2023-10-05	15.8	2.26	ME	Mussla2_SLU7_2023-10-05	LuS 19664	1.105	0.006
		2023-10-05	15.8	2.26	ME	Mussla3_SLU7_2023-10-05	LuS 19665	1.102	0.006
		2023-12-12	2.8	2.21	ME	Mussla123_SLU7_2023-12-12	LuS 20091	1.155	0.005
		2024-02-13	2.5	2.03	ME	Mussla123_SLU7_2024-02-13	LuS 20092	1.182	0.005
		2023-04-12	6.2	1.48	SM	SM_SLU7_2023-04-12_ind1	LuS 19188	1.554	0.006
		2023-04-12	6.8	1.42	SM	SM_SLU7_2023-04-12_ind2	LuS 19189	1.284	0.006
		2023-04-12	7.2	1.40	SM	SM_SLU7_2023-04-12_ind3	LuS 19190	2.419	0.008
		2023-08-02	17.80	2.03	SM	SM_SLU7_2023-08-02_ind1	LuS 19473	1.540	0.006
		2023-08-02	17.80	2.03	SM	SM_SLU7_2023-08-02_ind2	LuS 20089	1.312	0.006
		2023-08-02	17.80	2.03	SM	SM_SLU7_2023-08-02_ind3	LuS 20090	1.559	0.006
Knarrskär	SLU16	2023-05-02	10.40	1.53	FV	FV_SLU16_2023-05-02	LuS 19186	1.038	0.005
		2023-10-09	13.40	0.89	FV	FV_SLU16_2023-höst	LuS 19678	1.050	0.005
		2023-12-11	2.50	2.12	FV	FV_SLU16_2023-12-11	LuS 20036	1.054	0.005
		2024-02-13	2.40	2.00	FV	FV_SLU16_2024-02-13	LuS 20037	1.057	0.005

Table D3 $F^{14}C$ in *Fucus* spp., sediments and particulate carbon (PC) collected in Skagerrak by Lund University. Uncertainties in $F^{14}C$ represent the analytical uncertainty (one standard deviation), resulting from repeated measurements of the same sample. N.D. – No data. FV – *Fucus vesiculosus*. FS – *Fucus serratus*. N – *Ascophyllum nodosum*. V.A. – Vesicles and above. Salinity measurements should only be seen as relative and not absolute: the instrument may continually have drifted to show too low values.

Site	Site name	Date (YY-MM-DD)	Water temp (°C)	Salinity (%)	Species	Part	SSAMS sample code	$F^{14}C$	Ref
52	Svineund	2024-05-17	17.9	0.4	FV	All	LuS 20071	1.038 ±0.005	[1]
53	Saltbacken	2024-05-17	17.5	0.9	FV	All	LuS 20072	1.058 ±0.005	[1]
1	Båteviken, Strömstad	2020-04-08	9.1	2.2	FV	V.A.	LuS 15821	1.096 ± 0.008	[2]
		2020-10-15	14	2.7	FV	V.A.	LuS 18215	1.087 ± 0.005	[3]
		2022-10-12	12	2.1	FV	V.A.	LuS 18201	1.053 ± 0.005	[3]
		2023-05-04	13	1.8	FV	All	LuS 19048	1.056 ± 0.005	[3]
		2023-08-30	19.1	0.9	FV	All	LuS 19260	1.066 ± 0.006	[3]
					Sediment		LuS 19625	1.011 ± 0.005	
		2024-05-17	19.6	1.1	FV	All	LuS 19262	1.070 ± 0.006	[3]
3	Smögen, Kleven	2020-04-08	11.8	2.5	FV	V.A.	LuS 15822	1.099 ± 0.006	[2]
		2022-10-12	13.1	2.6	AN	Upper parts	LuS 18202	1.052 ± 0.005	[3]
46	Lysekil	2020-10-15	13.7	2.6	FV	V.A.	LuS 18223	1.078 ± 0.005	[3]
		2022-10-12	N.D.	2.5	FV	V.A.	LuS 18213	1.052 ± 0.005	[3]
		2023-05-04	14	1.9	FV	All	LuS 19062	1.050 ± 0.005	[3]
		2023-05-04	14	1.9	FS	All	LuS 19061	1.070 ± 0.005	[3]
		2023-08-30	20.3	1.9	FV	All	LuS 19214	1.068 ± 0.006	[3]
					Sediment		LuS 19629	1.035 ± 0.005	
		2024-05-18	17.2	1.3	PC		LuS 20111	1.028 ± 0.005	
					FV	All	LuS 20068	1.062 ± 0.006	[3]
4	Stockevik, Tjörn	2020-04-08	11.3	2.2	FV	V.A.	LuS 15823	1.072 ± 0.006	[2]
		2022-10-13	12	2.4	FV	V.A.	LuS 18203	1.048 ± 0.005	[3]
		2023-05-04	12	2	FV	All	LuS 19029	1.053 ± 0.005	[3]
		2023-08-30	20.1	1.6	FV	All	LuS 19207	1.061 ± 0.005	[3]
					Sediment		LuS 19626	1.004 ± 0.005	
		2024-05-18	21.3	1.2	FV	All	LuS 20063	1.049 ± 0.005	[3]

[1] S. Bjarheim, K. Eriksson Stenström, A. Lindskog, M. Olsson, P. Carlsson, S. Mattsson. The potential of shells of *Mytilus edulis* for retrospective analysis of marine ^{14}C discharges from nuclear power plants. Accepted for publication in Radiocarbon, 2025.

[2] K. Eriksson Stenström, S. Mattsson. Spatial and temporal variations of ^{14}C in *Fucus* spp. in Swedish coastal waters. Journal of Environmental Radioactivity Volume 242, February 2022, 106794.

[3] K. Eriksson Stenström, S. Mattsson. Current trends in radiocarbon in Skagerrak and Kattegat assessed by brown algae from Swedish coastal waters. Radiation Protection Dosimetry. ncaf032. <https://doi.org/10.1093/rpd/ncaf032>. 2025.

Table D4 $F^{14}C$ in *Fucus* spp., sediments and particulate carbon (PC) collected in Kattegat by Lund University. Uncertainties in $F^{14}C$ represent the analytical uncertainty (one standard deviation), resulting from repeated measurements of the same sample. N.D. – No data. FV – *Fucus vesiculosus*. FS – *Fucus serratus*. V.A. – Vesicles and above. Salinity measurements should only be seen as relative and not absolute: the instrument may continually have drifted to show too low values.

Site	Site name	Date (YY-MM-DD)	Water temp (°C)	Salinity (%)	Species	Part	SSAMS sample code	$F^{14}C$	Ref
1	Båteviken	2023-08-30			Sediment				
49	Åsa	2022-10-14	12.3	2.1	FV	Upper 10 cm	LuS 18214	1.062 ± 0.005	[3]
7	Frillesås	2020-03-31	5.4	1.9	FV	V.A.	LuS 15812	1.070 ± 0.006	[2]
		2020-10-01	14.6	1.9	FV	V.A.	LuS 18216	1.074 ± 0.005	[3]
		2022-10-14	12.7	2.1	FV	V.A.	LuS 18204	1.062 ± 0.005	[3]
		2024-05-18	22.8	1.1	FV	All	LuS 20064	1.067 ± 0.005	[3]
8	Sallebacka	2020-03-31	5.6	2.0	FV	V.A.	LuS 15813	1.097 ± 0.006	[2]
		2020-10-01	15.8	2.1	FV	V.A.	LuS 18217	1.153 ± 0.006	[3]
		2022-10-14	12.8	2.2	FV	All	LuS 18205	1.101 ± 0.005	[3]
9	Ringhals Gloppe	2020-03-31	6.5	2.0	FV	V.A.	LuS 15814	1.135 ± 0.007	[2]
		2020-10-01	15.4	2.1	FV	V.A.	LuS 18218	1.163 ± 0.006	[3]
		2022-10-13	n.d.	2.4	FV	V.A.	LuS 18206	1.150 ± 0.005	[3]
		2023-05-05	15.5	1.8	FV	All	LuS 19051	1.162 ± 0.005	[3]
		2023-05-05	15.5	1.8	FS	All	LuS 19050	1.121 ± 0.005	[3]
		2023-08-30	18.4	1.3	FV	All	LuS 19208	1.144 ± 0.006	[3]
10	Videbergs-hamn	2020-03-31	6.6	2	FV	V.A.	LuS 15815	1.234 ± 0.008	[2]
		2020-10-01	16	2.1	FV	V.A.	LuS 18219	1.237 ± 0.005	[3]
		2022-10-13	13.3	2.2	FV	V.A.	LuS 18207	1.361 ± 0.006	[3]
		2023-05-05	11.7	1.7	FV	All	LuS 19053	1.093 ± 0.005	[3]
		2023-08-31	20.4	1.0	FV	All	LuS 19209	1.237 ± 0.006	[3]
					Sediment		LuS 19627	1.435 ± 0.006	
		2024-05-18	20.4	1.1	PC		LuS 20108	2.407 ± 0.008	
					FV	All	LuS 20065	1.247 ± 0.008	[3]
11	Bua, at beacon	2020-03-31	N.D.	N.D.	FV	V.A.	LuS 15816	1.322 ± 0.007	[2]
		2020-10-01	15.5	2.1	FV	V.A.	LuS 18220	1.578 ± 0.006	[3]
		2020-10-01	15.5	2.1	FS	Upper 10 cm	LuS 18221	1.367 ± 0.006	[3]
		2022-10-13	12.9	2.3	FV	V.A.	LuS 18208	1.310 ± 0.006	[3]
		2023-05-05	16	1.7	FV	All	LuS 19057	1.230 ± 0.005	[3]
		2023-05-05	16	1.7	FS	Lower 10 cm	LuS 19055	1.345 ± 0.006	[3]
		2023-05-05	16	1.7	FS	Upper 40 cm	LuS 19056	1.235 ± 0.005	[3]
		2023-08-31	18.1	1.2	FV	All	LuS 19219	1.293 ± 0.006	[3]
					Sediment		LuS 19628	1.743 ± 0.010	
		2024-05-18	21.2	1.1	FV	All	LuS 20066	1.130 ± 0.005	[3]
11B	Bua pier	2022-10-13	12.9	2.3	FV	V.A.	LuS 18209	1.295 ± 0.006	[3]
11C	Bua strand	2022-10-14	12.8	2.1	FV	V.A.	LuS 18210	1.061 ± 0.006	[3]
17	Mölle	2020-04-20	9.1	1.4	FV	V.A.	LuS 15825	1.043 ± 0.006	[2]
		2022-10-14	14.6	2.0	FV	V.A.	LuS 18211	1.014 ± 0.005	[3]
50	Arild	2020-09-30	16.3	1.4	FS	Upper 10 cm	LuS 18224	1.047 ± 0.005	[3]
		2023-05-05	10.7	1.6	FS	All	LuS 19064	1.027 ± 0.005	[3]
		2023-08-31	20.1	1.1	FV	All	LuS 19215	1.034 ± 0.005	[3]
		2024-05-19	20.0	1.0	FV	All	LuS 20069	1.024 ± 0.005	[3]

[1] S. Bjarheim, K. Eriksson Stenström, A. Lindskog, M. Olsson, P. Carlsson, S. Mattsson. The potential of shells of *Mytilus edulis* for retrospective analysis of marine ^{14}C discharges from nuclear power plants. Accepted for publication in Radiocarbon, 2025.

[2] K. Eriksson Stenström, S. Mattsson. Spatial and temporal variations of ^{14}C in *Fucus* spp. in Swedish coastal waters. Journal of Environmental Radioactivity Volume 242, February 2022, 106794.

[3] K. Eriksson Stenström, S. Mattsson. Current trends in radiocarbon in Skagerrak and Kattegat assessed by brown algae from Swedish coastal waters. Radiation Protection Dosimetry. ncaf032. <https://doi.org/10.1093/rpd/ncaf032>. 2025.

Table D5 $F^{14}C$ in *Fucus* spp., sediments and particulate carbon (PC) collected in the Baltic Sea by Lund University. Uncertainties in $F^{14}C$ represent the analytical uncertainty (one standard deviation), resulting from repeated measurements of the same sample. N.D. – No data. FV – *Fucus vesiculosus*. FS – *Fucus serratus*. V.A. – Vesicles and above. Salinity measurements should only be seen as relative and not absolute: the instrument may continually have drifted to show too low values.

Site	Site name	Date (YY-MM-DD)	Water temp (°C)	Salinity (‰)	Species	Part	SSAMS sample code	$F^{14}C$	Ref
30	Skillinge	2020-03-11	10.3	0.7	FV	V.A.	LuS 15789	1.002 ± 0.004	[2]
		2020-03-11	10.3	0.7	FV	V.A.	LuS 15791	1.000 ± 0.004	[2]
		2020-03-11	10.3	0.7	FV	V.A.	LuS 15795	1.009 ± 0.004	[2]
		2020-05-13	10.7	0.7	FV	Top part	LuS 15847	0.990 ± 0.005	[2]
		2020-09-24	17.2	0.7	FV	V.A.	LuS 18222	1.017 ± 0.005	[3]
		2022-10-26	13.2	0.6	FV	V.A.	LuS 18212	1.005 ± 0.005	[3]
		2023-04-25	N.D.	0.6	FV	All	LuS 19059	0.980 ± 0.005	[3]
		2023-08-22	18.4	0.7	FV	All	LuS 19259	0.990 ± 0.005	[3]
		2024-02-15	4	0.2	FV	All	LuS 20043	0.986 ± 0.005	
					PC		LuS 20109	0.850 ± 0.004	
		2024-05-19	24.1	0.4	FV	All	LuS 20067	0.997 ± 0.005	[3]
					PC		LuS 20110	0.940 ± 0.004	
51	Åhus	2023-05-20	14.0	0.6	FV	All	LuS 19066	1.016 ± 0.006	[3]
		2023-09-01	17.2	0.5	FV	All	LuS 19216	1.002 ± 0.005	[3]
					Sediment		LuS 19630	0.913 ± 0.005	
		2024-05-19	17.9	0.5	FV	All	LuS 20070	1.000 ± 0.005	[3]

[1] S. Bjarheim, K. Eriksson Stenström, A. Lindskog, M. Olsson, P. Carlsson, S. Mattsson. The potential of shells of *Mytilus edulis* for retrospective analysis of marine ^{14}C discharges from nuclear power plants. Accepted for publication in Radiocarbon, 2025.

[2] K. Eriksson Stenström, S. Mattsson. Spatial and temporal variations of ^{14}C in *Fucus* spp. in Swedish coastal waters. Journal of Environmental Radioactivity Volume 242, February 2022, 106794.

[3] K. Eriksson Stenström, S. Mattsson. Current trends in radiocarbon in Skagerrak and Kattegat assessed by brown algae from Swedish coastal waters. Radiation Protection Dosimetry. ncaf032. <https://doi.org/10.1093/rpd/ncaf032>. 2025.

Appendix E – Trophic levels and carbon content

The results of the EA-IRMS measurements of some samples of *F. vesiculosus*, *M. edulis* (soft tissue), *S. melops* (soft tissue), *M. gigas* (soft tissue), and *C. pagurus* (soft tissue and butter) are shown in Table E1. *Fucus vesiculosus* was not subjected to acid-alkali-acid pretreatment prior to analysis (unlike the of *F. vesiculosus* samples for ^{14}C analysis).

For definition of $\delta^{13}\text{C}$ and $\delta^{15}\text{N}$, see e.g. [1, 2]. In brief, and simplified, $\delta^{13}\text{C}$ and $\delta^{15}\text{N}$ are measures of the changes of isotopic ratios that occur whenever carbon and nitrogen are transferred from one ecological compartment to another. Typical values of $\delta^{13}\text{C}$ range from about 0‰ (-4 to +4‰) for marine carbonates, -9‰ (-11 to +6‰) for atmospheric CO_2 , -15‰ (-19 to -11‰) for marine organisms and -27‰ (-32 to -22‰) for terrestrial tree leaves [1, 3]. $\delta^{15}\text{N}$ tend to increase through each step of the food chain, and can thus be used to reveal the trophic level (see e.g. [4-6]).

Table E1 EA-IRMS-data for selected samples of *Fucus vesiculosus* (FV), *Mytilus edulis* (ME) soft tissue, *Symphodus melops* (SM) soft tissue, *Magallana gigas* (MG) soft tissue, *Cancer pagurus* (CP) soft tissue and butter. Each measurement is from material from different individuals. * Affected by biofouling organisms. ω_N and ω_C are the mass fraction of nitrogen and carbon related to dry weight (g N per g dry mass and g C per g dry weight). $\delta^{15}N$ is the isotope fractionation using the atmospheric nitrogen scale. $\delta^{13}C$ is the isotope fractionation expressed using the VPDB scale. F_N = isotopic amount fraction $^{15}N/(^{14}N + ^{15}N)$; calculated from $\delta^{15}N$ using $R_{ref} = ^{15}N/^{14}N = 1/272$. F_C = isotopic amount fraction $^{13}C/(^{12}C + ^{13}C)$; calculated from $\delta^{13}C$ using $R_{ref} = ^{13}C/^{12}C = 0.0112372$.

Site	Sample type	Date (YYYY-MM-DD)	ω_N / %	$\delta^{15}N$ / ‰	Atom% F_N / %	ω_C / %	$\delta^{13}C$ / ‰	Atom% F_C / %	C/N ratio
1 Båteviken	FV*	2022-10-12	1.69	6.23	0.3686	34.64	-11.98	1.098066	20.5
		2023-05-04	1.97	6.64	0.3687	36.67	-11.67	1.098407	18.6
		2023-08-30	1.01	7.10	0.3689	22.24	-8.26	1.102155	22.0
	ME	2022-10-12	9.11	7.96	0.3692	38.96	-19.97	1.089283	4.3
11 Bua	FV	2022-10-13	0.71	4.18	0.3678	40.67	-12.87	1.097088	57.3
		2023-05-05	2.59	6.40	0.3686	40.29	-16.29	1.093329	15.6
		2023-08-31	1.24	7.98	0.3692	40.16	-16.26	1.093362	32.4
	ME	2022-10-13	9.29	7.20	0.3689	43.58	-19.54	1.089756	4.7
			9.28	5.88	0.3684	45.48	-20.15	1.089085	4.9
SLU3/22	SM	2023-04-05	13.98	12.53	0.3709	48.44	-19.63	1.089657	3.5
		2023-04-12	13.69	11.14	0.3704	48.65	-18.47	1.090932	3.6
		2023-08-02	14.09	11.29	0.3704	48.75	-19.41	1.089899	3.5
			14.13	10.88	0.3703	48.57	-18.64	1.090745	3.4
	MG	2023-05-11	8.10	7.62	0.3691	39.36	-22.14	1.086898	4.9
			8.30	8.32	0.3693	43.74	-21.87	1.087194	5.3
	ME	2023-09-08	9.11	8.11	0.3693	40.29	-19.65	1.089635	4.4
			9.47	8.16	0.3693	38.99	-19.32	1.089998	4.1
SLU7	ME	2023-10-05	7.31	7.65	0.3691	38.86	-20.30	1.088920	5.3
			5.88	7.37	0.3690	36.49	-20.59	1.088602	6.2
		2023-05-23	8.65	7.03	0.3689	42.78	-22.00	1.087051	4.9
			9.66	6.62	0.3687	42.08	-21.23	1.087898	4.4
SLU8	CP soft tissue	2023-04-20	12.92	12.97	0.3710	43.36	-19.50	1.089800	3.4
			11.82	14.27	0.3715	41.05	-19.20	1.090130	3.5
	CP butter	2023-04-20	8.50	11.31	0.3704	38.84	-21.72	1.087359	4.6
			9.11	12.43	0.3708	42.74	-21.37	1.087744	4.7

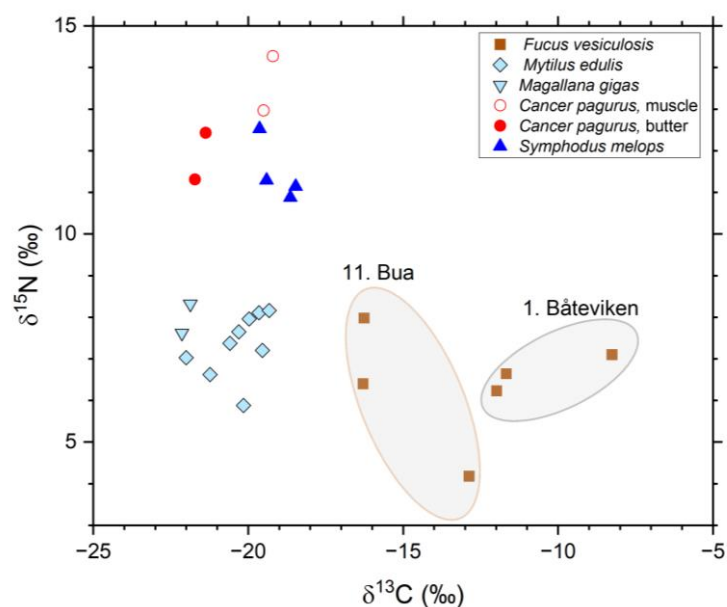


Figure E1 $\delta^{13}\text{C}$ and $\delta^{15}\text{N}$ for a selected number of samples.

The carbon content of the various samples is shown in Figure E2. These values can be used in converting F14C to Bq 14C per g dry weight (see Appendix A)

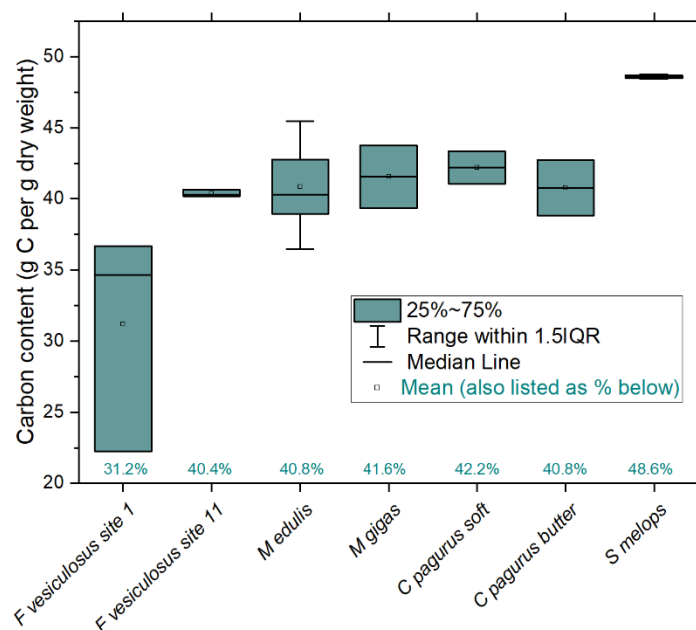


Figure E2 Carbon content for the different sample types in Table E1.

Some observations from the data EA-IRMS data:

1. As expected, the different species forms groups in the trophic level diagram (Figure E1). $\delta^{15}\text{N}$ is increasing throughout the food chain, with higher values in *C. pagurus* and *S. melops* than in *M. edulis* and *M. gigas*.
2. $\delta^{13}\text{C}$ (Figure E1) and carbon content (Figure E2) for *F. vesiculosus* differ for Site 1 Båtevik and Site 11 Bua. This is most likely due to the presence of biofouling organisms attached to *F. vesiculosus* at site 1 Båtevik.
3. As expected, $\delta^{13}\text{C}$ (Figure E1) for *F. vesiculosus* is higher than for filter feeders, arthropods and fish.

The results of the EA-IRMS results of the sediment samples are found in Table E2. Note that, in contrast to the sediment samples subjected to ^{14}C analysis, the sediment samples analysed with EA-IRMS have not been subjected to AAA pretreatment. Different physicochemical forms of the samples have thus been analysed for ^{14}C and for the stable isotopes. In future studies, the pretreatment should be the same for the two analytical methods to reveal useful information.


Table E2 EA-IRMS-data sediment samples. Shaded cells contain results which are outside the range of calibration. ω_{N} and ω_{C} are the mass fraction of nitrogen and carbon related to dry weight (g N per g dry mass and g C per g dry weight). $\delta^{15}\text{N}$ is the isotope fractionation using the atmospheric nitrogen scale. $\delta^{13}\text{C}$ is the isotope fractionation expressed using the VPDB scale. F_{N} = isotopic amount fraction $^{15}\text{N}/(^{14}\text{N} + ^{15}\text{N})$; calculated from $\delta^{15}\text{N}$ using $R_{\text{ref}} = ^{15}\text{N}/^{14}\text{N} = 1/272$. F_{C} = isotopic amount fraction $^{13}\text{C}/(^{12}\text{C} + ^{13}\text{C})$; calculated from $\delta^{13}\text{C}$ using $R_{\text{ref}} = ^{13}\text{C}/^{12}\text{C} = 0.0112372$.

Site	Date (YYYY-MM-DD)	$\omega_{\text{N}} / \%$	$\delta^{15}\text{N} / \text{‰}$	Atom% $F_{\text{N}} / \%$	$\omega_{\text{C}} / \%$	$\delta^{13}\text{C} / \text{‰}$	Atom% $F_{\text{C}} / \%$	C/N ratio
SLU11b S. Ledskär	2023-07-05	0.09	6.95	0.3688	0.87	-18.84	1.090526	9.7
SLU3/22 Outlet	2023-07-05	0.01	3.45	0.3676	0.09	-17.73	1.091746	9.0
1. Båtevik	2023-08-30	0.02	8.48	0.3694	0.15	-13.07	1.096868	7.5
46. Lysekil	2023-08-30	0.02	5.52	0.3683	0.17	-14.70	1.095077	8.5
4. Stockevik	2023-08-30	0.01	7.74	0.3691	0.09	-17.44	1.092065	9.0
9. Ringhals Glippe	2023-08-30	0.06	6.07	0.3685	1.38	-5.65	1.105024	23.0
10. Videbergshamn	2023-08-31	0.01	6.41	0.3686	0.09	-21.87	1.087194	9.0
11. Bua	2023-08-31	0.01	4.23	0.3678	0.26	-6.94	1.103606	26.0
50. Arild	2023-08-31	0.13	5.20	0.3682	1.99	-15.22	1.094505	15.3
51. Åhus	2023-09-01	0.01	5.65	0.3684	0.07	-19.16	1.090174	7.0

References

1. K. Eriksson Stenström, G. Skog, E. Georgiadou, J. Genberg and A. Johansson. *A guide to radiocarbon units and calculations*. LUNFD6(NFFR-3111)/1-17/(2011). Lund University. Dep of Physics. Div of Nuclear Physics.
<http://lup.lub.lu.se/search/ws/files/5555659/2173661.pdf>, 2011.
2. D. Robinson. $\delta^{15}\text{N}$ as an integrator of the nitrogen cycle. *Trends in Ecology & Evolution*, 16(3): 153-162, 2001.

3. M. Stuiver and H. A. Polach. *Discussion reporting of ^{14}C data*. Radiocarbon, 19(3): 355-363, 1977.
4. E. Georgiadou, K. Eriksson Stenström, C. B. Uvo, P. Nilsson, G. Skog and S. Mattsson. *Bomb-pulse ^{14}C analysis combined with ^{13}C and ^{15}N measurements in blood serum from residents of Malmö, Sweden*. Radiation and Environmental Biophysics, 52(2): 175-87, 2013.
5. M. Minagawa and E. Wada. *Stepwise enrichment of ^{15}N along food chains: Further evidence and the relation between $\delta^{15}\text{N}$ and animal age*. Geochimica et Cosmochimica Acta, 48(5): 1135-1140, 1984.
6. D. A. Schoeller, M. Minagawa, R. Slater and I. R. Kaplan. *Stable isotopes of carbon, nitrogen and hydrogen in the contemporary north American human food web*. Ecology of Food and Nutrition, 18(3): 159-170, 1986.



The Swedish Radiation Safety Authority (SSM) works proactively and preventively with nuclear safety, radiation protection, nuclear security, and nuclear non-proliferation to protect people and the environment from the harmful effects of radiation, now and in the future.

You can download our publications from www.stralsakerhetsmyndigheten.se/en/publications. If you need alternative formats such as easy-to-read, Braille or Daisy, contact us by email at registrator@ssm.se.

Strålsäkerhetsmyndigheten

SE-171 16 Stockholm

+46 (0) 8-799 40 00

www.stralsakerhetsmyndigheten.se

registrator@ssm.se

©Strålsäkerhetsmyndigheten